DEVELOPMENT OF PROTEIN LOADED MICROPARTICLES AND NANOPARTICLES FOR ANTIGEN DELIVERY

Dissertation

zur Erlangung des Doktorgrades (Dr. rer. nat.)
der Mathematisch-Naturwissenschaftlichen Fakultät
der Rheinischen Friedrich-Wilhelms-Universität Bonn

vorgelegt von
Donny Francis
aus Bad Honnef

Bonn 2014

Angefertigt mit Genehmigung der Mathematisch-Naturwissenschaftlichen Fakultät der Rheinischen Friedrich-Wilhelms-Universität Bonn

Erstgutachter:	Prof. Dr. A. Lamprecht
Zweitgutachter:	Prof. Dr. K. Wagner
Fachnaher Gutachter:	Prof. Dr. G. Bendas
Fachfremder Gutachter:	Prof. Dr. D. Dietrich

Tag der Promotion: 21.11.2014

Erscheinungsjahr: 2014

This work has been done under the supervision of

Prof. Dr. Alf Lamprecht

at the Institute of Pharmaceutical Technology

Rheinische Friedrich-Wilhelms-Universität Bonn

Acknowledgment

I would like to express my sincere thanks to my supervisor Prof. Dr. Alf Lamprecht for giving me the opportunity to work on this interesting research topic and for providing outstanding research conditions. I am grateful for your motivation and the constructive discussions throughout my work.

I like to thank Prof. Dr. Karl Wagner, Prof. Dr. Gerd Bendas and Prof. Dr. Dirk Dietrich very much for their attendance to be part of my examination committee.

Moreover, I would like to express the deepest appreciation to Boehringer Ingelheim Vetmedica GmbH for their financial support. I want to thank Dr. Martin Folger for enabling this project and for the interesting discussions and meetings. I want to thank Dr. Ragna Hoffmann for her continuous support, motivation and scientific discussions. I would like to thank Dr. Konrad Stadler and Dr. Philip Bridger for the collaboration and assistance for my in vivo studies. I am particularly grateful to Dr. Alfonso Martin-Fontecha for his insightful comments and suggestions.

Further, I would like to thank Dr. med. vet. Eichelkraut and all employees of the "Haus für Experimentelle Therapie" at the university hospital of Bonn. Especially, I would like to thank Andrea Lohmer for her great support during my in vivo experiments.

From the LIMES Institute in Bonn I would like to express my gratitude to Philipp Ebel for his assistance in the field of protein analysis.

Special thanks also to Martina Gerlitz for her friendly support in all situations. I also want to acknowledge Thomas Vidua, Jürgen Hohmann and especially Alexander Ramich for their help in technical issues.

I would like to sincerely thank my colleagues for the great time I had working at the Institute for Pharmaceutical Technology. First, I want to thank Philip Wachsmann and Angela Viehof for assistance and the nice time we had in the lab. I want to thank my office-colleagues and very good friends Montserrat Armengol and Thomas Kipping for all the fun time we spent together. I also want to thank my colleagues Mona Abdel-Mottaleb, Samiha Mouftah, Belal Al-Zaitone, Mert Serim, Alvaro Lopez, Ehab Ali, Tawfek Yazeji, Stefan Lorscheidt, Manu Singh, Leonie Grimm, Anna Schlüter, Henusha Jhundoo, Wiebke Niebel, Daniela Alhenn, Markus Jäger, Daniel

Lagudka, Vicky Riedel, Constantin Kerkfeld, Katharina Freischlad, Thomas Schmal, Florian Schorr, Maryam Shetab, Katrin Grüneberg, Kathrin Lange, Stefan Wanning, Chi-Wah Yeung and Bernadette Kettel for all the nice time we had, particularly on “Karneval”.

Further, I thank my colleagues Victor Rempel, Sören Eggerstedt, Alexander Fuchs, Matthias Mertens, Matthias Plaum and Philipp Ottersbach for the best lunch breaks and the occasional coffee breaks.

I am deeply grateful to my friends Lucas, Tobias, Nora, Philipp and my sister-in-law Eva for their encouragement and support.

I also would like to thank Daniela for your support and patience. Your continuous encouragement and motivation helped me a lot.

Finally, my biggest thanks go to my parents and my brother for the great support, encouragement and love that I receive from you. I accomplished my goals, because you are always there for me when I need you. THANK YOU!!!

Meiner Familie

“Always laugh when you can. It is cheap medicine.”

(Lord Byron)

Trademarks:

This work contains trademarks which are not always indicated explicitly in the text.

Table of contents

1 Introduction and Objective

Vaccines have led to the elimination or control of several infectious diseases, including measles, mumps, rubella, tetanus and smallpox. Generally, a long-lasting immune response can be achieved when using live, attenuated vaccines. However, mutation to the virulent version is always possible. Therefore, non-live vaccines, which are less dangerous, are desirable.

Novel vaccines consist of recombinant proteins that are safe to use, but often poorly immunogenic. In order to achieve a sufficient immune response adjuvants are essential. The requirements for an adjuvant are dependent on the type of immunogenic substance that is used as a vaccine. Despite the high demand only a few adjuvants are currently available for the use in humans and animals. At the moment, aluminum salts and oil-in-water (o/w)-emulsions are typically used as adjuvants (Tetsutani and Ishii, 2012). New adjuvants are needed for the challenges of finding vaccines for malaria, autoimmune diseases and cancer (Heegaard et al., 2011).

An innovative approach of developing modern adjuvants is the design of particulate antigen delivery systems. These, typically polymeric, particles that are in a size range of micro- and nanoparticles can be used as drug carrier systems. Such drug carriers can target antigen presenting cells, which is crucial for long-lasting immunity (Singh et al., 2007).

The mode of action of the drug delivery system can be modified by the particle size as well as the physicochemical property (Lamprecht, 2010). Therefore, the aim of this work was the development and characterization of polymeric micro- and nanoparticles for the antigen delivery using biodegradable and biocompatible polymers. In this work poly(D,L-lactide-co-glycolide) (PLGA) was used as a polymer, because PLGA-microparticles and PLGA-nanoparticles already showed a potential to be used as vaccine adjuvants (Kasturi et al., 2011; Singh et al., 2004).

This work deals with three major parts. First, protein loaded nanoparticles were prepared by the double-emulsion method. This method is the gold-standard to entrap hydrophilic drugs like proteins into polymeric nanoparticles (Lamprecht et al., 2000b). It has been assumed that the protein is entrapped inside the nanoparticles, although this notion was never accurately proven by

a suitable imaging technique (Lamprecht et al., 1999). Scanning electron microscopy (SEM), transmission electron microscopy (TEM) and atomic force microscopy (AFM) were mainly used in the past to characterize the morphology of microparticles and nanoparticles (Blanco and Alonso, 1997; Lamprecht et al., 2000b; Zambaux et al., 1998). However, only the shape and the particle size of the nanoparticles are visible using these imaging methods. In the presented work we characterized the physicochemical properties and investigated the interior morphology of the prepared nanoparticles using ion-milling coupled field-emission scanning electron microscopy. The goal was to achieve a comprehensive understanding of these nanocarriers regarding its morphology.

In the second part, polymeric nanoparticles for the parental use as vaccine adjuvants were prepared. Based on the findings about the morphology of nanoparticles prepared by the double-emulsion method, a simplified preparation method was employed. A comprehensive characterization of the nanoparticles, including analysis of the particles size, loading rate, zeta potential and release studies, to obtain a thorough understanding about the carrier system was the aim of this work. Furthermore, an investigation about the toxicity and uptake abilities of the prepared nanoparticles into a macrophage cell line and in-vivo experiments in mice to examine the adjuvant effect of the nanoparticles was of high importance. The aim was to find out, if protein loaded nanoparticles are beneficial as a vaccine adjuvant and if the surface properties of the nanoparticles have an influence on the immune response.

Microparticles also showed a potential as vaccine adjuvants (O'Hagan and Singh, 2003). Protein loaded micorparticles can be prepared using the double-emulsion method. In the third part of this work, the aim was to investigate the effect of different processing parameters of polymeric microparticles prepared by a double-emulsion method. Also the influence of different polymers on the microparticle properties was investigated.

2 Background

2.1 Vaccines

First achievements in the field of immunological research can be traced back to the 15th century. In China scabs of smallpox were pulverized and insufflated to gain immunity. This very dangerous procedure did have a mortality rate of around 2%. In 1798 Edward Jenner was able to describe a protective effect of cowpox against smallpox that was safe in children and adults (Schütt and Bröker, 2009).

The goal of vaccination is the induction of an immunologic memory to protect against a disease. Vaccines can be classified in live, attenuated vaccines, and inactivated vaccines (Foged et al., 2002). Live, attenuated vaccines contain a version of bacteria or viruses that cannot cause the disease but elicit a strong immune response. However, viruses and bacteria can mutate back into the virulent form leading to an outbreak of the illness. Targets for live, attenuated vaccines are measles, mumps, rubella, and chicken pox (NIH, 2012).

Inactivated vaccines contain killed and non-virulent microorganisms that cannot mutate to the virulent version. They are safer to use, but they also induce a reduced immune response. Toxoid vaccines, e.g. vaccines against diphtheria and tetanus, are inactivated bacterial toxins. Subunit vaccines contain only the antigens that stimulate the immune system the most. The antigens can be derived directly from the microorganism responsible for the disease or they are genetically engineered resulting in recombinant proteins that pose as antigens. Another vaccine type are conjugate vaccines. Some bacteria have polysaccharides as a compound of the cell wall material, linking these polysaccharides to proteins creates conjugate vaccines like the Haemophilus influenzae type B vaccine (Rosenthal and Zimmerman, 2006; Schütt and Bröker, 2009). All of these vaccines show a lower immune response than live, attenuated vaccines, therefore adjuvants are needed to enhance the immunogenic effect.

Fatal diseases like smallpox have been successfully eradicated through the use of vaccines. Other diseases like measles, mumps and chicken pox are not as common as they were before the use of vaccines. Some people cannot be immunized with all vaccines due to immunosuppression. That

is why it is important to vaccinate the majority of the population to decrease the likelihood of spreading a disease. This effect is referred to as herd immunity.

The Robert Koch Institute is responsible for recommending a vaccine schedule in Germany (Table 1). Standard vaccines should be taken by the whole population. Depending on the type of work, age, gender and travel destinations additional vaccines might be necessary.

Table 1: *Vaccine schedule for Germany recommended by the STIKO (STIKO, 2013)*

	Vaccine target
Standard vaccination	Diphtheria Haemophilus influenza type b Hepatitis B Measles Meningococcus Mumps Pertussis Pneumococcus Poliomyelitis Rubella Tetanus Varicella
Vaccination for high-risk groups	Cholera Hepatitis A Human papillomavirus Influenza Rabies Thick-borne encephalitis Typhoid

Even though a lot of diseases can already be prevented by using vaccines, there is still a vast number of infectious diseases for which vaccines or safer and more efficacious versions of those available are needed. There are unmet targets for vaccine development like the human immunodeficiency virus (HIV), and cytomegalovirus, bacteria such as Pseudomonas aeruginosa, Neisseria gonorrhea, Mycobacterium tuberculosis, and parasitic diseases like malaria. Other vaccine targets include cancer, autoimmune diseases, hypertension and Alzheimer's (Rosenthal and Zimmerman, 2006).

Vaccines help developing immunity by imitating an infection. Essential for initiating immune responses are antigen-presenting cells like dendritic cells and macrophages (Unanue, 1984). Immature dendritic cells are taking up proteins in the periphery to monitor the environment. After dendritic cells are activated by antigens, the cell matures and migrates to lymph nodes. During the maturation the antigen is processed into small fragments and these fragments are then presented at the cell surface by coupling the antigens to major histocompatibility complex (MHC) molecules. CD4+ T cells recognize antigenic peptides coupled with MHC class II molecules and CD8+ T cells bind to MHC class I molecules. Activated CD4+ T cells support the activation of B cells, whereas CD8+ T cells differentiate into cytotoxic cells capable of killing pathogens (Fig. 1) (Schütt and Bröker, 2009; Siegrist, 2008). T cell responses are part of the cellular immunity. The humoral immunity is triggered by B cell responses, which leads to antibody production. B cells are also activated by dendritic cells. They bind to the antigen presented by dendritic cells with immunoglobulins on their surface. This causes the B cells to differentiate to plasma cells that produce antibodies, which appear in low levels in the serum within a few days of immunization. Some B cells differentiate to memory B cells. These memory B cells are activated through contact with the specific antigen, which leads to maturation to plasma cells and the production of IgG antibodies. The short life span of the plasma cells has the consequence that antibody titers decline rapidly after one immunization. The antibodies will eventually disappear after a primary response, when using non live vaccines. That is why booster immunizations after several weeks are necessary. Following a secondary immunization, a rapid increase of the antibody titer can be observed, as memory B cells are activated. They differentiate to plasma cells and high-affinity antibodies are secreted (Rosenthal and Zimmerman, 2006; Siegrist, 2008).

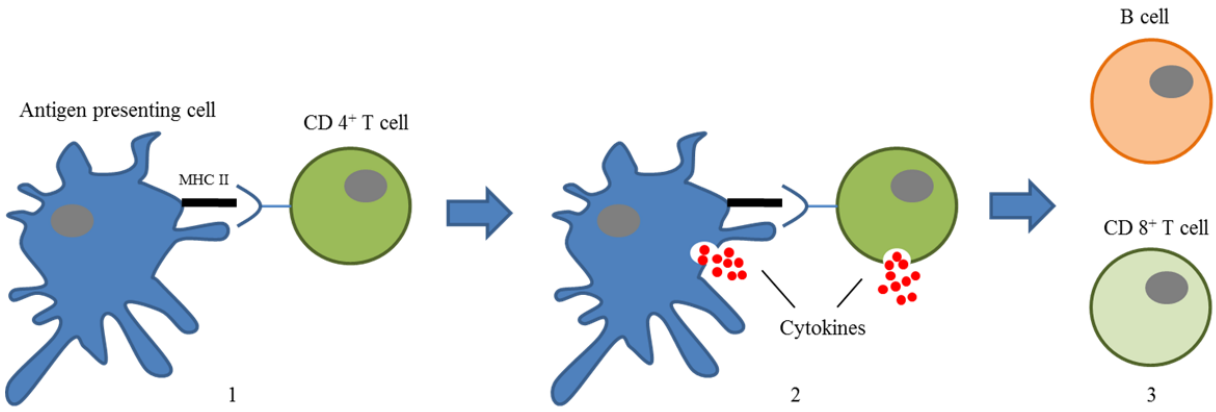

Fig. 1: *(1) CD 4^+ T cell binds on MHC II at cell surface of antigen presenting cells; (2) both antigen presenting cells and CD 4^+ T cells release cytokines that activate (3) B cells and CD 8^+ T cells; modified from (Dario-Becker, 2013; Meeusen et al., 2007; Siegrist, 2008)*

Live, attenuated vaccines rapidly spread throughout the body after injection and dendritic cells are activated at multiple sites, which is similar to the pattern occurring after a natural infection. They multiply at the injection site and in the periphery. Consequently, the immunogenicity of live vaccines is generally higher compared to non-live vaccines. Furthermore, the injection site is not important when using live vaccines, because of the fast dissemination of the viral or bacterial particles. Non live vaccines cannot multiply, therefore the activation of innate responses are limited in time and space, which is why the administration route is more important in comparison to live vaccines (Siegrist, 2008).

2.2 Adjuvants

Many vaccines are not immunogenic enough to elicit an immune response that would trigger immunity. Especially non live-vaccines are showing a low immunogenic potency when administered alone. Moreover, proteins posing as antigens have to withstand harsh conditions to maintain their composition and thereby maintaining their immunogenic potential. Recombinant proteins are safer to use than live, attenuated vaccines, but less immunogenic. Hence, substances that enhance the immune response of the safe, but poorly immunogenic antigens are in demand (Aucouturier et al., 2001).

Adjuvants are compounds that increase the immune response, when used in combination with a specific antigen (Singh and O'Hagan, 2003). The efficacy of many vaccines is dependent on the adjuvants as antigens have become more purified (Aucouturier et al., 2001; Korsholm, 2010).

The application of an adjuvant can have different benefits and different adjuvant types are available. Immunomodulatory adjuvants can induce either a predominantly Th1 or Th2 type immune response, dependent on which adjuvants are being used. Another type of adjuvants are substances that can prolong the interaction between the antigen and antigen presenting cells. Furthermore, adjuvants have the potential to be antigen delivery systems that target antigen presenting cells like dendritic cells (Cox and Coulter, 1997).

The exact mode of action of adjuvants is still not fully understood, but is has been suggested that a “depot effect” and an induction of an inflammation might be mechanisms of adjuvant effectiveness (Heegaard et al., 2011; Kuroda et al., 2013).

A lot of different adjuvants are available or currently in development (Table 2). The most commonly used adjuvants are aluminum salts. They are FDA approved and safe to use in humans and animals (Tetsutani and Ishii, 2012). Generally, an aluminum hydroxide or aluminum phosphate gel is used, which binds the immunogenic substance via electrostatic interaction. A prolonged interaction of the antigen with cells of the immune system is possible because of the gel-like structure. Furthermore, it is suggested that aluminum salts activate the innate immune response, which in combination with the immunogenic substance subsequently leads to an adaptive immunity (Kuroda et al., 2013).

Freund’s Adjuvant is an oil based adjuvant. It has been successfully used in veterinary vaccines, but remains inapplicable for humans, because of toxicity concerns. Freund’s Adjuvant does however elicit a strong immune response, which can also be contributed to the high inflammatory effect of the mineral oil after administration (Heegaard et al., 2011).

Table 2: *Ingredients of conventional adjuvants; modified from (Cox and Coulter, 1997; Heegaard et al., 2011; Rosenthal and Zimmerman, 2006; Singh and O'Hagan, 2003; Tetsutani and Ishii, 2012)*

Adjuvant	Ingredient
Freund's Adjuvant, complete	Mycobacterium tuberculosis, paraffin oil, mannide monooleate
Freund's Adjuvant, incomplete	Paraffin oil, mannide monooleate
Alum	Aluminium hydroxide, aluminium phosphate
MF59®	Squalene, polysorbate 80, Span 85
AS03	Squalene, polysorbate 80, DL-α-tocopherol
AS04	Aluminium hydroxide, monophophoryl lipid A
Immune stimulating complexes (ISCOMs)	Cholesterol, phospholipid, Quillaia saponins
MPL	Monophophoryl lipid A
CpG	Oligunecleotide
Carbopol	Synthetic, anionic polymer
Ribi®	Squalene, polysorbate 80, MPL,
Montanide ISA51	Mineral oil, surfactant, immunomodulator
Syntex adjuvant formulation (SAF)	Squalene, polysorbate 80, muramyl dipeptide derivative (threonyl-MDP)
Titermax®	Squalene, block copolymer, microparticulate stabilizer
Proteosomes	Aggregates of bacterial transmembrane proteins
Virosomes	Virus-derived transmembrane proteins
Mineral salts	Aluminium salts or calcium phosphate
LPS	Lipopolysaccharides
Particulate adjuvants	Microparticles, nanoparticles, liposomes

A better approach than oil based adjuvants is an o/w-emulsion. MF59® and AS03 are examples for o/w-emulsions and are currently used in influenza vaccines. MF59® and AS03 induce a high

degree of cell recruitment of monocytes and dendritic cells, which might be responsible for the adjuvant effects (Tetsutani and Ishii, 2012).

ISCOMs are matrices that are formed after interaction of saponins, cholesterol and phospholipids. These open cage-like structures have the immunogenic substance incorporated inside the cage. The mode of action is probably via targeting of immune cells (Cox and Coulter, 1997).

Immune cells have toll-like receptors on their surface, which are able to identify pathogens. The pathogens are detected by their pathogen-associated molecular pattern (PAMP). Adjuvants that pose as PAMPs can be ligands to toll-like receptors and therefore initiate an immune response. MPL as well as CpG have been identified as toll-like receptor agonists (Heegaard et al., 2011).

Adjuvants play an important role in vaccines and the battle against many diseases. However, only very few adjuvants have been approved for the use in humans. Novel, safe and efficient adjuvants are needed to overcome the challenges of new, poorly immunogenic antigens. Moreover, innovative adjuvants are needed for the challenging task of finding vaccines for malaria, cancer and autoimmune diseases.

2.3 Nanoparticles

Nanotechnology is an important and novel approach to overcome drug delivery challenges. Nanoparticles can be defined as particles with diameters ranging from 1 nm to 1000 nm. Further, they can be subdivided into nanocapsules and nanospheres (Fig. 2). Nanocapsules have the drug usually encapsulated in an inner liquid core that is surrounded by a polymeric shell. Nanospheres consist of a matrix in which the drug is encapsulated or the drug is adsorbed at the surface of the nanospheres (Pinto Reis et al., 2006).

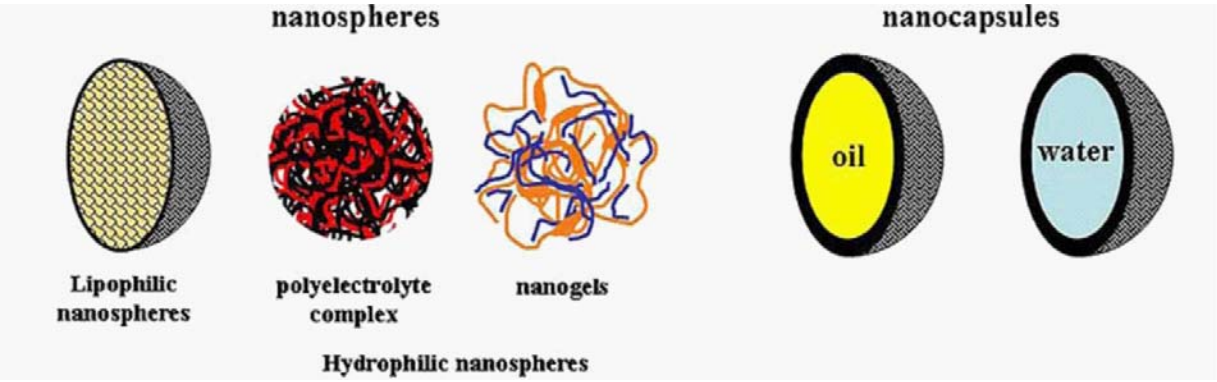

Fig. 2: *Different types of polymeric nanoparticles (Vauthier and Bouchemal, 2009)*

Polymeric nanoparticles are of great interest as carriers of therapeutic drugs in controlled release applications (Mundargi et al., 2008). With an improved drug delivery directly to the site of action the overall toxicity can be reduced (Cheng et al., 2012). Nanoparticles can penetrate deep into tissues and are usually taken up efficiently by cells. Moreover, the drug dosage can be reduced and drugs are protected from degradation, increasing the drug stability (Bala et al., 2004). Requirements for polymeric nanoparticles for parental use include biocompatibility, suitable biodegradation and drug compatibility (Lu et al., 2009). Due to a better transport of drugs across absorption membranes, oral delivery of APIs that normally have no bioavailability like heparin (Hoffart et al., 2006) or insulin (Viehof et al., 2013) is possible (Viehof and Lamprecht, 2013).

The uptake and pathway of nanoparticles into cells was the target of various studies (Fleischer and Payne, 2012; Hillaireau and Couvreur, 2009; Treuel et al., 2013; Wachsmann and Lamprecht, 2012; Walczyk et al., 2010). Nanoparticles can be internalized in cells through phagocytosis or other endocytic pathways. The other endocytic pathways can be further categorized in clathrin-mediated endocytosis, caveolae-mediated endocytosis and macropinocytosis (Fig. 3) (Hillaireau and Couvreur, 2009). Nanoparticles are being “tagged” by proteins (opsonins) if phagocytosis occurs. This opsonization enables the nanoparticles to attach to cells, and subsequently to be phagocytosed.

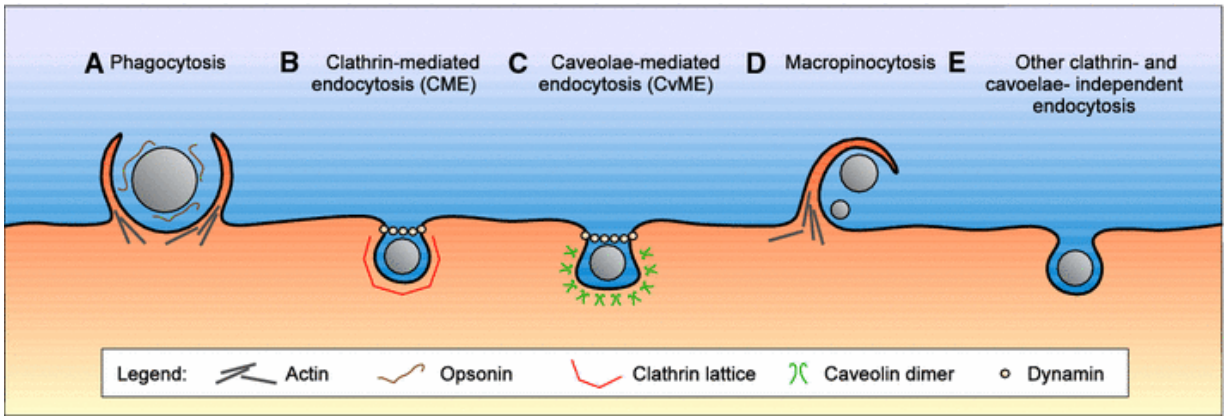

Fig. 3: *Pathways of nanoparticles into cells (Hillaireau and Couvreur, 2009)*

Nanoparticles have a benefit in the treatment of a wide range of diseases and also possess the ability to function as supporting agents for the diagnosis of diseases, e.g. imaging contrast agents in diagnostic ultrasound (Lu et al., 2009). Delivery of vaccines and adjuvants using nanoparticles is possible and needs to be further investigated (Singh et al., 2007). The delivery of interferon and the delivery of DNA with nanoscale drug carriers offer the potential of the treatment of a variety of diseases, e.g. neurodegenerative illnesses, cancer and cardiovascular diseases (Mundargi et al., 2008). Treatment of cancer with nanoparticles showed promising results in animal studies, as nanoparticles showed the ability to accumulate in tumor tissue (Doll et al., 2013). Furthermore, the delivery of drugs across the blood-brain barrier can be enhanced when using surfactant coated nanoparticles (Soppimath et al., 2001). Several products based on nanomedicine containing API's can already be found on the market (Table 3).

Table 3: *Selection of nanoparticulate drug delivery systems on the market; modified from (Patel, 2008; Wagner et al., 2006)*

Registered Trademark	API
Estrasorb®	Estradiol
Amphotec®	Amphotericin B
Abraxane®	Paclitaxel
Rapamune®	Sirolimus
Emend®	Aprepitant

In immunology vaccines are used to achieve adaptive immunity for various illnesses. Nanocarriers have been investigated as adjuvants formulations. Up to now, aluminium salts are the most common adjuvants used in current vaccine formulations. They are safe to use and they can generate an enlarged humoral immune response (Demento et al., 2009). Additional delivery carriers are necessary as many new antigens are only weakly immunogenic. A nano sized emulsion (MF59) is already approved for human use and on the market in Europe (Peek et al., 2008).

Polymeric nanoparticles have to meet strict requirement such as biocompatibility, biodegradability and compatibility with the antigen to be considered as vaccine formulations. PLGA is an FDA approved excipient that may be used to formulate nanoparticles that meet the necessary requirements (Drug Master File is registered with FDA) (Mitsui-Chemicals, 2010).

Nanoparticles can act as adjuvants as they can enhance the uptake of antigens into cells and they can be used as controlled delivery systems, prolonging the availability of an antigen (Rice-Ficht et al., 2010).

Nanoparticles are able to protect the drug of hostile environments like the conditions in the gastrointestinal tract. Nanoparticles can therefore improve the oral vaccination of proteins and peptides as they enhance their transmucosal transport (des Rieux et al., 2006). Mucosal

vaccination reduces the risk of infections at the injection site and has a better compliance. Further it is generally more cost efficient and makes large population immunization possible.

Nevertheless, immunization through the parental route is also important, as most antigens cannot be delivered orally, even when using nanoparticles. Nanoparticulate delivery systems may play an important role in vaccine formulation in the future as they can specifically deliver antigen to antigen presenting cells like dendritic cells (Cruz et al., 2010). Targeting dendritic cells enhances the immune response and also makes lower dosage of the antigen possible, leading to reduced side effects. PLGA nanoparticles also have a great potential as adjuvants as they facilitate dendritic cell maturation (Akagi et al., 2012).

Nanoparticles may also be used in immunotherapy to utilize the immune system in the treatment of cancer, which could lead to a prevention of the metastatic spread. Further, prophylactic cancer vaccines might be developed using nanoparticles as carriers to prevent cancer in the first place. Vaccines for hepatitis B and human papillomavirus are already being used to reduce the risk of liver cancer and cervical cancer, respectively (Hamdy et al., 2011).

Nanoparticles have several benefits over microparticles for antigen delivery, because their smaller size leads to better uptake by dendritic cells, which in turn leads to a better immune response (Li et al., 2011). The significant larger surface area also allows nanoparticles to adsorb more antigen per weight as microparticles (Oyewumi et al., 2010). The particle size and the surface properties appear to be central in vaccine formulations using nanoparticles. Nanoparticles may also be used to co-deliver antigens and adjuvants (Rice-Ficht et al., 2010).

FDA approved PLGA and its derivatives are common polymers for the preparation of polymeric nanoparticles (Drug Master File is registered with FDA) (Mitsui-Chemicals, 2010). Common nanoparticle preparation methods have already been established and include emulsification solvent evaporation method, emulsification solvent diffusion method, double-emulsion method, salting-out, nanoprecipitation method and ionic gelation (Bala et al., 2004; Pinto Reis et al., 2006; Vauthier and Bouchemal, 2009).

2.3.1 Preparation of protein loaded nanoparticles

Polymeric nanoparticles loaded with hydrophilic drugs such as proteins can be obtained by several preparation methods. Most common is the double-emulsion method. Adsorption of the protein on the nanoparticles following an emulsification solvent-evaporation method, a solvent displacement method and salting-out are also options to prepare protein loaded nanoparticles.

In the double-emulsion method the protein is dissolved in an aqueous phase and emulsified with an oil phase containing a polymer. This primary water in oil emulsion is then emulsified with an outer water phase containing PVA as a stabilizer. Solvent-extraction using a high amount of water or solvent-evaporation under reduced pressure leads to the precipitation of nanoparticles containing the hydrophilic drug (Bilati et al., 2005). The particle size is dependent on a lot of variables, including the concentration of the hydrophilic drug in the inner water phase, the viscosity of the organic phase, the concentration of the stabilizer in the outer water phase, the emulsification conditions and the organic solvent removal method. Nanoparticles prepared by the double-emulsion method have been widely described and characterized in regard to their particle size, loading rate and dissolution kinetics (Lamprecht et al., 2000b), their potential for clinical application (Cheng et al., 2012) and their in-vivo effects (Gutierro et al., 2002b; Kasturi et al., 2011). The morphology of the nanoparticles has been investigated using SEM (Giovino et al., 2012; Khoee et al., 2012), FE-SEM (Sahana et al., 2010), atomic force microscopy (Lamprecht et al., 1999) and transmission electron microscopy (Cohen-Sela et al., 2009; He et al., 2004). These imaging techniques were used to determine the shape and to confirm the particle size of the prepared nanoparticles. However, the inner morphology of the nanoparticles could not be revealed.

The emulsification solvent-evaporation method is a frequently used method to prepare polymeric nanoparticles. Briefly, the polymer is dissolved in an organic phase and afterwards emulsified in a water phase. This water phase usually contains a surfactant to stabilize the emulsion that is formed following the emulsification process. The organic solvent is removed from the emulsion under reduced pressure, leading to the formation of solid nanoparticles (Desgouilles et al., 2003). The protein is then adsorbed at the surface on the nanoparticles via incubation of the protein with the nanoparticles on a horizontal shaker. This method is advantageous as compared to the double-emulsion method in that respect that it does not stress the protein during the emulsification

process and therefore reduces the problem of protein degradation and degeneration during the preparation. The particle size can be easily controlled by the surfactant concentration in the aqueous phase and the emulsification conditions.

A modified solvent displacement method was described to obtain protein loaded nanoparticles using polyethylene glycol as a solvent for the polymer (Ali and Lamprecht, 2013). The solvent containing the polymer is mixed with an aqueous phase containing a protein and added to a disperse phase under magnetic stirring, causing the polymer-rich solvent phase to form nanodroplets. The polyethylene glycol is then extracted with water and protein loaded nanoparticles precipitate.

The salting-out method is based on an aqueous phase that contains electrolytes and a stabilizer, e.g. PVA, forming an emulsion with an inner phase, e.g. acetone that contains the polymer and the drug. After homogenization the o/w-emulsion is diluted with water, which leads to a diffusion of acetone to the aqueous phase, which induces the formation of nanoparticles (Pinto Reis et al., 2006). The encapsulation efficiency is dependent on the salting-out agent. Suitable electrolytes include magnesium chloride, calcium chloride and magnesium acetate. Even though the process is not as harsh as the double-emulsion method, proteins do not show high encapsulation rate, therefore the salting-out method is mainly used for lipophilic drugs.

2.4 Microparticles

Microparticles have a particle size of 1 µm – 1000 µm and a spherical morphology. They can be classified as microcapsules that have a polymeric shell and an API core, and microspheres, where the API is homogenously dispersed in the polymeric matrix (Mäder and Weidenauer, 2010; van de Weert et al., 2000) (Fig. 4). Polymeric microparticles can consist of a biodegradable and biocompatible polymer and an API. They can be used as parental drug delivery systems (Jain, 2000), furthermore, oral delivery (Lamprecht et al., 2004), nasal delivery (Garmise et al., 2007) and pulmonary delivery (Fu et al., 2002) have been investigated. However, parental applications are used for the most part, as they cause a sustained release of an API for a prolonged period of time (Ye et al., 2010).

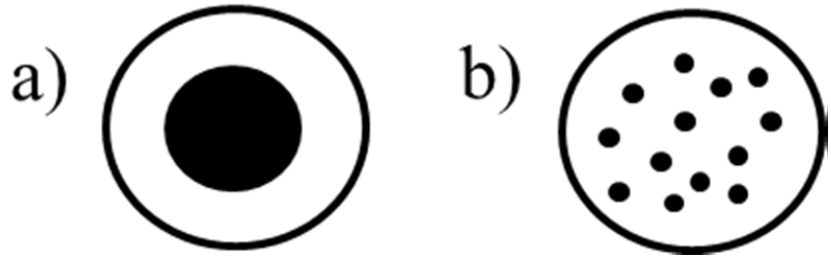

Fig. 4: *Morphology of microparticles: a) Microcapsule with polymeric shell and solid or liquid API core; b) Microsphere with API dispersed in polymer matrix*

Many injectable microparticulate drug carriers are already on the market (Table 4), since microparticles offer many advantages compared to conventional dosage forms, e.g. the possibility of a controlled release of the API over a prolonged period of time (Faisant et al., 2006), no need for surgical removal, easy administration (Siepmann et al., 2004) and a better compliance due to the fact that the number of injections can be reduced. Microparticles can be used as drug delivery systems for a wide variety of therapeutics. Therefore, they have the potential to be used in many different fields, e.g. the antigen delivery (O'Hagan and Singh, 2003), cancer treatment (Allhenn et al., 2013) and as antipsychotics (Bobo and Shelton, 2010).

Table 4: *Selection of injectable microparticulate drug carriers on the market (Mäder and Weidenauer, 2010; Mundargi et al., 2008)*

Registered Trademark	API	Preparation Technique
Decapeptyl® SR	Triptorelin	Phase separation
Lupron Depot®	Leuprorelin	Emulsion method
Suprecur® MP	Buserelin	Spray drying
Sandostatin® LAR®	Octreotide	Phase separation, Spray drying
Risperdal® Consta®	Risperidon	Emulsion method

Biodegradable and biocompatible polymers like PLGA are the excipients of choice for the particulate delivery of antigens via microparticles. PLGA microparticles are proven to be safe to use in humans and are very promising systems that present multiple copies of the antigen to the immune system (Wendorf et al., 2008).

In vaccine research particulate formulations such as microparticles are generally used as vaccine delivery systems to target antigens into antigen-presenting cells. However, microparticles can also be used as delivery systems for adjuvants to increase their immunostimulatory effect. A controlled release of the adjuvant causes a reduced toxicity and limits the systemic distribution of the adjuvant, which could reduce adverse effects (O'Hagan and Singh, 2003).

Particulate carriers like microparticles are able to be internalized by antigen presenting cells and macrophages, since they are of similar size as many pathogens (O'Hagan et al., 2006). Therefore, they can increase the amount of antigen that reaches the intracellular space, which could lead to a higher efficiency of the vaccine formulation.

Injectable microparticles have the potential to act as single-dose vaccines, combining the initial immunization with a booster vaccination. Therefore a higher compliance could be achieved and costs could be lowered significantly. Ideally, an initial burst release of the antigen is followed by a "lag time", in which no antigen is released. The release can be tailored with different polymeric types. Pulse releases of the antigen after several weeks to provide booster responses are desired (Singh et al., 2007). However, a benefit of pulse releases has not been proven yet in vivo.

Microparticles might also be used for oral immunization and offer advantageous like a better compliance, less side effects and easier administration. Microparticles have the ability to be taken up by mucosal-associated lymphoid tissue, which is crucial for the delivery of the antigen to the lymphoid tissue. Another promising immunization route is the intranasal route as the environment for the antigen is better, since there are less proteolytic enzymes and a less acidic pH (Gutierro et al., 2002a).

A key issue in the antigen delivery with microparticles remains the stability of the antigen. Due to the conditions in the particle and during the encapsulation process, aggregation and denaturation might reduce the immunogenicity of the antigen (Caputo et al., 2008). To avoid this problem, surface adsorbed proteins that can easily be released from the surface might be a

promising alternative. Another approach is the adsorbtion of DNA onto the surface of cationic microparticles. Like for surface adsorbed proteins, this technique reduces the high stress the API is submitted to during the particle preparation (Singh et al., 2004).

A few immunization studies in vivo in mice and pigs were performed using mostly PLGA microspheres. Particle sizes of ≤ 10 µm were favorable to bigger particles in regard to their immune response, however the effect of microparticulate vaccine formulations has not been tested in humans, yet (Gutierro et al., 2002a; Heegaard et al., 2011; O'Hagan et al., 2006; Waeckerle-Men and Groettrup, 2005).

There are a number of manufacturing techniques to prepare microparticles. Depending on the API and the intended release profile a suitable preparation method must be chosen. Microencapsulation methods include phase separation, spray drying, emulsion methods, electrospray method, microfluidic methods and micro fabrication methods (Ye et al., 2010).

The phase separation yields mainly microcapsules. A polymer is dissolved in an organic solution and the API is dispersed in the polymer solution. For each API a proper polymer with suitable interface characteristics must be selected. An organic non-solvent that does not dissolve either the polymer or the drug and is miscible with the polymer solvent is added. Phase separation sets in and the polymer accumulates around the API, leading to coacervate droplets. Using solvent extraction the microdroplets are formed to microparticles (Jalil and Nixon, 1990).

A one step and continous process to obtain microparticles is spray drying. The scale up is manageable, the method is very rapid and the solubility of the API and the polymer are less crucial, compared to phase separation and emulsion methods (Takada et al., 1995; Wagenaar and Müller, 1994). A liquid is dispersed from a spray nozzle and the suspension or solution separates as solid and the solvent evaporates. When using suitable nozzles, microparticles can be prepared. Another method is spray freeze drying, where the liquid is sprayed into liquid nitrogen and the frozen droplets are later freeze dried (Eggerstedt et al., 2012). This is especially advantageous for thermo labile APIs.

Common techniques to prepare polymeric microparticles containing polyesters for the application as implants or injectable, parental drug delivery systems are emulsion methods. With a single emulsion process and a subsequent solvent evaporation or solvent extraction process, particles can be formed. A polymer and a drug are dissolved in an organic solvent that is immiscible with water. The organic phase is then emulsified with water containing a surfactant, e.g. PVA. The organic solvent is then removed by adding huge quantities of water and therefore extracting the organic solvent or by evaporating the organic solvent under reduced pressure (Arshady, 1991). The microparticle suspension can be filtrated and dried under appropriate conditions to obtain an injectable product (Jain, 2000). When using o/w-emulsions water soluble drugs diffuse into the aqueous phase, leading to poor encapsulation rates. Hence, this method is more frequently used for lipid-soluble APIs. Encapsulation of water soluble drugs can be obtained by using an oil-in-oil (o/o)-emulsion method, in which a water miscible organic solvent is used. It must be able to dissolve the drug and the polymer. As an outer phase a mineral oil is used, after emulsification and evaporation microparticles are formed containing the API. To wash off the mineral oil, another organic solvent, e.g. n-hexane, is used.

Due to the use of a lot of toxic solvents, other methods to encapsulate hydrophilic drugs are preferable. An alternative to the emulsion methods using methylene chloride or other toxic organic solvents is the preparation of microparticles using glycofurol as a solvent (Allhenn and Lamprecht, 2011). The double-emulsion method is best suited to encapsulate hydrophilic drugs.

2.4.1 Preparation of protein loaded microparticles

Polymers containing proteins as a sustained release formulation have been investigated since 1976 (Langer and Folkman, 1976). The preparation of biodegradable and biocompatible microparticles containing proteins as an API have various advantages compared to traditional dosage forms, which include reduced toxicity, improved compliance and a controlled-release drug delivery system (Luan et al., 2006; Meng et al., 2003).

Manufacturing of protein loaded microparticles can be achieved with multiple methods. Spray drying and spray freeze drying are suitable options, however they require expensive and complex

manufacturing processes. A common method to prepare protein loaded microparticles in the laboratory scale is the w/o/w-double-emulsion method (Coombes et al., 1998; Crotts and Park, 1998). This technique has been further developed and w/o/o-, s/o/w-, s/o/o, s/o/o/w-emulsion methods (Paillard-Giteau et al., 2010; Ye et al., 2010; Yuan et al., 2009) are potential ways to encapsulate proteins.

The double emulsion technique starts with dissolving a suitable polymer, e.g. PLGA, cellulose or polylactide in an organic solvent, e.g. ethyl acetate or methylene chloride (Porjazoska et al., 2004). Then a protein is dissolved in water and emulsified in the organic phase, forming a water-in-oil emulsion. This emulsion is commonly referred to as the primary emulsion (Sah, 1999). After this first emulsification step the primary emulsion is dispersed in an outer aqueous phase containing a stabilizer, e.g. PVA. During this second emulsification step a w/o/w-double emulsion is formed (Jain, 2000). To remove the organic solvent a solvent extraction or a solvent evaporation method can be applied. For the solvent extraction method the double emulsion is introduced into a high volume of water. The organic solvent is thereby extracted from the double emulsion and then, under continuous stirring of the formulation, evaporates at room temperature. For the solvent evaporation method the organic solvent of the double emulsion is removed by evaporation under reduced pressure using a rotary evaporator (Uchida et al., 1995). The resulting microparticle suspension can then be centrifuged or filtrated to obtain the particles.

PLGA is a commonly used polymer for this method, since it is not soluble in water. It also has major advantages compared to other polymers, because it is a safe to use FDA approved excipient that is biodegradable and biocompatible. The double emulsion technique is easy to handle and offers relatively mild conditions for the protein. However, the double emulsion method also faces a lot of challenges, e.g. instability of the encapsulated protein, an incomplete release of the protein and loss of the protein during the encapsulation process (Putney and Burke, 1998; Yeo and Park, 2004). Due to the acidic environment in PLGA hydrolysis of peptide bonds of the protein has been observed (Jiang et al., 2005). Modifications of the protein, like the hydrolysis of peptide bonds or changes in the tertiary structure through aggregation or denaturation, can lead to a loss of functionality of the protein (Schwendeman, 2002). During the double emulsion method the protein is confronted with several conditions that could lead to protein denaturation. During the emulsification steps, the protein may be submitted to heat or

shear forces. Cooling can be beneficial to maintain protein stability. The protein is exposed to an organic surface during the preparation process, which can lead to aggregation of the proteins (Sah, 1999).

2.5 In vivo immunization studies

The immune system of a mammal is too complex to be sufficiently simulated in cell culture experiments. The effect of an antigen and an adjuvant on the immune response can only be adequately determined by an in vivo vaccination study.

Mice are commonly used in immunization studies, as they can be easily handled in a laboratory scale. Ovalbumin can act as a model antigen that provokes antibody response in mice (Kasturi et al., 2011). The potency of this response can be used to compare and to evaluate different adjuvants that are administered in combination with the antigen. In general, two injections three to four weeks apart from one another of the antigen are given to the test animal. Blood samples are usually drawn before the first injection to confirm that no antibodies for the given antigen are present in the beginning of the experiment. Furthermore, five to seven weeks after the first injection blood samples are drawn to evaluate the antibody titers after two injections of the antigen (Gutierro et al., 2002b; TVT, 2010). For immunization purposes, intravenous, subcutaneous, intramuscular, intradermal or intraperitoneal injections are established parental delivery routes for vaccines in mice (Mohanan et al., 2010; TVT, 2010).

3 Materials and Methods

3.1 Substances

3.1.1 Poly(lactic-co-glycolic acid) (PLGA)

The PLGA copolymers (Table 5) were kindly provided by Boehringer Ingelheim (Ingelheim, Germany) and Evonik (Essen, Germany). PLGA (Fig. 5) is synthesized by ring-opening copolymerization of two different monomers, the cyclic dimers (1,4-dioxane-2,5-diones) of glycolic acid and lactic acid. Common catalysts used for this reaction include tin(II) 2-ethylhexanoate, tin(II) alkoxides or aluminum isopropoxide (Lu et al., 2009; Mäder and Weidenauer, 2010). PLGA is a FDA approved excipient (Drug Master File is registered with FDA) (Ji et al., 2012), which is biocompatible and biodegradable (Anderson and Shive, 1997).

Table 5: *Polymers used to prepare microparticles and nanoparticles*

Trademark	End group	Composition
RG 502 H	Acid	Poly(D,L-lactide-co-glycolide) 50:50
RG 503 H	Acid	Poly(D,L-lactide-co-glycolide) 50:50
RG 504 H	Acid	Poly(D,L-lactide-co-glycolide) 50:50
RG 505	Ester	Poly(D,L-lactide-co-glycolide) 50:50

The glass transition temperature of the PLGA copolymers is above 37 °C and the biodegradation occurs by non-enzymatic hydrolysis of the ester backbone (Jain, 2000; Yoo et al., 2005). Each polymer that was used to prepare micro- and nanoparticles has a composition of equal amounts of lactic acid and glycolic acid and they degrade in approximately one to two months in vitro (Nair and Laurencin, 2007).

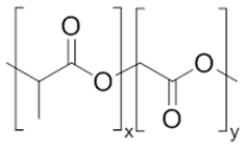

Fig. 5: *Chemical structure of PLGA (x = number of units of lactic acid, y = number of units of glycolic acid)*

3.1.2 Bovine Serum Albumin (BSA)

BSA was purchased from Sigma Aldrich (Munich, Germany). BSA consists of 583 amino acids and has a molecular weight of 66.4 kDa (Hirayama et al., 1990). The isoelectric point is 4.7 (Ge et al., 1998). BSA was used as a model protein for the development of different micro- and nanoparticle formulations. It has already been widely used as a model protein for the preparation of micro- and nanoparticles due to its stability (Lamprecht et al., 2000b) and low cost. For studies with the FE-SEM BSA was substituted with Gold-BSA (Aurion®, Netherlands) as the hydrophilic compound due to its characteristics to be visible under the FE-SEM.

3.1.3 Ovalbumin (OVA)

OVA was obtained from Sigma Aldrich (Munich, Germany). OVA has a molecular weight of 45 kDa, consists of 386 amino acids (Huntington and Stein, 2001; Nisbet et al., 1981), and has an isoelectric point of 4.86 (Smith, 1935). OVA is the major protein in avian egg-white (60-65%), however its function is unknown (Huntington and Stein, 2001). Nevertheless, OVA has been used as a model antigen in many vaccine studies (Kasturi et al., 2011; Singh et al., 2007; Uchida et al., 1995), since it is a safe to use and well characterized immunogen. Here, we used OVA as a model protein for formulation experiments with nanoparticles and as a model antigen for in-vivo studies with mice.

3.1.4 Lysozyme

Lysozyme was kindly provided by Boehringer Ingelheim Vetmedica GmbH (Ingelheim, Germany). Lysozyme is obtained from hen egg white. It consists of 129 amino acids and has a molecular weight of 14.3 kDa (Blake et al., 1965; Canfield, 1963). It has an isoelectric point of 11.35 (Wetter and Deutsch, 1951). Lysozymes are enzymes that catalyze the hydrolysis of β-1,4 glycosidic bonds between *N*-acetylmuramic acid and *N*-acetly-D-glucosamine residues in peptidoglycans. Peptidoglycans can be found in bacteria, especially in Gram positive bacteria. Therefore, lysozymes have antibacterial properties and are part of the immune system (McKenzie and White, 1991). In this work lysozyme was used as a model antigen for a small protein with a basic isoelectric point in various nanoparticle formulation studies.

3.1.5 α-toxin

Clostridium perfringens is a Gram-positive anaerobe pathogen that causes gas gangrene (Leslie et al., 1989; Titball, 2009) . Every Clostridium perfringens strain possess the gene encoding α-toxin (Titball et al., 1999). Formaldehyde α-toxins have already been used as experimental vaccines in humans and toxoid vaccines for sheep and goats are commercially available (Titball, 2005).

Two different C. perfringens α-toxoid antigens were kindly provided by Boehringer Ingelheim (Hannover, Germany). One antigen is α-toxoid derived from C. perfringens cell culture, the other antigen is E.coli derived α-toxoid. The Clostridium perfringens derived α-toxoid was inactivated with formaldehyde and neutralized with sodium bisulfite. E.coli express mutated which is therefore already inactived α-toxoid. Both antigens were used for nanoparticle formulation experiments, as results are more likely to be applicable to other recombinant proteins. α-Toxin has a molecular weight of 43 kDa (Leslie et al., 1989).

3.1.6 Carbopol

Carbopol was kindly provided by Boehringer Ingelheim (BIV Inc., St. Joseph, USA). Carbopol is a cross-linked polyanionic carbomer (Rachel et al., 2012) which is used as an adjuvant in in-vivo studies in this work. Carbopol has shown the property to increase the antibody response for veterinary vaccines, while also being well tolerated (Dey et al., 2012).

3.1.7 Emulsigen D

Emulsigen D was purchased from MVP Laboratories (Omaha, USA). Emulsigen D is an oil-in-water emulsified adjuvant combined with dimethyldioctadecylammonium bromide (DDA) as an immunostimulant (Hiszczyńska-Sawicka et al., 2010). Here, it was used for stabilization and formulation studies with protein loaded nanoparticles.

3.1.8 Lipopolysaccharides (LPS)

LPS is a component of the cell wall of Gram-negative bacteria. LPS consists of three parts, a hydrophobic lipid (lipid A), a polysaccharide chain as the hydrophilic core and a hydrophilic O-antigenic polysaccharide side chain (Sigma-Aldrich, 2013c). LPS stimulates cells of the innate immune system by Toll-like receptor 4 (TLR4) (Dement o et al., 2009).

Lipopolysaccharides from salmonella enterica serotype abortus equi (LPS) and fluorescein isothiocyanate labeled lipopolysaccharide (FITC-LPS) were obtained from Sigma Aldrich (Munich, Germany). LPS was used to formulate PLGA-nanoparticles with surface adsorbed LPS (LPS-NP). These nanoparticles were used as adjuvants in in-vivo studies for this work. LPS was substituted with FITC-LPS to quantify the amount of LPS that was adsorbed on the particles.

3.1.9 Freund's Adjuvant

Freund's Adjuvant (CFA) and Incomplete Freund's Adjuvant (IFA) were purchased from Sigma Aldrich (Munich, Germany). CFA is an emulsion that consists of heat killed and dried Mycobacterium tuberculosis, paraffin oil and mannide monooleate as the outer oil phase. The inner water phase contains the antigen, in this case OVA (Sigma-Aldrich, 2013b). IFA consists of paraffin oil and mannide monooleate and lacks the bacteria. It also forms an emulsion with an inner water phase, which contains the antigen (Williams and Mahaguna, 1998). For in-vivo study III in this work CFA and IFA were used as adjuvants. They were prepared by adding 2.5 ml of the oil phase to 2.5 ml of the water phase containing 0.01% OVA in PBS. The emulsion was formed by using an Ultra turrax® (T 10 basic Ultra turrax®, IKA®, Staufen, Germany) at 10000 rpm for 4 minutes. The resulting thick emulsion was tested by placing one drop of the emulsion on the surface of PBS. The drop of the emulsion was not allowed to disperse; if the drop disperses on the surface of PBS the emulsion is not stable and not suitable for injection.

3.1.10 Polyvinyl alcohol (PVA)

Polyvinyl alcohol (PVA) (Mowiol® 4-88, Kuraray Europe GmbH, Germany) (Fig. 49) was a gift from Kuraray Europe GmbH. PVA is a synthetic and water soluble polymer. After polymerization of vinyl acetate to polyvinyl acetate the hydrolysis of polyvinyl acetate results in PVA (Marvel and Denoon, 1938). PVA was used as a stabilizer in the outer water phase for the preparation of micro- and nanoparticles with the double emulsion method. It was also used as a surfactant for the preparation of nanoparticles with the o/w-emulsification-evaporation-method.

3.1.11 Polysorbate 20

Polysorbate 20 (Tween® 20) was purchased from Carl Roth® (Karlsruhe, Germany). Tween 20 (Fig. 50) is a polyoxyethylene sorbitan ester and has a molecular weight of 1225 g/mol. Tween 20 is a nonionic surfactant with a critical micelle concentration (CMC) of approximately

0.05 mmol/l (Zhu et al., 2011). It was used as a surfactant for the preparation of nanoparticles with the o/w-emulsification-evaporation-method.

3.1.12 Sodium dodecyl sulfate (SDS)

Sodium dodecyl sulfate (SDS) (Fig. 51) was obtained from Sigma Aldrich (Munich, Germany): SDS is an anionic surfactant with a molecular weight of 288 g/mol and a CMC of 8 mmol/l (Fuguet et al., 2005). It was used as a surfactant for the preparation of nanoparticles with the o/w-emulsification-evaporation-method and to linearize proteins in the polyacrylamide gel electrophoresis (SDS-PAGE).

3.1.13 Sodium cholate

Sodium cholate (Fig. 52) was purchased from Sigma Aldrich (Munich, Germany). Sodium cholate is an anionic surfactant with a molecular weight of 431 g/mol and a CMC of approximately 12 mmol/l (Sigma-Aldrich, 2013a). It was used as a surfactant for the preparation of nanoparticles with the o/w-emulsification-evaporation-method.

3.1.14 Cetyltrimethylammonium bromide (CTAB)

Cetyltrimethylammonium bromide (CTAB) (Fig. 53) was purchased from Carl Roth® (Karlsruhe, Germany). CTAB is a cationic surfactant with a molecular weight of 364 g/mol and a CMC of approximately 0.9 mmol/l (Zdziennicka et al., 2012).It was used as a surfactant for the preparation of nanoparticles with the o/w-emulsification-evaporation-method.

3.1.15 Nile red

Nile red was purchased from Sigma Aldrich (Munich, Germany). Nile red has a molecular weight of 318 g/mol. It is a lipohilic fluorescent stain that has an excitation wavelength of 544 nm and that emits at 615 nm in ethanol (Greenspan et al., 1985). Nile red was used to stain nanoparticles that were further used in cell culture experiments.

3.1.16 Dithiothreitol (DTT)

Dithiothreitol (DTT) was obtained from Carl Roth® (Karlsruhe, Germany). It has a molecular weight of 154 g/mol. DTT is a reducing agent. It was used in combination with SDS for quantification of adsorbed protein. DTT reduces disulfide bonds of the protein and SDS linearizes the protein (Wu and Narsimhan, 2008). Furthermore, SDS causes the protein to desorb from the particle surface as it replaces the protein on the surface (Crotts and Park, 1997).

3.2 Oil-in-water-emulsification-evaporation method

Biodegradable polymers, such as PLGA, can be used to prepare polymeric nanoparticles (Gurny et al., 1981). For the purpose of preparing protein loaded nanoparticles an oil-in-water-emulsification-evaporation-method (Fig. 6) was used as previously described (Vauthier and Bouchemal, 2009; Wachsmann and Lamprecht, 2012). First an oil-in-water emulsion was formed. PLGA (20 mg/ml- 100 mg/ml) dissolved in ethyl acetate acted as the oil phase. The outer water phase contained a surfactant (Table 6).

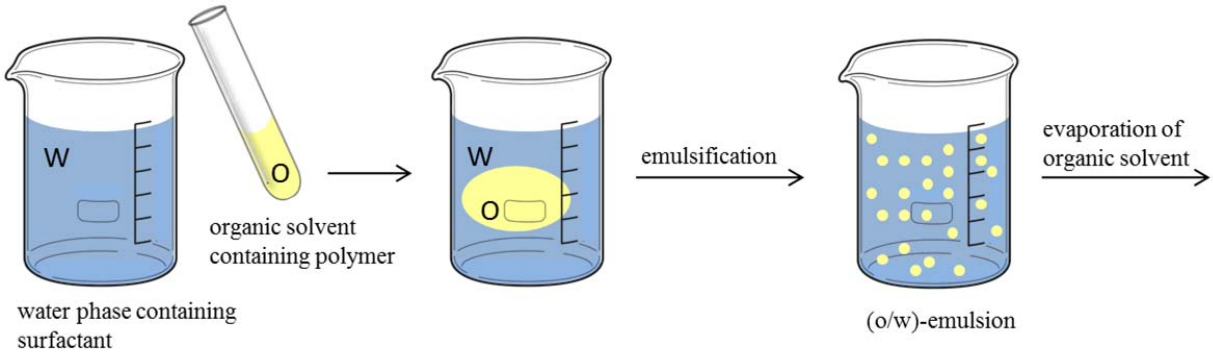

Fig. 6: *Schematic presentation of nanoparticle preparation using an oil-in-water emulsification evaporation method*

The organic phase was emulsified with the outer water phase by ultrasound using a Sonopuls HD 2200 sonicator (Bandelin electronic, Germany). The organic solvent of the resulting o/w-emulsion was then removed using a rotary evaporator at 45 °C under reduced pressure. The water insoluble PLGA precipitated as nanoparticles (o/w-NP).

Table 6: *Surfactants used for the preparation of polymeric nanoparticles loaded with proteins*

Surfactant	Concentration [g/100 ml]
PVA	1; 0.3; 0.1
Tween 20	1; 0.3; 0.1
Sodium cholate	0.1; 0.05; 0.01
SDS	0.1; 0.05; 0.01
CTAB	0.1; 0.05; 0.03; 0.01

3.2.1 Preparation of nanoparticles with adsorbed proteins

Polymeric nanoparticles that were prepared as described previously (3.2) were incubated with a protein solution (BSA, OVA or Lysozyme) in various concentrations (0.1 mg/ml – 2 mg/ml) for 3 hours on a horizontal shaker (Edmund Bühler, Tübingen, Germany). Nanoparticles that were incubated with α-toxin were freeze-dried (see section 3.4) before incubation with the protein solution.

3.2.2 Preparation of LPS loaded nanoparticles

LPS loaded polymeric particles were prepared by an oil-in-water-emulsification-evaporation-method as described above (see section 3.2). PLGA (10 mg/ml) dissolved in ethyl acetate acted as the oil phase. LPS (1 mg/ml) was used in the outer water phase and no surfactant was necessary for the preparation of nanoparticles.

3.3 Water-in-oil-in-water double emulsion method

For the preparation of protein loaded micro- and nanoparticles a double-emulsion method (Fig. 7) was performed as previously described (Buske et al., 2012; Cho and Sah, 2005; Okada et al., 1988). Briefly, the protein was dissolved in PBS (w_1-phase) and emulsified in an organic solvent containing dissolved PLGA (o-phase). This water-in-oil (w_1/o) primary emulsion was emulsified into the outer water phase (w_2) containing PVA as a stabilizer and a water-in-oil-in-water double-emulsion is formed (w_1/o/w_2). The organic solvent was removed by extraction (solvent extraction method) with water and evaporation of the organic solvent at room temperature or the organic solvent was removed by using a rotary evaporator (solvent evaporation method). The precipitating particles were then either filtrated using a cellulose acetate membrane filter (2.7 µm, Whatman, United Kingdom) or centrifuged using a Hermle Z 233 M-2 (Hermle Labortechnik, Wehingen, Germany) at 19000 rpm for 20 min. and dried overnight in an exsiccator.

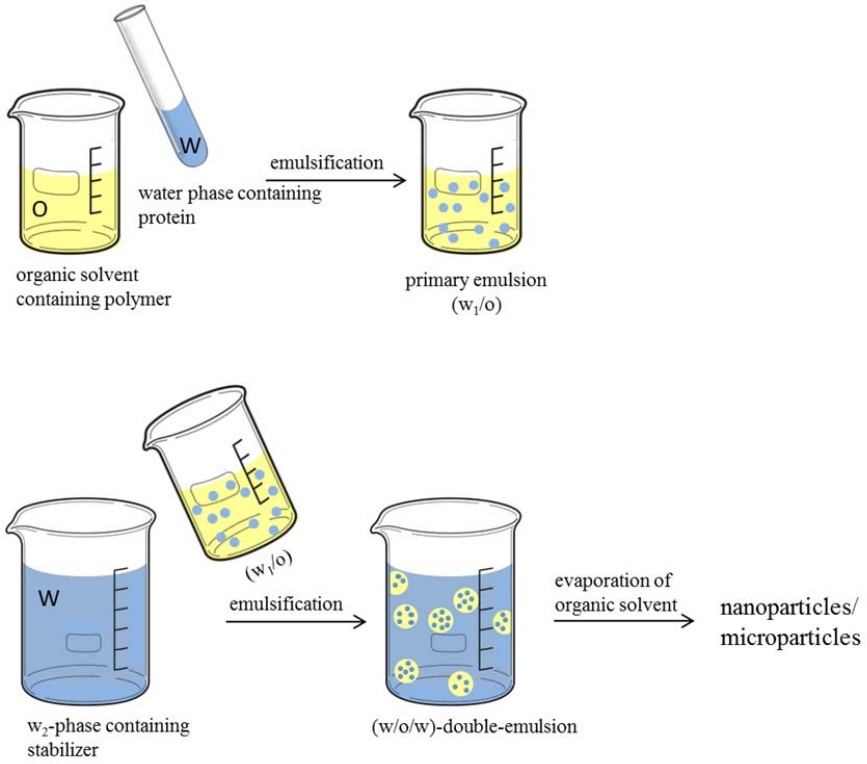

Fig. 7: *Scheme of double emulsion method*

3.3.1 Preparation of protein loaded microparticles

PLGA microparticles were prepared by a double emulsion method as described above (see 3.3). BSA dissolved in PBS (w_1) was used as a model protein (10 mg/ml). PLGA in various concentrations was dissolved in ethyl acetate (33.3 mg/ml - 83.3 mg/ml) and the primary emulsion was generated by using ultrasonication or an Ultra turrax® (T 10 basic Ultra turrax® or T 18 Ultra turrax®, IKA®, Staufen, Germany) at varying speeds for 30 seconds. The w_1/o-emulsion was emulsified in PVA (0.1% - 1% (m/V)) using a propeller stirrer (IKA® RW 20 digital, IKA®, Staufen, Germany) at varying speeds (500 rpm - 1000 rpm) for 2 minutes. Then, water was used to extract ethyl acetate and the formulation was stirred for 2 h to evaporate the organic solvent. The resulting microparticle suspension was then filtrated and dried overnight in an exsiccator.

3.3.2 Preparation of protein loaded nanoparticles

PLGA nanoparticles (w/o/w-NP) were prepared by a double emulsion technique (Fig. 7) (Blanco and Alonso, 1997; Lamprecht et al., 1999; Zambaux et al., 1998). BSA dissolved in PBS (w_1) was used as a model protein (10 mg/ml). PLGA was dissolved in ethyl acetate or methylene chloride (33.3 mg/ml) and the primary emulsion was generated by using a Sonopuls HD 2200 sonicator (Bandelin electronic, Germany) for 90 seconds. The w_1/o-emulsion was emulsified in PVA (0.1%-5% (m/V)) using ultrasonication for 60 seconds. The organic solvent was removed under reduced pressure at 45 °C for 20 minutes which led to the precipitation of nanoparticles (w/o/w-NP). For imaging studies of the cross-section of the nanoparticles (see 3.5.7) BSA was substituted with Gold-BSA.

3.4 Freeze drying of nanoparticles

For stability studies of the nanoparticles that were loaded with the α-toxin, nanoparticles were freeze dried using a Lyovac® GT2 (Steris, Germany). Trehalose (5% (m/V)) was added to the nanoparticle formulation as a cryoprotectant.

3.5 Analytical methods

3.5.1 Particle size analysis

3.5.1.1 Photon Correlation Spectroscopy (PCS)

Particle size and polydispersity index (PDI) of nanoparticles were determined by photon-correlation spectroscopy (PCS) using a ZetaPlus particle sizer (Brookhaven Instruments Corporation, UK) at a fixed angle of 90 ° at 25 °C. 100 µl of the nanoparticle sample was diluted with water in a UV-Cuvette macro (Brand GmbH, Germany). Each sample was measured in triplicates. Each measurement consisted of 5 runs with a duration of 1 min. each. The analysis was done using the Brookhaven Instruments Particle Sizing Software Version 3.88.

3.5.1.2 Laser diffraction

The particle size and the particle size distribution of microparticles were determined by laser diffraction analysis using a Helos 12 KA/ LA (Sympatec, Clausthal-Zellerfeld, Germany) equipped with a helium-neon laser. The measurement is based on the concept that particles of a certain size diffract light through a given angle and intensity. The angle increases when the particle size decreases (McCave et al., 1986), and the intensity increases when the particle size increases. The diffraction pattern is detected and the particle size distribution can be generated. The analysis was performed with the Windox Software Version 3.4 (Sympatec, Clausthal-Zellerfeld, Germany) and the measured laser diffraction pattern was evaluated by the Fraunhofer diffraction model. Briefly, 10 mg of dried microparticle sample was suspended in 40 ml 0.2% Polysorbate 80 and aggregates were separated using ultrasonication. One ml of the suspended sample was deposited into a glass cuvette containing 40 ml of an aqueous 0.2 % Polysorbate 80 solution and a magnetic stirrer that operated at 50%. Each sample was measured in triplicates.

3.5.2 Encapsulation/loading-rate of protein

The loading rate of the o/w-NP and w/o/w-NP with the model proteins BSA and OVA was determined using a BCA-Assay. The NP-samples were centrifuged at 19000 rcf for 15 minutes and the supernatant was collected and measured by a BCA-Assay. Thus, an indirect quantification of the protein content was performed. The encapsulation rate of the microparticle samples were also measured indirectly. After filtration of the obtained microparticle suspension, the protein content of the filtrate was investigated using a BCA-Assay. The loading rate of the o/w-NP with the α-toxin was handled as the o/w-NP samples with BSA and OVA. However, the supernatant was not examined by BCA-Assay, but SDS-PAGE gel electrophoresis (see 3.5.2.2).

3.5.2.1 BCA-Assay

Protein contents of the micro- and nanoparticle samples were measured by a BCA-Assay (Roti-quant universal assay, Carl Roth®, Germany). Cu^{2+} ions are being reduced to Cu^{1+} ions by

protein bonds (Lowry et al., 1951). The principle of the BCA-Assay is that bicinchoninic acid forms an intense purple complex with cuprous ions (Cu^{1+}) in alkaline environment (Smith et al., 1985). 100 µl of the samples and standards were placed in a 96-well plate (PerkinElmer, Waltham, USA) and mixed with 100 µl of reagent solution of the BCA-Assay Kit. After incubation at 37 °C for 30 minutes the absorbance was measured at 490 nm using a plate reader (1420 Multilabel Counter Victor3 V, PerkinElmer, USA).

3.5.2.2 SDS-PAGE gel electrophoresis

To quantify the α-toxin content on the o/w-NP a SDS-polyacrylamide gel electrophoresis (PAGE) was performed. SDS-PAGE is widely used to separate proteins according to their molecular weight (Laemmli, 1970; Schagger and von Jagow, 1987). The samples were mixed with "Laemmli-buffer" containing SDS to linearize the protein and additionally to apply a negative charge to each protein. The buffer also contained glycerol to increase the density of the sample and Bromphenol blue as a tracking dye. The sample was further heated to 95 °C for 5 minutes using a heating block (Thermomixer® comfort, Eppendorf®, Germany) and 2-mercaptoethanol was added to reduce disulfide linkages. SDS-PAGE was performed using a MINI-PROTEAN®-system (Bio-Rad Laboratories, USA). The self-prepared separating gels had an acrylamide content of 12% and the stacking gels had an acrylamide content of 4%. Polymerization was initiated by adding ammonium persulfate and tetramethylethylenediamine. After adding the samples to the gels an electric field was applied, which led to the negatively charged proteins migrating to the positive electrode (anode). The gel was run for 2 h at 20 mA. The gels were then stained with Coomassie Brilliant Blue for 8 h and bleached with water, methanol and acetic acid afterwards. To calculate the protein content, α-toxin samples with a known concentration were used as a standard. Further a marker (Roti®-Mark Standard, Carl Roth®, Germany) was used to estimate the molecular weight of the separated proteins. To quantify the α-toxin content the stained gels were placed on a reflecta® L 300 light panel (Intas Science Imaging Instruments GmbH, Göttingen, Germany) and photographed with an Intas® camera system (Intas Science Imaging Instruments GmbH, Göttingen, Germany) and then a densitometric analysis was put out with ImageJ analysis system.

3.5.3 Release test

The in-vitro dissolution tests were all carried out in PBS. A defined amount of the dried microparticle sample was suspended in a conical flask with PBS. The conical flask was incubated in a shaking water bath (GFL, Burgwedel, Germany) at 37 °C at 80 rpm. Samples were withdrawn at various times for the analyses of drug release. The protein content was determined as described above. The in-vitro dissolution tests of the nanoparticle samples were carried out in Eppendorf cups. 100 µl of nanoparticle suspension was mixed with 900 µl of PBS. Samples were withdrawn at various times for the analyses of drug release. The protein content was determined as described above.

3.5.4 Zeta potential

The measurement of the zeta potential was carried out using a ZetaPlus particle sizer (Brookhaven Instruments Corporation, UK). The analysis was done using the Brookhaven Instruments Zeta Potential Analyzer Software Version 3.54.

3.5.5 Drop shape analysis

The surface tension of protein and surfactant samples was measured using an Easy Drop FM 40 (Krüss, Hamburg, Germany).

After the samples were dissolved in various concentrations in water, a drop was formed using a syringe. This drop was further visualized with the camera of the Easy Drop FM 40. Using the Drop Shape Analysis Software (Krüss, Hamburg, Germany) the surface tensions was determined by the Young-Laplace-Equation (Eq. 1) (Lin et al., 1995). The “pendant drop method” was applied to measure the samples. For the measurement of interfacial tensions between methylene chloride and a water phase containing various samples the drop was injected into a glass vial containing methylene chloride.

$$\delta p = \sigma \times \left(\frac{1}{r_1} + \frac{1}{r_2}\right)$$

Eq. 1: p = Laplace pressure

σ = surface tension

r_1 = radius of curvature r_1

r_2 = radius of curvature r_2

3.5.6 Scanning electron microscopy (SEM)

To investigate the morphology of micro- and nanoparticles SEM was used. The images were also used to confirm the findings regarding the particle size of micro- and nanoparticles. Before examining the sample in the SEM, a thin layer of gold was coated on the sample to prevent electrostatic charge at the surface (Rein, 2010). The samples in this work were attached to the sample carrier with double adhesive tape. Therefore, dried microparticles were simply put on the double adhesive tape. However, for the nanoparticle samples, one drop of the nanoparticle suspension was put on a cover slip and dried overnight. Afterwards, the cover slip was put on the double adhesive tape. Then the samples were coated with gold using a Polaron Sputter Coater (SC 7640, Quorum Technologies Ltd., UK) for 6 min. (microparticles) or 2 min. (nanoparticles). Afterwards, the samples were fixed at a sample table and put into the SEM (S 2460 N, Hitachi, Japan). The samples were investigated at various magnifications at 15 kV acceleration voltage, using a secondary electron detector.

3.5.7 Field emission-scanning electron microscopy (FE-SEM) coupled with ion milling

The FE-SEM was used to investigate the morphology of nanoparticles. The experiments were conducted at the Hitachi facility in Krefeld. The preceding ion milling was used to cut the

nanoparticles with an ion beam to examine the interior morphology afterwards in the FE-SEM. Due to the high accelerating voltages used in SEM, the specimen can be damaged (Jongebloed et al., 1999). Furthermore, charging of the specimen increases with high accelerating voltages (Kim et al., 1992). The FE-SEM produces images using very low accelerating voltages (≤ 5kV). Coating therefore becomes unnecessary, because the conductivity of the specimen is less important (Dunnebier et al., 1995) and less beam induced damage can be observed (Kim et al., 1992). The electrons were emitted by a field emission electron gun. In this work a cold field emission source as a cathode was used. Here, we analyzed the w/o/w-NP with a SU8030 (Hitachi, Tokyo, Japan) after ion milling with an IM4000 (Hitachi, Tokyo, Japan). One drop of the w/o/w-NP sample was put on a silicium plate and dried overnight. The silicium plate was then scratched with a diamond scriber and fractured in several pieces. A piece with a beveled edge was put in the IM4000 with the sample facing downwards and a mask on top of the silicium plate (Fig. 8). The IM4000 was then cooled down with liquid nitrogen to -100 °C. Afterwards an argon beam (4 keV) cut the sample for 40 min. at an ion current of 140 µA. The sample was then recovered from the ion milling machine and investigated in the FE-SEM at 0.5-1 kV using various magnifications. A secondary electron detector, a low angle backscattered electron detector or a combination of the two detectors was used to visualize the signals emitted by the sample.

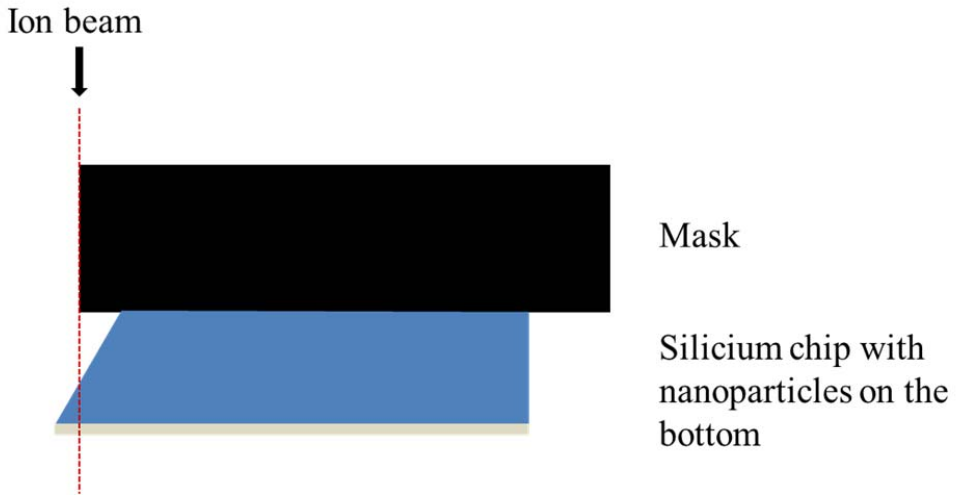

Fig. 8: *Schematic layout of ion milling process*

3.5.8 Confocal laser scanning microscopy (CLSM)

Using CLSM images of specimens at selected depths can be acquired, making it possible to visualize interior structures (Nikon, 2014). By using different fluorescent labels multiple compounds can be determined with CLSM (Lamprecht et al., 2000a). The location of Nile red nanoparticles in macrophages was investigated using CLSM. The staining of the nanoparticles and macrophages was performed as described by Wachsmann and Lamprecht (Wachsmann and Lamprecht, 2012). Briefly, 200000 macrophages were seeded and incubated for 24 h in a 24-well plate containing cover slips. After the removal of the medium 500 µl of Nile red nanoparticles (0.1 mg*ml^{-1}) were then incubated with the cells for 2 h at 37 °C. After washing with 500 µl PBS twice, the cells were kept at 4 °C for 30 minutes. Afterwards, the PBS was removed the cells were incubated with 500 µl concanavalin A (0.1 mg*ml^{-1}) for 5 min. at 4 °C to stain the cell membrane. After washing with PBS twice, cells were fixed with 200 µl formaldehyde solution (4%) for 10 min. at room temperature. After washing with PBS twice the cells were incubated with 200 µl 4',6-diamidino-2-phenylindole (DAPI, 300 nM) for 5 min. to stain the cell nuclei. The cells were washed with PBS and after removal of the PBS the cover slips were put on a microscope slide to further examine the cells via CLSM. A Nikon Eclipse Ti A1 (Nikon Corporation Inc., Tokyo, Japan) was used to investigate the location of Nile red nanoparticles in the macrophages. The examination was performed using various magnifications. In order to see all three fluorescent labeled compounds (nanoparticles, cell membrane, cell nuclei) the excitation wavelength of the laser was set on 405 nm, 488 nm and 543 nm. The fluorescence signals were collected using a filter of 450/525/640 nm. To avoid elevated signals a control sample without Nile red nanoparticles was examined.

3.5.9 Calculation of surface area of nanoparticles

The surface area was calculated as explained in the following. The mass of a single particle was determined by multiplication of the volume of the particle and the density. A density of 1.2 g/cm^3 was used (Cu and Saltzman, 2008). The amount of particles was then calculated by dividing 1 g by the mass of one particle. The number of particles was then multiplied with the surface area of a single particle to obtain the surface area of 1 g w/o/w-NP.

3.6 Cell culture

To investigate the different o/w-NP formulations in regard to toxicity and cell uptake, cell culture experiments were used. Cell culture experiments cannot simulate the complexity of an immune system of an animal, but it does allow for a comparison among the different formulations (Nicolete et al., 2011; Treuel et al., 2013). Here, the toxicity, the cell uptake and the location of the o/w-NP in the cells were determined. The resuscitation, sub cultivation and cryopreservation of the RAW 264.7 cell-line was conducted as previously described (Schmitz, 2011).

3.6.1 Macrophages

The cell culture experiments were performed with a macrophage cell line (RAW 267.4). The cells were kindly provided by the pharmaceutical institute of Besancon (Pharmaceutical Technology and Biopharmaceutics). The cell line has been established from murine tumors induced with Abelson leukemia virus (Raschke et al., 1978). This mouse-derived cell line (BALB/c) exhibits adherent growth (ATCC, 2014).

A hemocytometer (Neubauer Chamber) was used to count the cells. The hemocytometer is a glass slide with a rectangular indentation in the middle that creates a chamber. First, the cover slip was properly positioned on the surface of the hemacytometer. 200 µl of the cell suspension was then added to the chamber, due to capillary effects the chamber gets completely filled with the cell suspension. The number of cells was then counted using a microscope (Motic AE21, Wetzlar, Germany). The cells on the 4 large squares, with each square consisting of small 20 squares, were counted (Fig. 9). The volume of one large square is 0.1 mm^3. The concentration of the cells was calculated as follows:

$$A \times V \times 10^4 = Number\ of\ cells\ in\ entire\ volume$$

Eq. 2: *A = mean of counted cells in 4 large squares*

V = volume in which cell pellet was resuspended

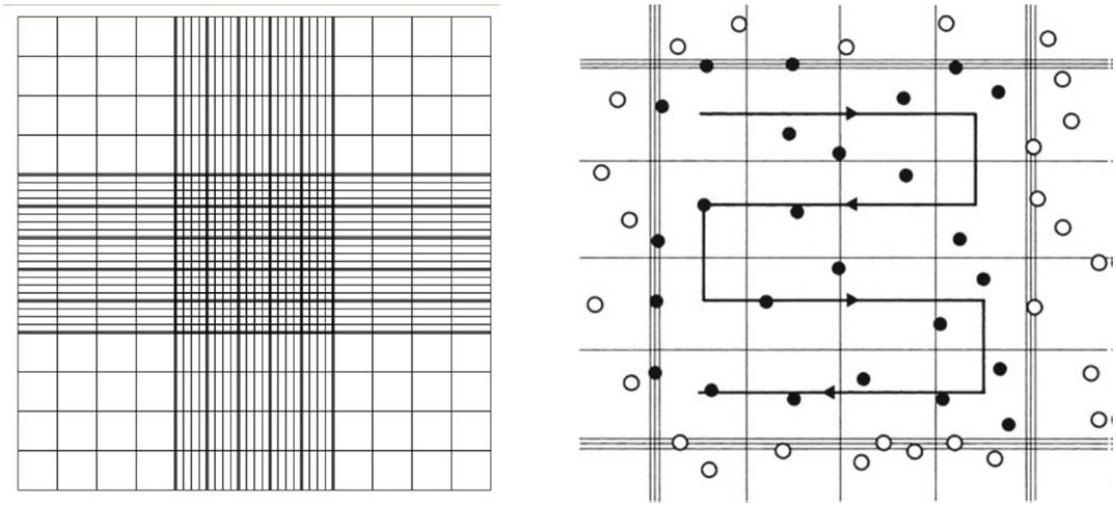

Fig. 9: *Hemacytometer grid (left) and counting method (right)*

3.6.2 Cell culture experiments

The toxic effects of the o/w-NP on macrophages were tested using a MTT-assay. The cell uptake and the location of the o/w-NP were investigated using Nile red nanoparticles. Here, Nile red was added during the preparation of the o/w-NP. 1 mg of Nile red was dissolved in 1 ml ethyl acetate. 100 µl of this solution was added to the organic phase during the preparation of the o/w-NP which resulted in a final concentration of 10 µg/ml Nile red in the nanoparticle formulation.

3.6.2.1 MTT assay

The MTT-assay was used to determine the toxicity of nanoparticles on macrophages. It is based on the principle that 3-(4,5-dimethylthiazol-2-yl)-2,5-diphenyl tetrazolium bromide (MTT) is reduced to its corresponding insoluble purple colored formazan in living cells (Mosmann, 1983). It was shown that the cofactors NADH and NADPH play an important role in the reduction of MTT (Berridge and Tan, 1993). The MTT reduction does not only occur in mitochondria, but also the cytoplasm and membranes including endosome, lysosome and the plasma membrane (Berridge et al., 2005). The assay was used to investigate the toxicity of the different o/w-NP formulations and to determine the concentration in which the o/w-NP formulation can be used for further studies without harming the cells. 100000 cells/well were seeded in a 96-well plate and incubated for 24 h at 37 °C and 5% CO_2 in an incubator. After 24 h the medium was removed and 200 µl of different concentrations (3 mg/ml; 1 mg/ml; 0.3 mg/ml; 0.1 mg/ml; 0.03 mg/ml) of the o/w-NP were added into the wells. PBS was used as a control. After 8 h of incubation at 37 °C and 5% CO_2 the wells were washed two times with PBS. Then 20 µl of MTT (5 mg/ml) and 180 µl of medium were added and again incubated for 2 hours. Then the medium was carefully withdrawn without syphoning off any formazan crystals. A mixture of DMSO, acetic acid and SDS (99.4 ml/0.6 ml/10 g) was then added to dissolve the formazan crystals. The amount of formazan was determined photometrically at 570 nm using a plate reader (1420 Multilabel Counter Victor3 V, PerkinElmer, USA).

3.6.2.2 Uptake of Nile red nanoparticles into macrophages

Nanocarriers can be internalized by mammalian cells via different pathways, e.g. phagocytosis, clathrin-mediated endocytosis, caveolae-mediated endocytosis, macropinocytosis or other clathrin- and cavoelae- independent endocytosis (Hillaireau and Couvreur, 2009). It was already reported, that the internalization can be dependent on size (Gaumet et al., 2009) and surface properties (Foged et al., 2005; Wachsmann et al., 2013). In the present work, we determined the quantitative cell interaction between macrophages and Nile red nanoparticles. 100000 cells/well were seeded in a 96-well plate and incubated for 24 h at 37 °C and 5% CO_2 in an incubator. After 24 h the medium was removed and 200 µl of the Nile red nanoparticle formulations (0.1 mg/ml)

was added to the wells. The plates were then incubated for various amounts of time (0.5 h; 1 h; 2 h; 4 h; 6 h; 8 h). PBS was used as a control. When the incubation was done, the supernatant was removed and the wells were washed with PBS to get rid of any nanoparticles that were not internalized. The fluorescent dye was then extracted by adding 200 µl of ethanol. The 96-well plate was agitated and the fluorescence was measured using a plate reader (1420 Multilabel Counter Victor3 V, PerkinElmer, USA) at 544 nm/615 nm.

3.7 In vivo experiments

The immune response of the o/w-NP and the LPS-NP was determined by animal experiments using BALB/c mice. As a model protein OVA was used. This is a well-established in-vivo model to simulate adjuvant effects (Demento et al., 2009; Gutierro et al., 2002b; Kasturi et al., 2011).

3.7.1 BALB/c mouse

The BALB/c mice were purchased from Charles River (Sulzfeld, Germany). The BALB/c mouse is an albino and laboratory bred strain. All experiments were carried out in the "Haus für Experimentelle Therapie" (HET) in Bonn. The mice were 4 weeks old and weighed 25-35 g. Only male mice were used. The animal trial began after an acclimation period of seven days. The mice were fed with autoclaved standard food (ssniff, Soest, Germany) and water ad libitum. 3-5 mice were kept in one cage and the cages were changed once a week. Individually Ventilated Cages (IVCs) were used in this study. The cages were kept in a room with a temperature of 22 °C and an overpressure of 150 Pa. The relative humidity was approximately 50-60%.

3.7.2 Study outline

The influence of OVA loaded carriers was investigated using a mouse-model. Therefore, five in-vivo studies were conducted. The immune response of nanoparticles and different adjuvant formulation was tested. PLGA particles have already shown that they can have an effect on the

immune response (Gutierro et al., 2002a; Waeckerle-Men and Groettrup, 2005). In the presented work, we investigated different adjuvant formulations (in-vivo study III) and the effect of different o/w-NP formulations (in-vivo study I-II and IV-V). For all in-vivo trials the animals were immunized two times and blood samples were drawn three (in vivo study III-V) or four times (in vivo study I-II) (Fig. 10).

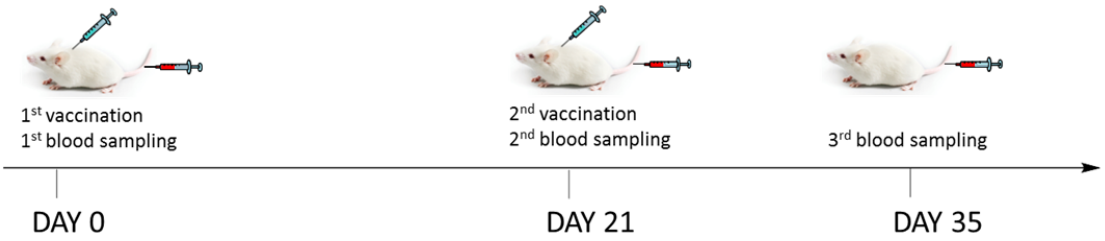

Fig. 10: *Study outline of in vivo studies with BALB/c mice*

All animal experiments started with marking the mice. Therefore, an ear puncher that was kindly provided by the HET was used. Depending on the number of mice in one cage, either 4 mice or 2 mice were marked.

The immunization was performed subcutaneously in the neck using a 23 G needle (B. Braun, Melsungen, Germany) on study day (SD) 0 and on SD 21. The OVA solution or nanoparticle formulation was drawn up in the syringe and 100 µl was injected in each mouse. The needle was always changed for each mouse. The blood withdrawal from the tail was done using a 22 G needle (B. Braun, Melsingen, Germany) and micro haematocrit tubes (Brand, Wertheim, Germany). Approximately 50-100 µl blood was drawn and put in an Eppendorf cup, while the mouse was fixed in a restrainer. The blood was stored at room temperature for approximately one hour. Then it was stored at 4 °C for 24 hours. Afterwards, it was centrifuged at 19000 rcf for 15 min. using a Hermle Z 233 M-2 (Hermle Labortechnik, Wehingen, Germany). Then approximately 10-20 µl of the blood serum (supernatant) was collected and stored at -20 °C.

The injection site of the animals was monitored daily after the subcutaneous injection for three days and then once a week. Several abort criteria were set to guarantee minimal distress for the

animals (GV-SOLAS, 2009). If any of the following signs were observed, the experiment with this animal was terminated by euthanizing:

a) abnormal body posture
b) loss of mobility
c) visible inflammations
d) weight loss ≥ 20%

3.7.2.1 Carbopol and ovalbumin loaded nanoparticles in mice

In the first two in-vivo studies the immune response of OVA loaded PVA (1%)-NP and OVA loaded Tween (1%)-NP was investigated (Table 7 and

Table 8). Six groups containing 4-5 mice were tested. Carbopol was used as an adjuvant (0.1% w/v) and the OVA concentration was 10 µg per dose in all groups. To see the effect of the adjuvant Carbopol, three groups were immunized with addition of Carbopol and three groups had no Carbopol. PBS with Carbopol and PBS without Carbopol were used as a control to see the effect of the PVA-NP and the Tween-NP. The blood samples were taken on SD 0, SD 21, SD 35 and SD 42.

Table 7: *Experimental groups – in vivo study I*

Group	Formulation	Ovalbumin	Adjuvant	Number of mice
I	Tween 20 (1%)-NP	10 µg	100 µg Carbopol	5
II	Tween 20 (1%)-NP	10 µg	-	4
III	PVA (1%)-NP	10 µg	100 µg Carbopol	5
IV	PVA (1%)-NP	10 µg	-	4
V	PBS	10 µg	100 µg Carbopol	4
VI	PBS	10 µg	-	4

Table 8: *Experimental groups – in vivo study II*

Group	Formulation	Ovalbumin	Adjuvant	Number of mice
I	Tween 20 (1%)-NP	10 µg	100 µg Carbopol	5
II	Tween 20 (1%)-NP	10 µg	-	5
III	PVA (1%)-NP	10 µg	100 µg Carbopol	5
IV	PVA (1%)-NP	10 µg	-	5
V	PBS	10 µg	100 µg Carbopol	5
VI	PBS	10 µg	-	5

3.7.2.2 In vivo testing of different Adjuvants

In the third animal experiment (Table 9) different adjuvant formulations were tested in regard to the immune response. The OVA concentration was 10 µg per dose in all groups. PBS with OVA acted as a control group. The second group contained OVA and CFA for the first immunization and IFA for the second immunization. The adjuvant protein emulsion was formed as described above (3.1.9). This group acted as a positive control, since the intense immune response in mice after the administration of CFA is widely known (Aucouturier et al., 2001; Schnare et al., 2001; Singh and O'Hagan, 2003). The third group and fourth group were the experimental groups. Here we compared the immune response of LPS-NP combined with CpG with soluble LPS combined with CpG. Since CFA and IFA are highly toxic and dangerous, the mice in this group were anesthetized with isofluran (Forene®, Abbott, Germany) during the immunization. The blood withdrawal took place on SD 0, SD 21 and SD 35.

Table 9: *Experimental groups – in vivo study III*

Group	Formulation	Ovalbumin	Adjuvant	Number of mice
I	PBS	10 µg	-	5
II	PBS	10 µg	CFA/IFA (50%)	6
III	LPS (1 µg)-NP	10 µg	5 µg CpG	6
IV	PBS	10 µg	5 µg CpG; 1 µg LPS	5

3.7.2.3 Lipopolysaccharide loaded nanoparticles and ovalbumin loaded nanoparticles in mice

In the fourth in-vivo study (Table 10) the effect of five different o/w-NP formulations on the immune response was tested. The OVA concentration was 10 µg per dose in all groups and LPS-NP (LPS concentration 1 µg per dose) coupled with CpG (5 µg per dose) was used as an adjuvant in all groups. The first group was the control group, containing free OVA and the adjuvant formulation. The eighth group was also a control group, containing free OVA without the adjuvant formulation. The other groups were the experimental groups. OVA was loaded on nanoparticles as described above (see 3.2.1). The resulting nanoparticle formulations were tested. Group II contained the Tween 20 (1%)-NP, Group III the PVA (1%)-NP, Group IV the Sodium cholate (0.05%)-NP, Group V the SDS (0.01%)-NP and Group VI the CTAB (0,05%)-NP. The blood withdrawal was on SD 0, SD 21 and SD 35.

Table 10: *Experimental groups – in vivo study IV*

Group	Formulation	Ovalbumin	Adjuvant	Number of mice
I	LPS-NP	10 µg	LPS (1 µg)-NP; 5 µg CpG	6
II	Tween 20 (1%)-NP	10 µg	LPS (1 µg)-NP; 5 µg CpG	6
III	PVA (1%)-NP	10 µg	LPS (1 µg)-NP; 5 µg CpG	6
IV	Sodium cholate (0.05%)-NP	10 µg	LPS (1 µg)-NP; 5 µg CpG	6
V	SDS (0,01%)-NP	10 µg	LPS (1 µg)-NP; 5 µg CpG	5
VI	CTAB (0,05%)-NP	10 µg	LPS (1 µg)-NP; 5 µg CpG	6
VII	PBS	10 µg	-	6

3.7.2.4 Influence of nanoparticle concentration on immune response in mice

In the fifth in-vivo study (Table 11) the effects of the nanoparticle concentration on the immune response was investigated. An OVA solution in PBS coupled with LPS-NP (LPS concentration 1 µg per dose) and CpG (5 µg per dose) was used as an adjuvant in all groups, including the control group. The nine experimental groups had all the same amount of OVA in their formulation (10 µg per dose). CTAB (0,05%)-NP, Tween 20 (1%)-NP and PVA (1%)-NP were tested in different concentrations. The particles were prepared as described before (see 3.2.1) with slight deviations. Briefly, the PLGA amount was changed (100 mg/ml and 4 mg/ml instead of 20 mg/ml) and the sonication duration was adjusted, in order to obtain comparable nanoparticle sizes. The blood withdrawal was performed on SD 0, SD 21 and SD 35.

Table 11: *Experimental groups – in vivo study V*

Group	Formulation	PLGA concentration [mg/ml]	Adjuvant	Number of mice
I	LPS-NP	-	LPS (1 µg)-NP; 5 µg CpG	5
II	CTAB (0,05%)-NP	2	LPS (1 µg)-NP; 5 µg CpG	5
III	Tween 20 (1%)-NP	2	LPS (1 µg)-NP; 5 µg CpG	5
IV	PVA (1%)-NP	2	LPS (1 µg)-NP; 5 µg CpG	5
V	CTAB (0,05%)-NP	10	LPS (1 µg)-NP; 5 µg CpG	5
VI	Tween 20 (1%)-NP	10	LPS (1 µg)-NP; 5 µg CpG	5
VII	PVA (1%)-NP	10	LPS (1 µg)-NP; 5 µg CpG	5
VIII	CTAB (0,05%)-NP	50	LPS (1 µg)-NP; 5 µg CpG	4
IX	Tween 20 (1%)-NP	50	LPS (1 µg)-NP; 5 µg CpG	5
X	PVA (1%)-NP	50	LPS (1 µg)-NP; 5 µg CpG	5

3.7.2.5 IgG-ELISA

The blood samples of the in-vivo studies were left to thaw overnight in a fridge (-20 °C) and then measured using the Mouse Anti-Ovalbumin IgG kit from Alpha Diagnostics (San Antonio, USA). The ELISA (Fig. 11) was carried out as described in the manual (Instruction Manual No. M-600-105-OGG). Briefly, after preparing a "washing solution" as well as a solution to dilute the samples, the 96-well plate that was covered with OVA was washed using the "washing solution". Meanwhile, all samples were appropriately diluted (100-500000x). 100 µl of standards and samples were added to the plate and incubated for 60 min. to bind the IgG on the immobilized OVA on the wells. After several washing steps, 100 µl of an IgG-specific antibody conjugated with horseradish peroxidase (HRP) was added and incubated for 30 minutes. The IgG-specific antibody was bound to IgG. After several washing steps the excess of the free IgG- specific antibody conjugated with HRP was washed off. Then 100 µl of 3,3',5,5'-Tetramethylbenzidine (TMB) was added as a chromogenic substrate. The HRP reacted with the TMB to a blue colored

product. TMB was oxidized by HRP, resulting in a diimine (Veitch, 2004). By adding 100 µl sulfuric acid (1%) the TMB turned yellow. The absorbance was then measured at 450 nm using a plate reader (1420 Multilabel Counter Victor3 V, PerkinElmer, USA). The amount of mouse IgG in the samples was calculated relative to anti-ovalbumin reference calibrators. The results were indicated as IgG Antibody Activity Units ($U*ml^{-1}$).

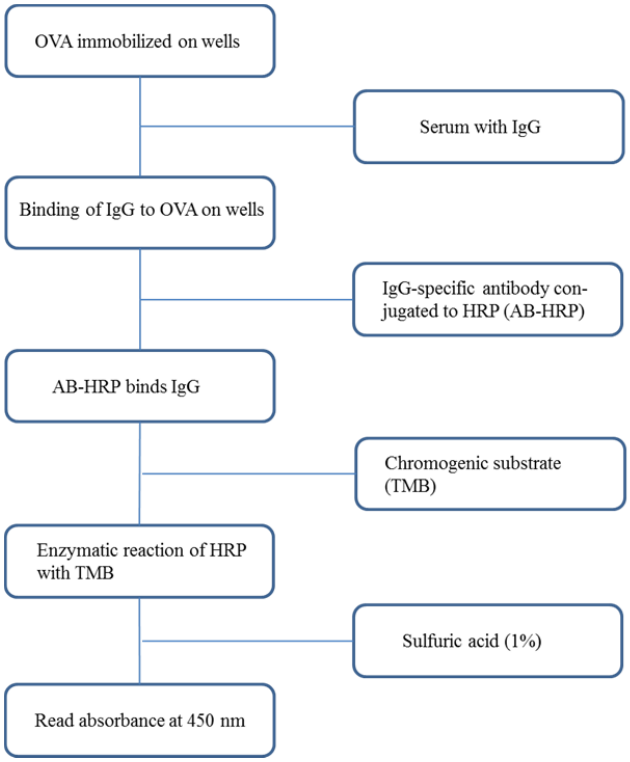

Fig. 11: *Principle of mouse anti-OVA IgG-ELISA*

3.8 Statistical analysis

The statistical analysis was carried out using Sigmastat 2.0 Software. Statistical difference was investigated by Kruskal-Wallis Anova on Ranks followed by multiple comparisons with Student Newman-Keuls test. The data was expressed as mean ± SD, $p < 0.05$ was considered to be significant.

4 Results and Discussion

4.1 Nanoparticles prepared with the double-emulsion-solvent-evaporation method

The encapsulation of hydrophilic drugs, such as proteins and peptides, into nanoparticles is challenging. The double-emulsion method is the gold-standard for this process (Bilati et al., 2005). However, there is still a lack of understanding concerning the morphology of nanoparticles, as imaging techniques used to determine the morphology only provide pictures showcasing the external structure. Mostly SEM (Gutierro et al., 2002b) or transmission electron microscopy (Khoee and Yaghoobian, 2009) were used to investigate the morphology. Basically, most analyses concerning the morphology came to the conclusion that spherical nanoparticles were obtained (Zambaux et al., 1998), conclusions about the interior morphology could not be drawn. Nevertheless, the current understanding is that the hydrophilic drug is encapsulated inside the nanoparticles when utilizing the double-emulsion method (Lamprecht et al., 2000b). This postulated structure does not comply with the findings made in this thesis. As explained in the following, the understanding regarding the structure of nanoparticles prepared by the double-emulsion method needs to be revisited.

4.1.1 Physicochemical characterization of nanoparticle properties

4.1.1.1 Influence of surfactant and organic solvent on particle size and polydispersity

Particles were prepared using various amounts of PVA in the outer water phase and BSA in the inner phase. In agreement with previous studies (Lamprecht et al., 2000b; Zambaux et al., 1998) nanoparticles could be obtained, using a double-emulsion evaporation method. Actually, also microparticles were obtained, when using less than 0.1% PVA in the outer water phase (Fig. 12).

The aim was to get nanoparticle formulations of different particle sizes for the studies regarding the interior morphology. A first approach was simply changing the concentration of PVA in the outer water phase, without varying any other parameter, e.g emulsification duration or PLGA concentration, in the production of the nanoparticles.

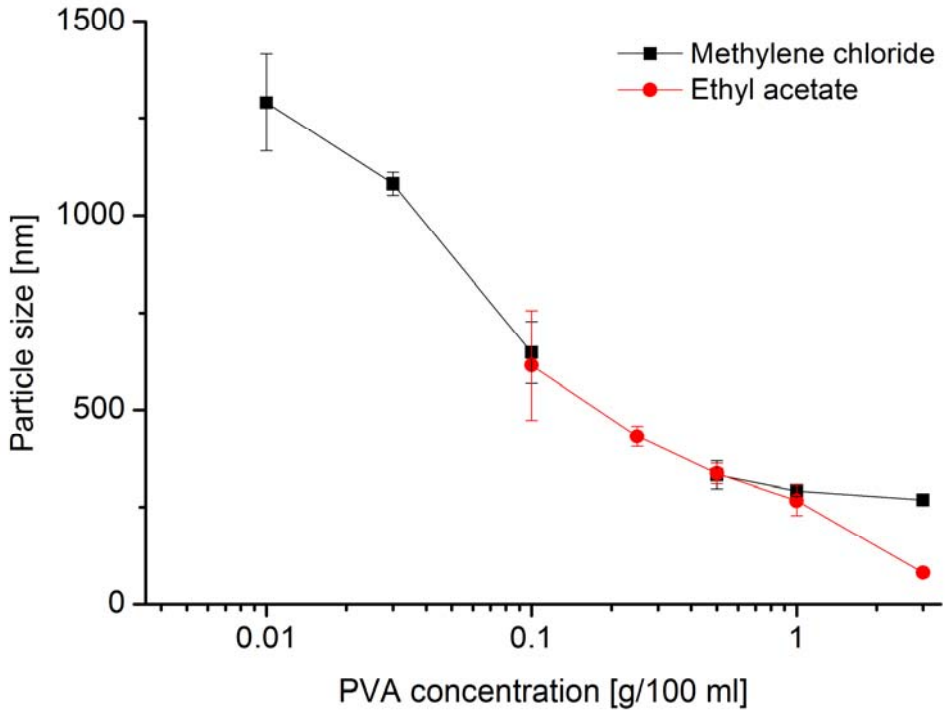

Fig. 12: *Particle size of w/o/w-NP prepared with methylene chloride or ethyl acetate at various PVA concentrations (mean diameter ± SD, n = 3)*

A higher amount of PVA has two effects: Firstly, the primary emulsion is better stabilized, due to more PVA that can stabilize the interface. Secondly, the viscosity of the outer water phase increases, thereby mechanically preventing the formed droplets from merging again. This leads to smaller particles, with increasing concentrations of PVA. However, nanoparticles could only be obtained at a PVA concentration above 0.1%. The viscosity of the continuous phase is too low and PVA does not have sufficient surfactant activity otherwise.

In regard to the mean diameter of the particles, methylene chloride and ethyl acetate showed similar results. Only at 3% PVA a significant difference could be observed.

The goal was to prepare nanoparticle formulations with different particle sizes to compare them with regard to their release profile and morphology. Instead of changing a lot of parameters, only the amount of PVA was altered to keep the set up as simple as possible.

Depending on the application, w/o/w-NP are prepared in different size ranges. If an uptake into cells is desired, smaller nanoparticles, with a mean diameter of around 200 nm showed to have an advantage over bigger particles in the sub-micron to microparticle range (Foged et al., 2005). Nanoparticles prepared by the double emulsion method that showed promising results in-vivo regarding the enhancement of an immune response were in a size range of 250 nm – 400 nm (Kasturi et al., 2011). Therefore, this size range is of particular interest, as an in-vivo success has already been reported; however, the structural morphology of the nanoparticles applied in that study was apparently not investigated. Methylene chloride was mainly used as an organic solvent in most studies (Kasturi et al., 2011; Lamprecht et al., 2000b; Zambaux et al., 1998), which is why further characterization of the w/o/w-NP was performed with particles prepared using methylene chloride. Using 0.5% PVA, nanoparticles with a mean diameter of 332 nm ± 35 nm were obtained, which lies in the desired particle size range mentioned above. Furthermore, bigger particles of 648 nm ± 80 nm were obtained, using 0.1% PVA. To determine if the particle size has an influence on the morphology and release kinetics, these w/o/w-NP types were also further characterized in that respect.

The polydispersity index is dimensionless and provides information about the size distribution. A value close to 0.005 indicates that the investigated particle collective has a monomodal size distribution. Higher values of above 0.05-0.1 indicate that the particle collective exhibits a bimodal size distribution. In the case of the w/o/w-NP that were prepared a low polydispersity index was seen for formulations that were prepared using PVA concentration up to 0.5% (Fig. 13). Higher PVA concentrations led to smaller nanoparticles that are reported to generally have bigger polydispersity indices (Zambaux et al., 1998). To lower the polydispersity index for smaller nanoparticles the double-emulsion would require stabilization with additional surfactants. Our goal was to characterize the w/o/w-NP that are usually obtained, when applying the double-emulsion method. Therefore, attempts to obtain a monomodal size distribution for nanoparticles

that were prepared with 1% PVA or even higher amounts of PVA were not made. Besides, when using 0.5% PVA, nanoparticles of around 300 nm were obtained. These nanoparticles have a monomodal size distribution and are sufficient for further characterization, making the w/o/w-NP with high PVA concentrations and a high polydispersity expendable for the investigation of the interior morphology of the nanoparticles.

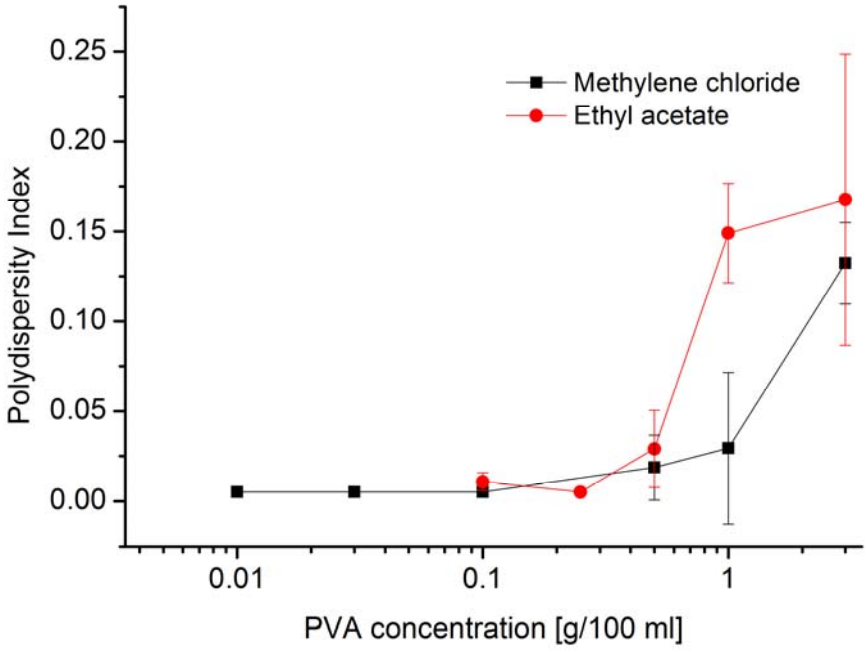

Fig. 13: *Polydispersity Index of w/o/w-NP prepared with methylene chloride or ethyl acetate at increasing PVA concentrations (mean ± SD, n = 3)*

4.1.1.2 Loading rate of nanoparticles

The encapsulation efficiency of the nanoparticles was determined by an indirect method as the supernatant of a centrifuged w/o/w-NP sample was measured regarding its BSA content. The amount of BSA encapsulated increased with higher PVA concentrations (Fig. 14). This is due to

the fact that PVA stabilizes the double-emulsion. Apparently, higher PVA concentrations stabilize the double-emulsion better, and leaking of the protein to the continuous phase, which is the major cause for low encapsulation efficiency when preparing w/o/w NPs, can be minimized (Bilati et al., 2005).

Another reason for high loading rates with higher PVA concentrations is the fact, that smaller w/o/w-NP, which were obtained with increasing amount of PVA, have a larger surface area. Thereby, more protein that is present in the continuous phase is able to adsorb to the surface of the nanoparticles.

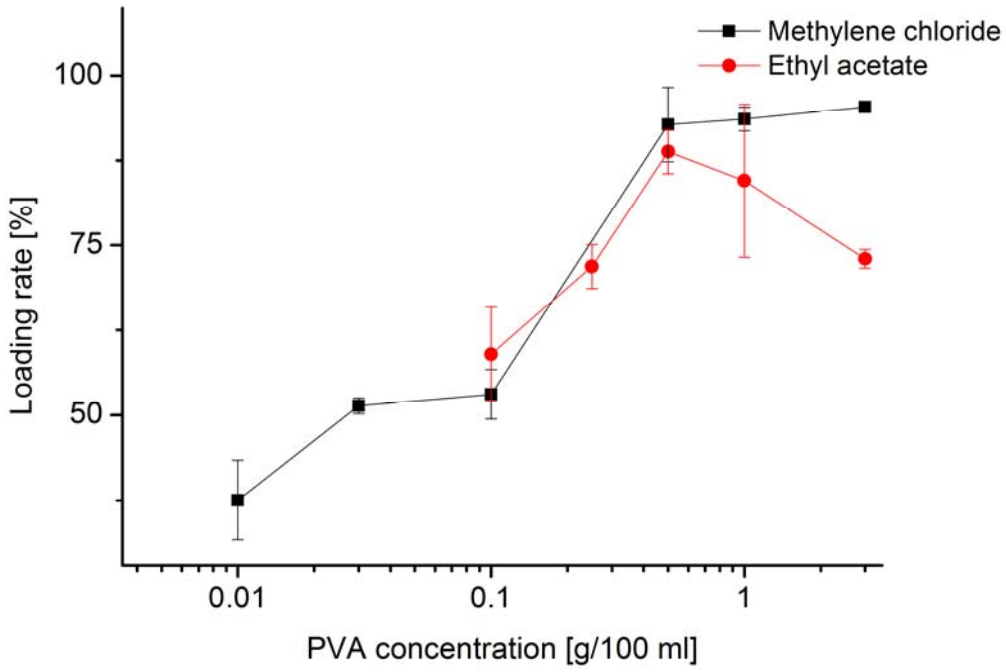

Fig. 14: *Loading rate of w/o/w-NP loaded with BSA (1 mg/ml) at various PVA concentrations using methylene chloride or ethyl acetate as the organic solvent for the polymer (mean ± SD; n = 3)*

Nanoparticles prepared with methylene chloride as an organic solvent showed a steady increase of the loading rate with decreasing particle sizes (Fig. 15). For particles with a mean diameter of

648 nm ± 80 nm to 1.29 µm ± 0.13 µm the encapsulation efficiency is between 37% ± 6% to 53% ± 4%. An increase of the encapsulation efficiency can be seen when using nanoparticles with a mean diameter of less than 332 nm. The encapsulation efficiency is more than 90%, which can be attributed to the large surface area existing in such small particles. The data indicate that the particle size is the deciding factor in regard to the particle size.

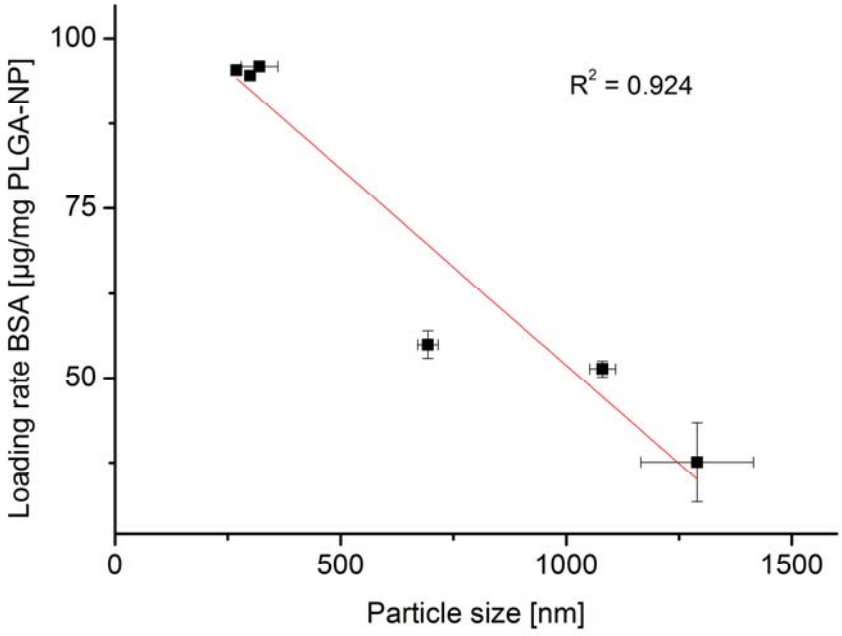

Fig. 15: *Loading rate of w/o/w-NP loaded with BSA (100 µg/mg PLGA-NP; mean ± SD; n = 3)) for different particle sizes (mean diameter ± SD; n = 3) using methylene chloride as the organic solvent for the polymer*

The surface area of the w/o/w-NP decreased with increasing PVA concentrations (Table 12). The surface area is logarithmically proportional to the particle size. A larger surface area on the nanoparticles enables more protein to adsorb at the surface (Fig. 14). Hence, higher loading rates for particles with a larger surface area, lead to the assumption that adsorption of the protein on the surface occurs.

Table 12: *Surface area of w/o/w-NP prepared by double-emulsion method with either methylene chloride or ethyl acetate as an organic solvent*

PVA	Surface area of 1 g w/o/w-NP [nm^2]	
[g/100 ml]	Methylene chloride	Ethyl acetate
0.01	3.87×10^{18}	
0.03	4.63×10^{18}	
0.1	7.72×10^{18}	8.14×10^{18}
0.5	1.51×10^{19}	1.49×10^{19}
1	1.72×10^{19}	1.88×10^{19}
3	1.86×10^{19}	6.26×10^{19}

Using ethyl acetate as an organic solvent is reported to be challenging when targeting high encapsulation rates, as it is partly miscible with water. Because of that, parts of the inner phase may leak into the continuous phase more easily compared to the usage of methylene chloride as an organic solvent. Consequently, lower encapsulation rates are typically achieved when using ethyl acetate as an organic solvent for the double-emulsion method (Bilati et al., 2005). Interestingly, encapsulation rates were similar when using ethyl acetate and methylene chloride in this work. Only when using high amounts of PVA (more than 1%), the encapsulation was different, and nanoparticles prepared with ethyl acetate showed a lower encapsulation rate. This can be attributed to the properties of the ethyl acetate mentioned above.

4.1.1.3 Release test of protein loaded nanoparticles

It had been suggested previously that the hydrophilic drug is encapsulated inside of the polymeric matrix (Lamprecht et al., 2000b). The release profile of the tested w/o/w-NP formulations in PBS gave surprising insights. Almost every w/o/w-NP formulation showed an immediate release of BSA within 1 hour (Fig. 16). These findings are in strong contrast to the postulated structure of the nanoparticles prepared by the double-emulsion method (Bilati et al., 2005; Blanco and Alonso, 1997; Zambaux et al., 1998).

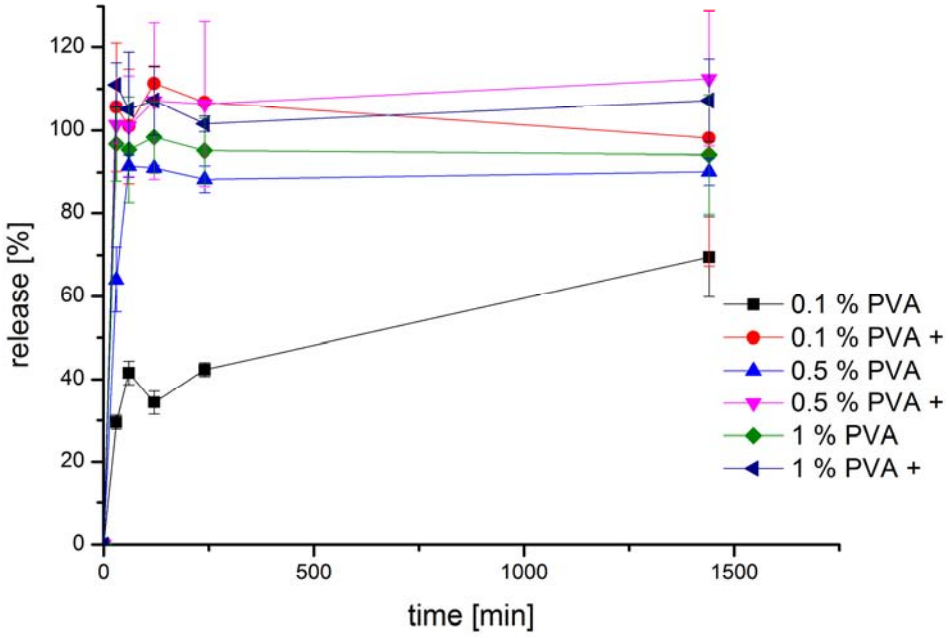

Fig. 16: *In-vitro BSA release of w/o/w-NP prepared with different PVA concentrations in the outer water phase. + indicates that BSA was added to the outer water phase, instead of the inner water phase (mean ± SD; n = 3)*

However, a fast release like it was observed in the presented experiments cannot be attributed to polymer degradation, as it takes several weeks for PLGA to degrade under these conditions (Mäder et al., 1998).

An immediate diffusion of the active ingredient through the polymer matrix would also take more time than monitored (Mäder and Weidenauer, 2010). Hence, it is much more likely that BSA is simply adsorbed to the surface and not dispersed within the polymeric matrix. Only for w/o/w-NP at a size range of above 650 nm a slower release of BSA was seen. Here, about 40% was immediately released, whereas after 24 h 70% of BSA was released. This suggests that about 40% of the BSA was located at the surface of the nanoparticles and that 60% were in fact encapsulated inside.

To confirm this hypothesis, w/o/w-NP were prepared with the alteration that BSA was added to the continuous phase (w_2) instead of the inner water phase (w_1). These nanoparticles had the

protein definitely adsorbed to the surface, because the inner water phase did not contain BSA. Therefore, nanoparticles were obtained that possessed a distinct structure. The obtained nanoparticles showed release profiles that were very similar to those of the particles in which BSA was present in the inner w_1–phase (Fig. 16).

A difference was visible for particles with a mean particle size larger than 650 nm. As mentioned above the w/o/w-NP with the BSA in the inner phase did not show a complete release of the BSA within 24 hours. Particles in a similar size range with BSA present in the continuous phase, but not the inner phase, did show an immediate release of the hydrophilic drug. The difference can be contributed to the fact that, for particles above a certain size, a part of the BSA is really encapsulated inside the particles.

A fast release within 4 hours has been previously reported for PLGA nanoparticles, prepared by the double-emulsion method, containing alendronate (Cohen-Sela et al., 2009). However, our findings differ from previous studies, in which proteins or glycosaminoglycans have been used as the API, with regard to the observed release profiles (Jiao et al., 2002; Lamprecht et al., 1999; Sahana et al., 2010). This can partly be attributed to conditions during the drug release test. There is no standardized method to measure the release profile of nanoparticles, consequently results cannot be sufficiently compared.

4.1.1.4 Morphology of nanoparticles

The release profile of the w/o/w-NP is contradictory to the common understanding of nanoparticles with encapsulated API, because the immediate release of BSA would not occur if it was in fact encapsulated inside a polymeric matrix. There also seems to be a size dependent effect, as particles larger than 650 nm did not show a complete release after 24 h, indicating that BSA is partly encapsulated inside the nanoparticles.

To determine the characteristic of the w/o/w-NP further, the morphology was investigated. The interior morphology is of particular interest, as it might explain the findings of the release profile that do not fit with current perception of the structural characteristics.

Until now, the interior morphology of w/o/w-NP remained undiscovered as imaging techniques like transmission electron microscopy (He et al., 2004; Khoee and Yaghoobian, 2009), SEM (Giovino et al., 2012), FE-SEM (Sahana et al., 2010) and atomic force microscopy (Lamprecht et al., 2000b) were able to confirm the size and determine the shape of w/o/w-NP, but failed to give information about the interior morphology and consequently the localization of the hydrophilic drug.

First, w/o/w-NP were investigated using an SEM (Fig. 17). As anticipated, nanoparticles showed a spherical shape and the particle size, measured by PCS earlier, could be confirmed. These findings were already described multiple times in previous studies as mentioned above.

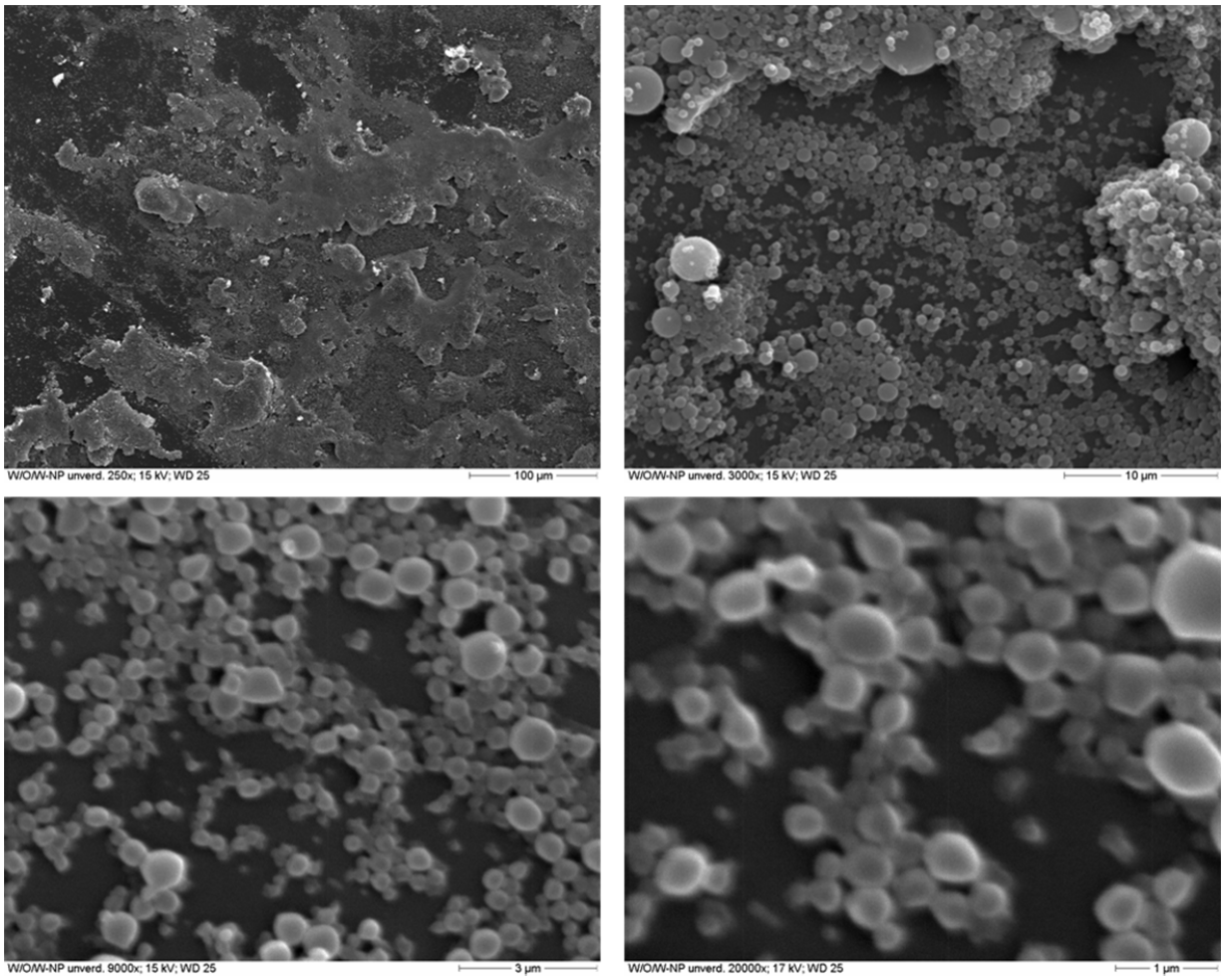

Fig. 17: *SEM images of w/o/w-NP prepared with 0.1% PVA at 15 - 17 kV with magnifications of 250 - 20000 x*

Further investigations regarding the morphology were conducted using an FE-SEM. As the resolution is much better it is more suitable as imaging technique for nanoparticles compared to SEM.

To obtain satisfactory results about the interior morphology of w/o/w-NP the preparation was modified. Instead of BSA a mixture of BSA and Gold-BSA was used. The Gold-BSA is visible under the FE-SEM as bright spots.

To get a comprehensive insight of the interior morphology of w/o/w-NP different formulations were tested. Particles in a size range of about 600 nm prepared with 0.1% PVA and w/o/w-NP in a size range of about 300 nm prepared with 0.5% PVA were investigated.

Gold-BSA is visible on the surface of w/o/w-NP in a size range of 600 nm, proving that at least not the entire drug is encapsulated (Fig. 18).

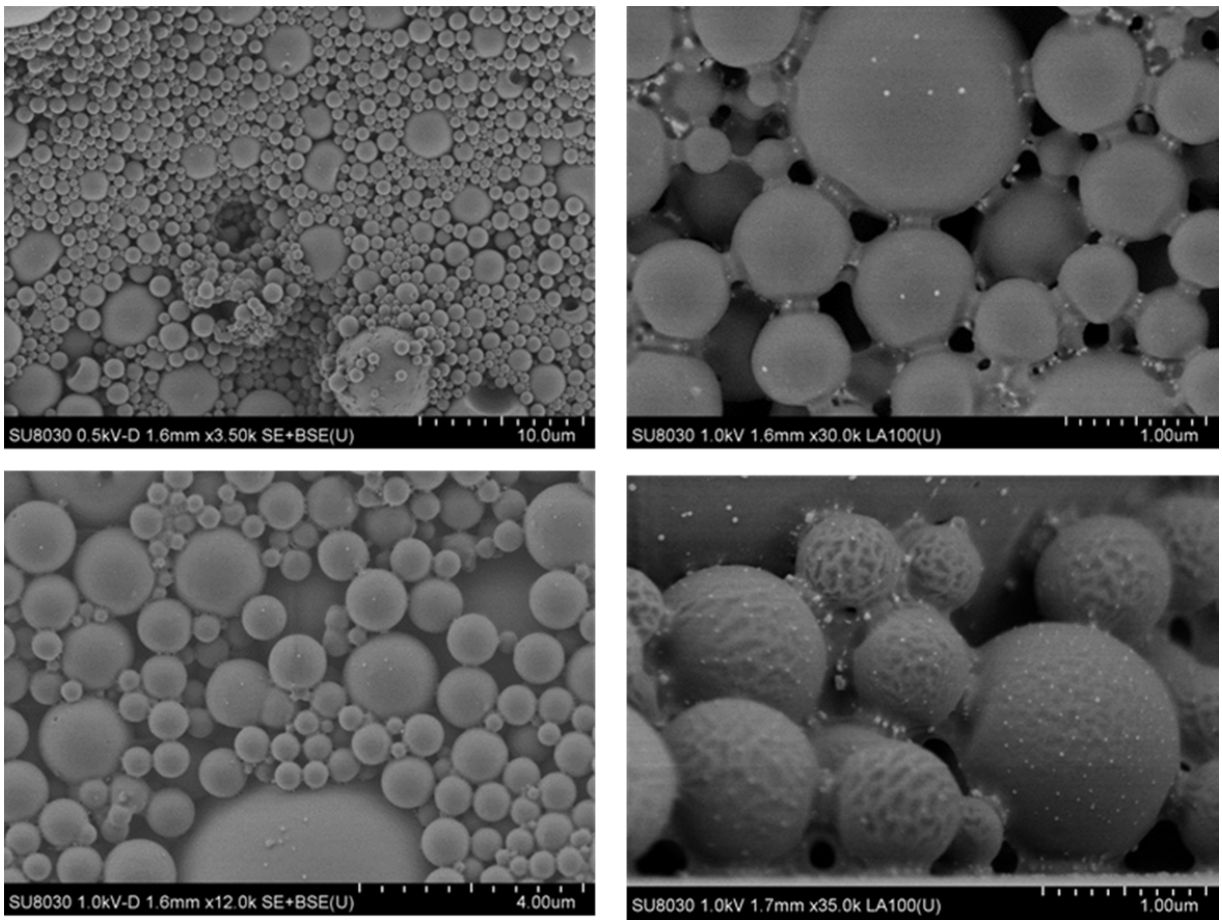

Fig. 18: *FE-SEM images of w/o/w-NP prepared with 0.1% PVA at 0.1 – 1 kV with magnifications of 3500 – 35000 x*

The pictures reveal "polymeric bridges" between the w/o/w-NP. These are most likely measurement artefacts derived from the drying of the w/o/w-NP. The situation in suspension

must be different; otherwise the measured particle size would be substantially bigger. Moreover, if the particles were aggregated they would not be homogenously dispersed.

Another aspect of interest is the surface of the w/o/w-NP, which seems to be either smooth or furrowed (Fig. 18). These are also most likely measurement artefacts as the surface is smooth at low magnifications and furrowed at high magnifications. The polymeric shell appears to be affected by the electron beam leading to damages of the specimen. During the examination of the nanoparticles, a change of the surface was discovered when the electron beam remained stationary on one area of the sample for a prolonged period. The surface was smooth in the beginning, but then a formation of wrinkles could be noted.

Even though the particle size analysis showed a monomodal size distribution, some microscale particles were visible in the FE-SEM pictures. Nevertheless, counting the particles displayed that only less than 2% of the total number of particles were bigger than 2 µm, confirming the results of the particle size experiments.

The discoveries and the consequent understanding about the morphology of w/o/w-NP were limited, when using FE-SEM on w/o/w-NP with Gold-BSA. Gold-BSA is clearly visible on the surface of the particles leading to the conclusion that at least part of the drug is not encapsulated. On the other hand, encapsulation rates are rarely 100%. That is why part of the drug is adsorbed at the surface, when proper interactions of the drug and the polymer prevail. As reported previously, this is the case for PLGA nanoparticles and BSA (Singh et al., 2004).

To get an insight into the interior morphology of the w/o/w-NP ion milling coupled FE-SEM was used. The sample was cut with an argon beam and investigated using FE-SEM in the same manner as the sample that was not subjected to ion milling.

By applying this sample preparation technique, the interior morphology of w/o/w-NP becomes visible (Fig. 19). Surprisingly, only very few particles with an inner hollow attributable to an inner aqueous phase could be found. Moreover, particles that contained an inner water phase were typically in the microscale and not nanoparticles. In fact, the smallest particle with an inner aqueous phase had a size of 658 nm. The mean particle size for particles with an inner phase was 2.32 µm. This is significantly larger than the mean particle size for particles without an inner phase, which was 606 nm

Besides, only about 11% of all particles even had an inner aqueous phase. It is clearly visible that most Gold-BSA is located on the outside of the nanoparticles. The lack of an inner phase prevents the drug from being encapsulated. Therefore, the drug is mainly adsorbed at the surface of the w/o/w-NP.

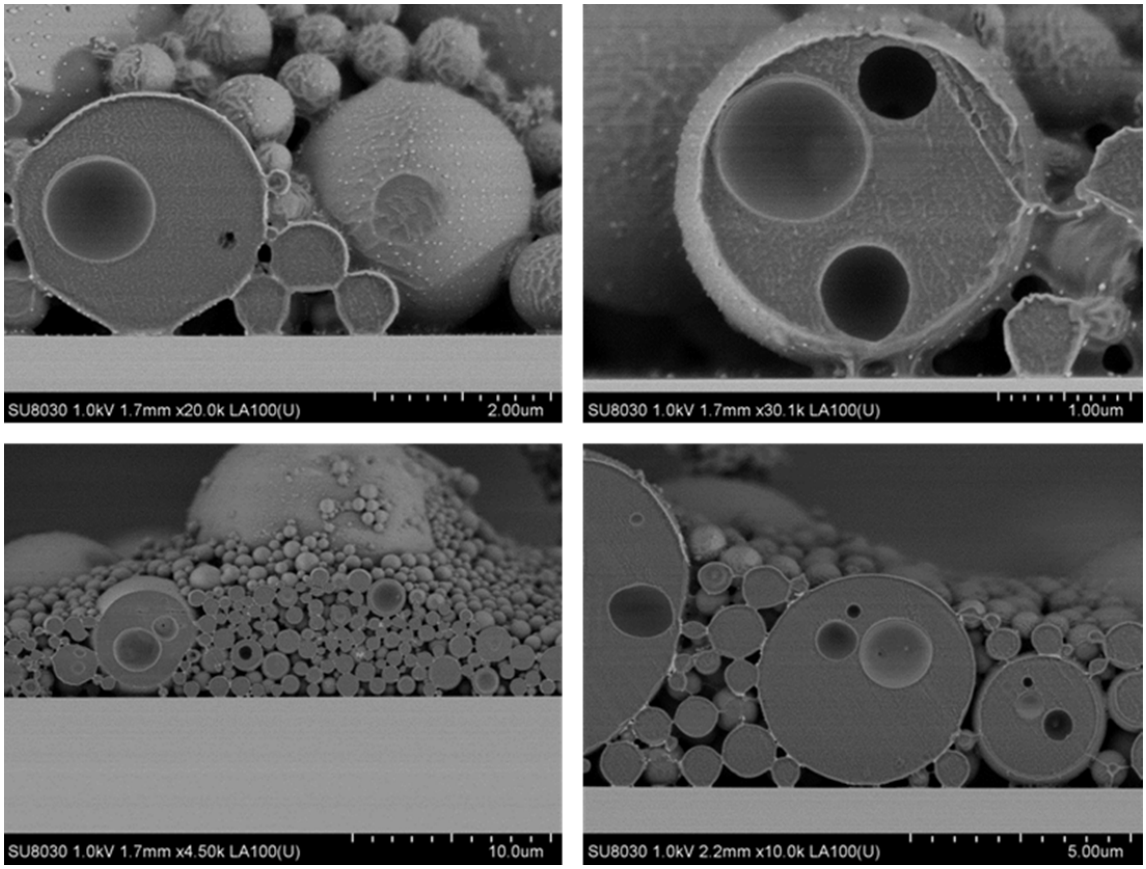

Fig. 19: *FE-SEM images of w/o/w-NP prepared with 0.1% PVA at 1 kV with magnifications of 4500 – 30000 x after ion milling with an argon beam*

Taking these discoveries into consideration, the encapsulation rates (Fig. 14) can be put in context. The amount of BSA loaded on the surface is dependent on the surface area of the w/o/w-NP. Therefore, a higher loading of the particles with BSA can be observed with smaller particles.

The findings of the interior morphology also correspond better with the findings of the dissolution test. The previously prevailing understanding of the morphology of w/o/w-NP was not suitable to explain the release profile (Fig. 16) sufficiently.

Based on the FE-SEM images it is consistent that most of the BSA is immediately released and only a small fraction remains inside the particles after 24 h. BSA on the surface is desorbed from the surface, when the properties of the surrounding media change, as they do when conducting a dissolution test.

To obtain informations about the morphology of smaller w/o/w-NP, particles with a mean particle size of 350 nm were prepared with 0.5% PVA were investigated using ion milling coupled FE-SEM (Fig. 20). It must be stated that the nanoparticles were not all cut at the exact center. Ion milling was applied to the nanoparticle sample on a silicium chip with an argon beam; consequently particles were not cut individually, leading to the previously shown images.

As already showcased for the bigger particles prepared with 0.1% PVA, the w/o/w-NP prepared with 0.5% PVA also showed almost no inner aqueous phase at all. Actually, for only about 2% of the particles an inner aqueous phase was visible. This is consistent with the results discussed above, as smaller particles are apparently not able to have an inner aqueous phase. The smallest particle with an aqueous phase had a particle diameter of 603 nm. This is similar to the smallest particle with an inner aqueous phase found in the earlier experiment, where the mean particle size was substantially bigger.

These findings reveal that the current understanding of the morphology of w/o/w-NP is not appropriate for nanoparticles with a mean diameter of below 600 nm and needs to be revisited. The protein is mainly adsorbed at the surface of the nanoparticles and it is not encapsulated inside the polymeric matrix.

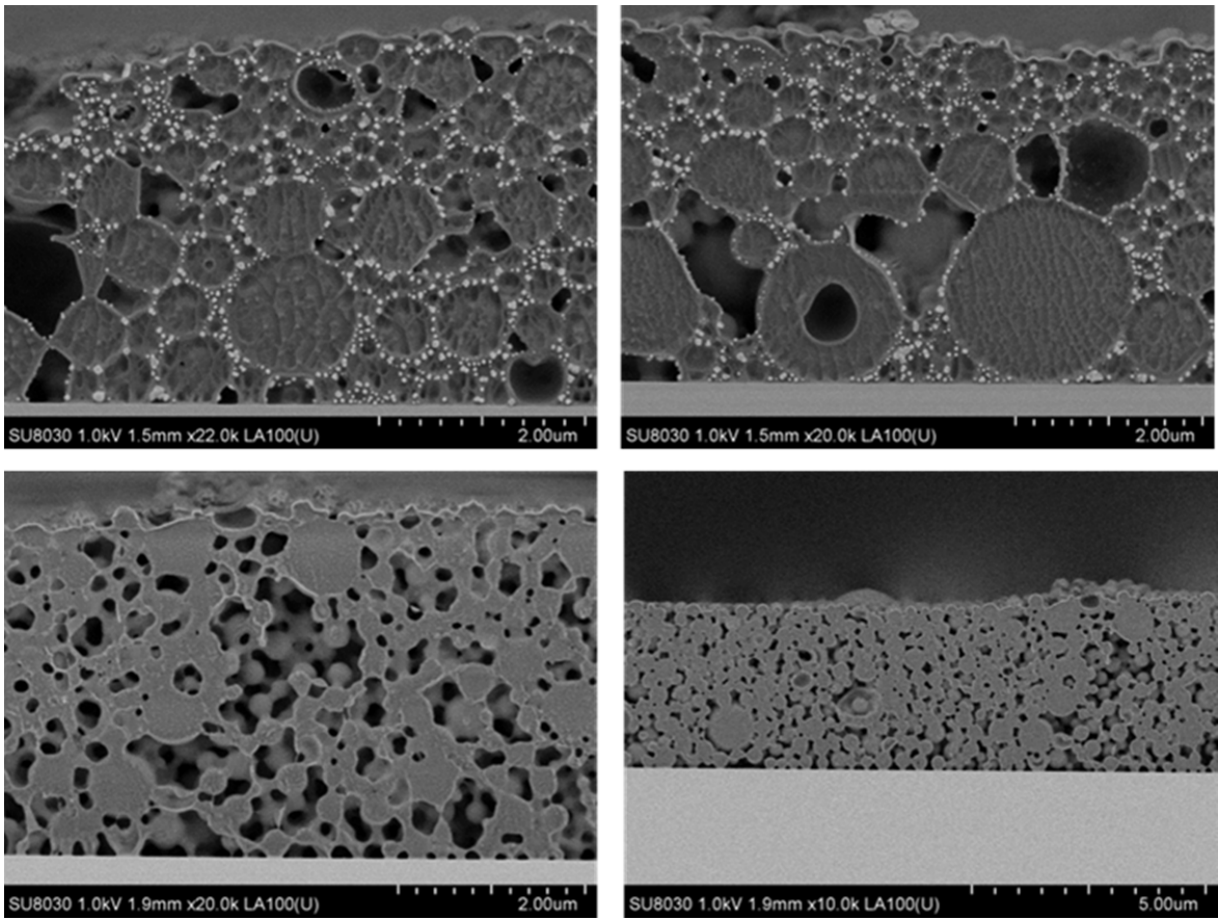

Fig. 20: *FE-SEM images of w/o/w-NP prepared with 0.5% PVA at 1 kV with magnifications of 10000 – 20000 x after ion milling with an argon beam*

4.1.1.5 Investigation of structural peculiarities of nanoparticles

A double-emulsion method was used to incorporate the hydrophilic drug inside nanoparticles consisting of a polymeric matrix. This postulated structure can now be dismissed as the images of the ion milling coupled FE-SEM of w/o/w-NP clearly show that the protein is not located inside the nanoparticles, but mostly outside at the surface of the nanoparticles.

Comparing the loading rates of w/o/w-NP in which the BSA was either added to the inner water phase or the outer water phase does only show slight differences between the formulations (Fig.

21). The loading rate is a little bit higher for the formulations in which the protein was added to the inner water phase. It must be stated that the loading rate was measured indirectly by analyzing the supernatant of the nanoparticle formulation after centrifugation. Both formulations showed an increased loading rate for decreasing particle sizes. This can be simply explained by the larger surface area that is available when using smaller particles. This correlation between particle size and encapsulation efficiency was expected for samples where BSA had only been added to the continuous phase, but not for samples with BSA in the inner phase, as encapsulation rates for e.g. microparticles are usually not expected to be dependent on the size when applying the double-emulsion method. However, this finding becomes plausible in view of the microscopic results reported in chapter 4.1.1.4, showing that for w/o/w-NPs where BSA had been added to the inner phase during manufacture, BSA was only detectable on the particle surfaces for particles smaller than 603 nm. It is also interesting that regardless of the mean particle size of a w/o/w-NP sample the size of the inner aqueous phase is similar, making it much more likely for big particles to have an inner aqueous phase (Table 13).

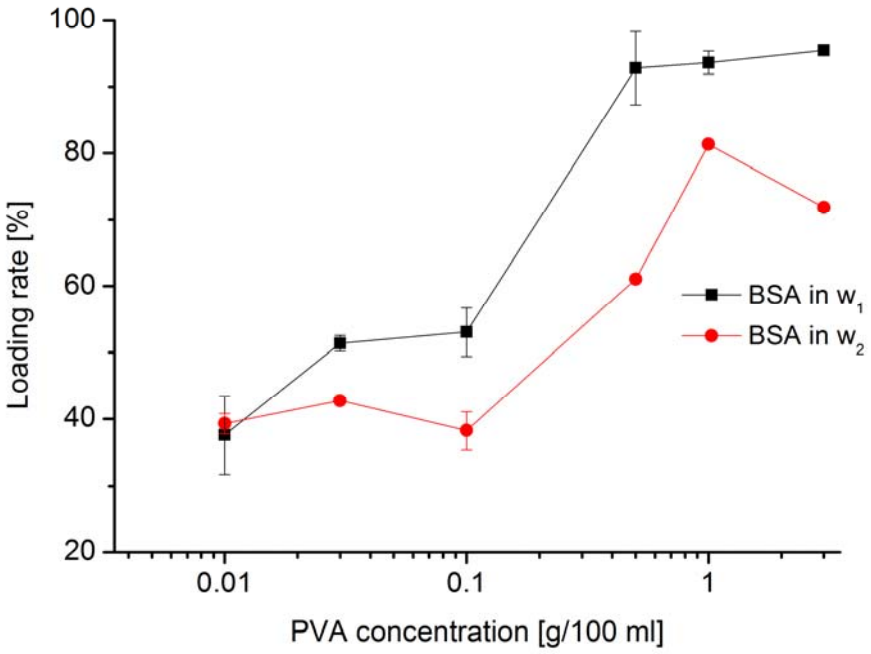

Fig. 21: *Loading rate of w/o/w-NP with BSA (1 mg/ml) either dissolved in the inner water phase (w_1) or the outer water phase (w_2) (mean ± SD; n = 3)*

Table 13: *Analysis of FE-SEM images regarding the particle size and interior particle morphology*

	w/o/w-NP-0.1% PVA	w/o/w-NP-0.5% PVA
Number of particles with an inner phase	13	2
Total number of particles	113	90
Fraction of particles with inner phase	11.5%	2.2%
Particle size (mean diameter) of all particles	790 nm	370 nm
Particle size (mean diameter) of particles with an inner phase	2327 nm	1037 nm
Particle size (mean diameter) of particles without an inner phase	606 nm	356 nm
Smallest particle (diameter) with an inner phase	658 nm	603 nm

Even though the double-emulsion method is used as a gold-standard to encapsulate hydrophilic drugs there are a lot of accompanying challenges with it. The hydrophilic drug, e.g. a protein or DNA, has to overcome shear stress from the emulsification process. This can, very likely, lead to destabilization or even denaturation of many proteins. Furthermore, the hydrophilic drug may have to deal with heat during the emulsification process and it comes in contact with an organic solvent at the interface of the primary emulsion. All of these hurdles can lead to inactivation of the hydrophilic drug. Therefore, the active ingredient used for the preparation must be robust enough to withstand the manufacturing conditions associated with this technique. Hence, results of model proteins like BSA cannot be transferred to other proteins like antibodies that have different properties in terms of size and overall composition. A scale-up to an industrial scale is also challenging, because of the complex preparation method.

As described earlier, the aim of loading a hydrophilic drug inside nanoparticles (particle size $\leq$ 600 nm) cannot be successfully carried out using the previously described double-emulsion method applied in this work. It cannot, in fact, be called a double emulsion method, as the droplets from which the nanoparticles are formed appear to not being capable of holding droplets of an inner phase.

A simpler and better transferable method would be to prepare polymeric nanoparticles of a desired particle size and then letting the hydrophilic drug adsorb onto the surface of the nanoparticles.

4.2 Nanoparticles prepared with oil-in-water-emulsification-evaporation method

As shown previously, nanoparticles prepared by the double-emulsion method do not encapsulate the hydrophilic drug inside at a particle size below 600 nm. The hydrophilic drug is adsorbed at the surface. Hence, preparing nanoparticles using a simpler approach is beneficial in terms of stability of the hydrophilic drug, since it is exposed to shear stress, heat and to an organic solvent, when applying the double-emulsion method.

Therefore, nanoparticles were prepared using an oil-in-water-emulsification-evaporation method. The "blank" PLGA-NP were then incubated with the hydrophilic drug, BSA, OVA or α-toxin.

4.2.1 Physicochemical characterization of nanoparticle properties

4.2.1.1 Influence of surfactants on particle size and polydispersity

Five different surfactants were used to prepare the PLGA-NP. The nonionic surfactants PVA and Tween 20, the anionic surfactants SDS and sodium cholate and the cationic surfactant CTAB were used for the preparation. As the protein was adsorbed after the preparation of the PLGA-NP it was anticipated that modified surface properties of the PLGA-NP, as a result of different surfactants, would have an effect on the loading rates (Fleischer and Payne, 2012).

As expected, higher amounts of surfactant led to a smaller particle size of the PLGA-NP (Fig. 22). The emulsion is stabilized with surfactants during the emulsification process via ultrasonication. A higher amount of surfactant can stabilize smaller droplets compared to lower amounts of surfactants. This ultimately yields smaller particles.

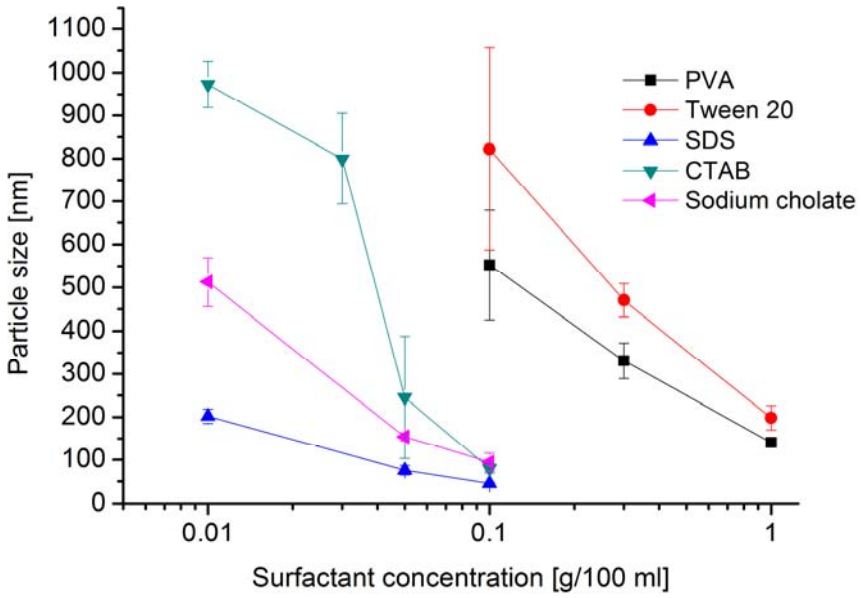

Fig. 22: *Influence of surfactant concentration on particle size of o/w-nanoparticles (mean diameter ± SD, n=3)*

The goal was to obtain nanoparticles in the size range of 100 nm – 200 nm (mean diameter). This was possible for all formulations, using sufficient amount of the respective surfactant. For PVA-NP and Tween 20-NP a surfactant concentration of 1% w/v was used to get nanoparticles below 200 nm, SDS-NP in the desired particle size range were obtained using 0.01% w/v SDS and for the CTAB-NP 0.1% w/v CTAB was necessary. Sodium cholate-NP had a particle size of 154 nm ± 10 nm, when using 0.05% w/v sodium cholate.

As another important aspect, the polydispersity of the nanoparticle formulations was investigated. As mentioned earlier, a high polydispersity indicates that the particle distribution is not monomodal. A polydispersity index above 0.05 – 0.1 suggests a bimodal particle size distribution.

The polydispersity index increases with higher amounts of surfactants and consequently increases for smaller particles (Fig. 23).

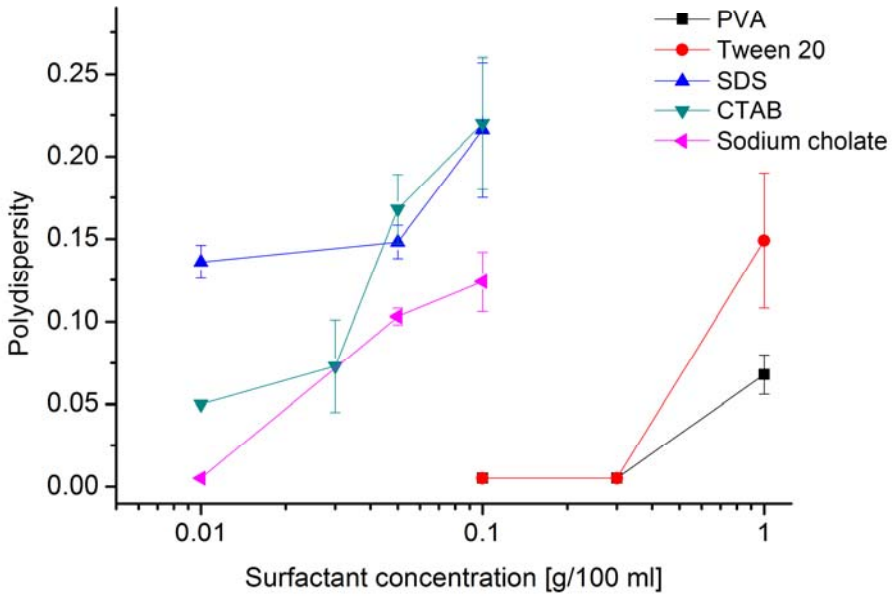

Fig. 23: *Influence of surfactant concentration on polydispersity of o/w-nanoparticles (mean ± SD, n=3)*

Polydispersity values close to 0.005 indicate monomodal particle size distributions. This could only be observed for particles above 300 nm. Higher amounts of surfactants were evidently sufficient to obtain small particles, but failed to obtain nanoparticles with a monomodal particle size distribution at a size range of 100 nm – 200 nm.

4.2.1.2 Zeta potential of nanoparticles

The surface properties of the PLGA-NP were characterized by measurement of the zeta potential as described in 3.5.4. The zeta potential changed for each surfactant and showed values of -7 mV - -25 mV for the nonionic and anionic surfactants (Fig. 24). The CTAB-NP had a zeta potential of -4 mV to 2 mV.

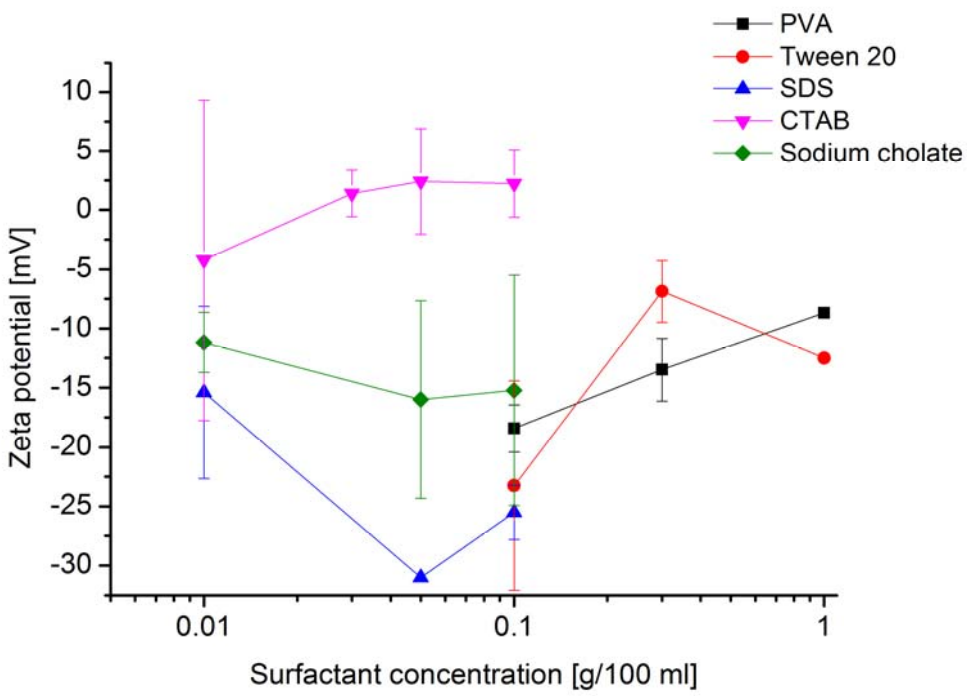

Fig. 24: *Influence of surfactant concentration on zeta potential of o/w-nanoparticles (mean ± SD, n=2)*

4.2.1.3 Loading rate of adsorbed proteins on nanoparticles

The prepared PLGA-NP were further tested regarding their potential to adsorb protein onto the surface, using OVA or BSA as model proteins. All formulations, using PVA, Tween 20, SDS, sodium cholate, and CTAB were prepared as described in chapter 3.2.1 and investigated.

OVA showed a high loading to the surface of the nanoparticles at a size below 200 nm (Fig. 25).

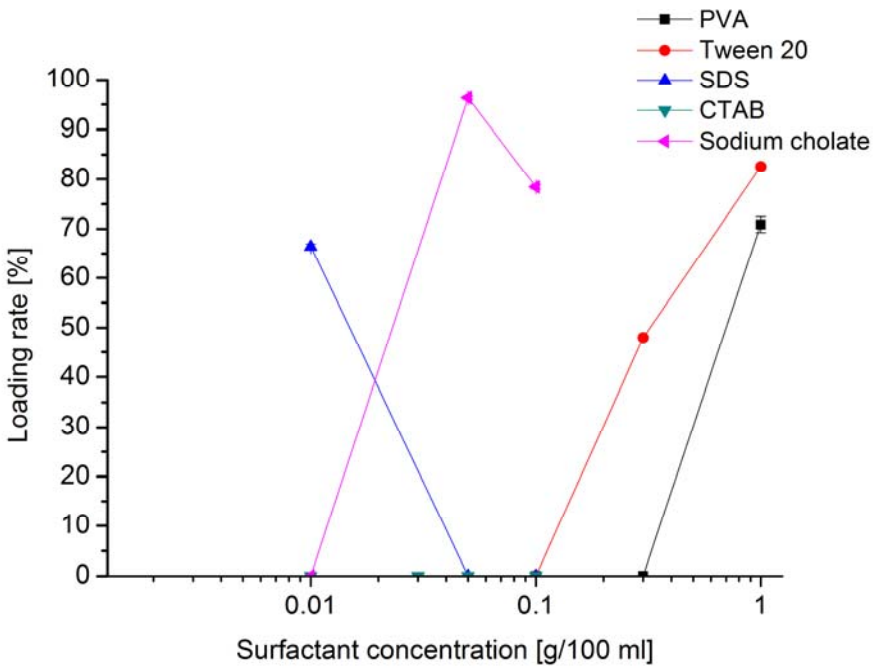

Fig. 25: *Loading rate of O/W-Nanoparticles (10 mg/ml) with 0.1 mg/ml Ovalbumin (mean ± SD, n=3)*

The amount of OVA adsorbed at the surface of the NP increased for smaller particles, when using PVA and Tween 20 as surfactants. However, this was not the case for the SDS- and sodium cholate- formulations. Especially for SDS-NP the loading rate decreases to 0%, meaning that no protein is adsorbed to the surface at a concentration of 0.1% SDS. Even though the particle size of the SDS-NP is smaller when using 0.1% SDS (46 nm ± 2 nm) instead of 0.01% (202 nm ± 16 nm), the loading rate decreases. This is most likely due to the fact that the SDS is repulsing the protein on the surface of the PLGA-NP. At low concentrations of SDS OVA is able to adsorb at the surface, but not at high SDS concentrations. A similar, but not as drastic effect, can be seen when using sodium cholate as a surfactant. The highest loading of OVA can be observed for sodium cholate-NP prepared with 0.05% sodium cholate. Increasing the sodium cholate concentration to 0.1% results in a lower loading rate, however the difference is not as substantial as for the SDS-NP. Like for all other tested surfactants, the particle size also decreases with higher surfactant concentrations, which, in theory, should lead to an increase in loading rate as smaller particles provide a larger surface available for adsorption. This means, that surface

properties such as zeta potential and hydrophobicity are of high importance as the surface area is apparently not itself solely responsible for the protein adsorption.

For the nonionic surfactants PVA and Tween 20 the loading rate follows the understanding that higher loading rates can be observed for smaller particles. Here, increasing surfactant concentrations yield smaller particles that have a bigger surface area (Table 14). A high amount of surfactant does not hinder OVA adsorbtion at the surface, when using the nonionic surfactants PVA and Tween 20. Both appear advantageous compared to the anionic surfactants SDS and sodium cholate.

CTAB was used as a cationic surfactant. Surprisingly, OVA does not adsorb at the surface of CTAB-NP. Independent of the size of the CTAB-NP and the amount of CTAB used, a loading of the CTAB-NP with OVA could not be obtained.

Table 14: *Surface area of o/w-NP prepared with different surfactants at various concentrations*

Surfactant concentration [g/100 ml]	Surface area of 1 g w/o/w-NP [nm^2]				
	PVA-NP	Tween 20-NP	SDS-NP	Sodium cholate-NP	CTAB-NP
1	35.5×10^{18}	25.2×10^{18}			
0.3	15.1×10^{18}	10.6×10^{18}			
0.1	9.1×10^{18}	6.1×10^{18}	110×10^{18}	53.0×10^{18}	62.5×10^{18}
0.05			65.7×10^{18}	32.4×10^{18}	20.4×10^{18}
0.035					6.25×10^{18}
0.01			24.8×10^{18}	9.75×10^{18}	5.14×10^{18}

Another model protein that was used in this work was BSA. The results regarding the loading rate of BSA onto the surface of PLGA-NP are similar to those obtained when using OVA as a protein. For the nonionic surfactants PVA and Tween 20 the loading rate increases with a bigger surface area. PVA-NP do show a slight decrease of the loading rate for 1%, here the high amount of PVA affects the loading with BSA negatively. For Tween 20-NP and sodium cholate-NP a

higher loading of BSA was observed for smaller nanoparticles, which have a bigger surface area (Fig. 26).

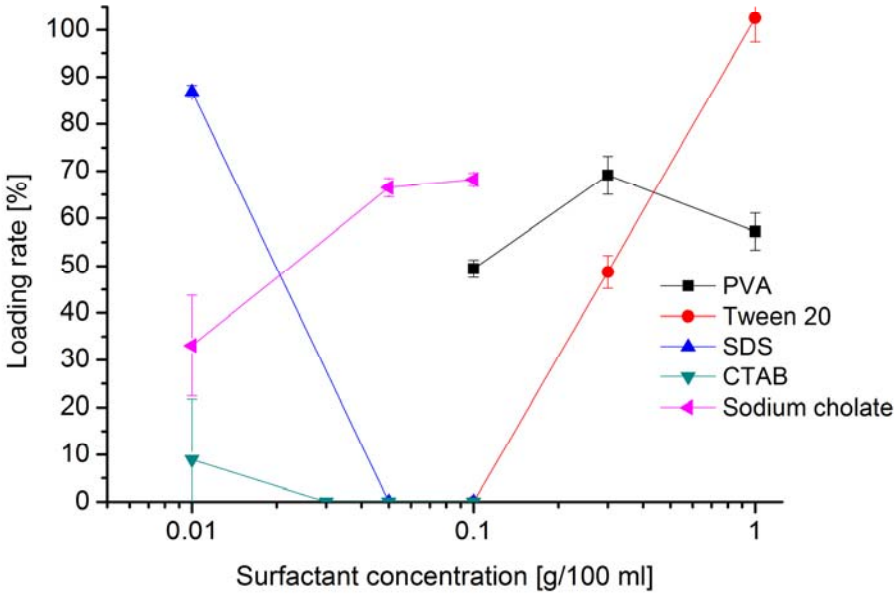

Fig. 26: *Loading rate of O/W-Nanoparticles (10 mg/ml) with 0.1 mg/ml BSA (mean ± SD, n=3)*

SDS-NP showed a similar behavior when comparing the loading of BSA and OVA. Only at a concentration of 0.01% a loading with BSA could be observed. This may also be the effect of SDS competing with BSA on the surface of the nanoparticles, making an adsorption of BSA at high SDS concentrations impossible.

A loading with BSA on CTAB-NP could also only be observed at the lowest used CTAB concentration. This is an improvement compared to the loading with OVA, where a loading was not observed. The low loading rate at 0.01% CTAB combined with the fact that no loading was possible at higher CTAB concentrations suggests that CTAB competes with the proteins at the surface of the nanoparticles, making a loading with the proteins unlikely.

When comparing the nanoparticle formulations that produced the highest loading with the proteins at different protein concentrations, it can be observed that BSA tends to be more

adsorbed at the nanoparticle surface compared to OVA (Fig. 27). However, this was not observed for all formulations, but for the majority of nanoparticle formulations. The CTAB-NP were not included for the comparison of OVA and BSA as a loading with protein on the CTAB-NP surface was not observed. BSA causes a lower surface tension in PBS than OVA (Table 18). Therefore, it can be assumed that BSA, compared to OVA, accumulates more on interfaces, which could explain why the loading rate of BSA is higher on most o/w-NP formulation. However, the surface-active properties of the protein are not the only determining factors for the adsorption of the protein onto the nanoparticle surface, hydrophobic and ionic interaction also impact the ability of the protein to adsorb at the nanoparticle surface (Hillaireau and Couvreur, 2009; Lundqvist et al., 2008). The surfactant used for the preparation of the o/w-NP causes a modified nanoparticle surface (Singh et al., 2007). Thereby, the loading rate of each protein onto the nanoparticle surface must be tested for each o/w-NP formulation as the surface properties of the o/w-NP surface changes with each formulation leading to different intensities of ionic and hydrophobic interactions with the protein.

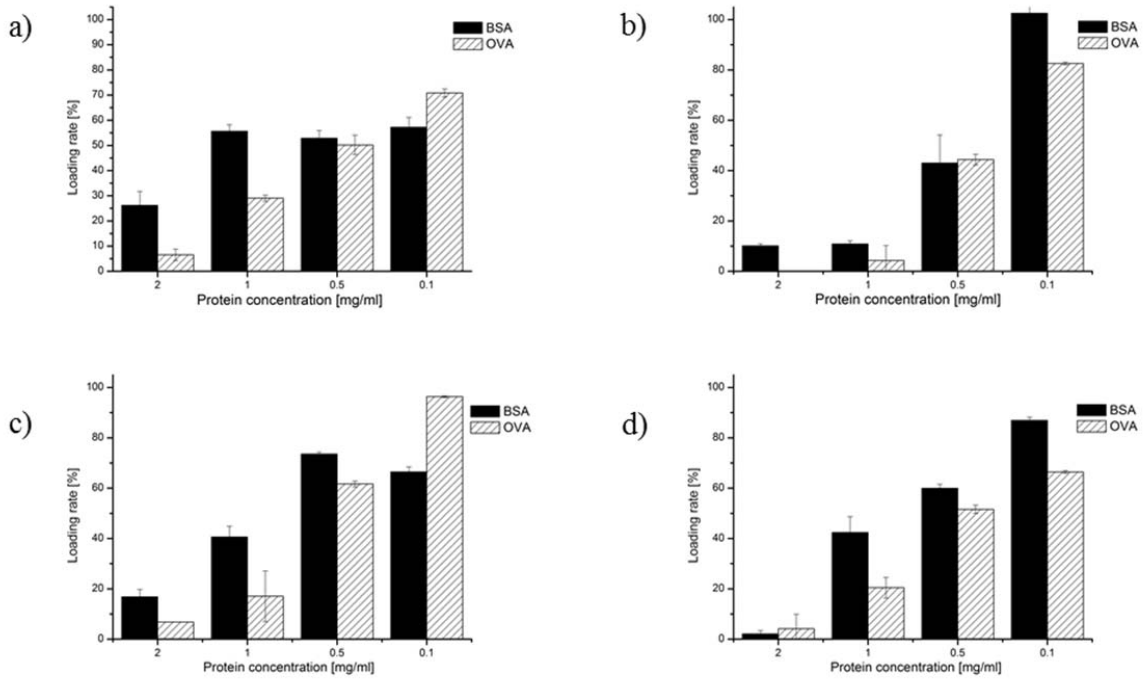

Fig. 27: *Influence of protein concentration on loading rate on (a) PVA (1%)-Nanoparticles, (b) Tween 20 (1%)-Nanoparticles, (c) Sodium cholate (0.05%)-Nanoparticles and (d) SDS (0.01%)-Nanoparticles (mean ± SD, n=3)*

The studies regarding release kinetics, stability, morphology, cell interaction and in-vivo experiments were conducted using nanoparticle formulations that had a relatively good loading rate combined with a small particle size (Table 15).

Table 15: *Particle formulations used for futher studies*

Nanoparticle formulation (10 mg/ml)	Loading rate (OVA 0.1 mg/ml) [%]	Mean diameter [nm]
PVA (1%)	71 ± 2	141 ± 9
Tween 20 (1%)	83 ± 2	198 ± 28
Sodium cholate (0.05%)	96 ± 1	154 ± 10
SDS (0.01%)	66 ± 2	202 ± 16
CTAB (0.05%)	0	246 ± 142

4.2.1.4 Release profile of protein loaded nanoparticles

The in-vitro release profile of the o/w-nanoparticle formulations (Table 15) prepared using different surfactants showed similar results to the nanoparticles prepared with the double emulsion method, using only PVA (Fig. 16).

The o/w-NP showed an immediate release of OVA in PBS (Fig. 28) within 30 minutes. The Protein is just adsorbed at the surface, making a fast release possible. A release of about 100% was achieved for all nanoparticle formulations. Therefore, the surface modification with the surfactants has no influence on the release profile.

The results of the release profile are slightly defective as the release of the protein was over 100%. This can be attributed to the fact that the nanoparticle samples were directly measured after sampling. The samples were drawn at a temperature of 37°C, the increased temperature of the nanoparticle samples compared to the standards led to an increase in the absorption of the detected bicinchoninic acid, which is measured when determining the protein content with a BCA-assay.

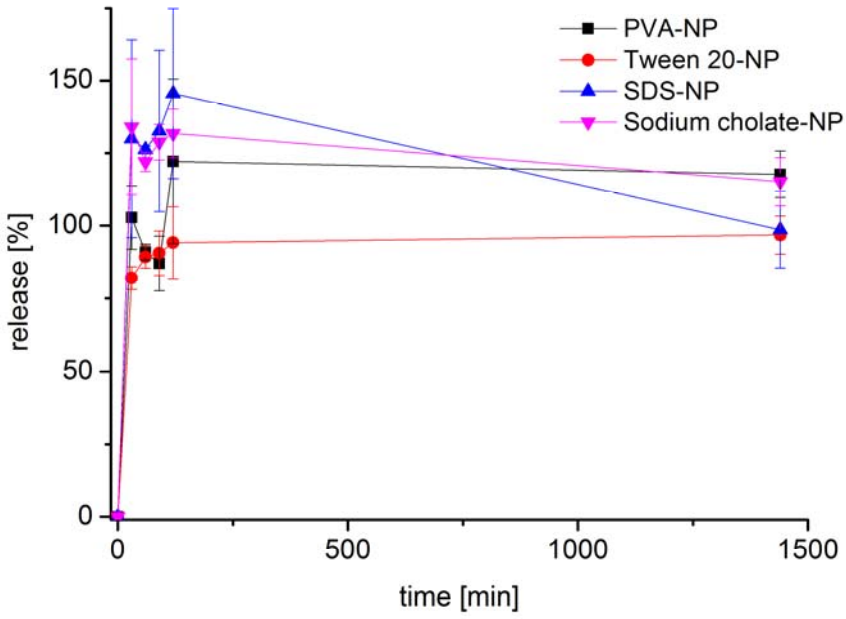

Fig. 28: *In-vitro OVA release of o/w-NP in PBS at 37 °C (mean ± SD; n = 3)*

4.2.1.5 Characterization of α-toxoid loaded nanoparticles

Recombinant proteins are in high demand in vaccine research as they pose as a safer choice compared to live, attenuated vaccines. Challenges regarding the immunogenicity have been discussed earlier (2.1). In addition to those challenges, recombinant proteins are rarely of a high purity making the formulation development difficult. Residual host cell impurities like proteins and DNA can interact with the nanoparticles leading to aggregation.

In this work, α-toxoid from E. coli and α-toxoid from Clostridium perfringens, which can be used as vaccines to protect animals against gas gangrene, was tested regarding its compatibility and loading rate with o/w-NP.

The o/w-NP showed promising properties concerning loading rate, stability and compatibility when model proteins like BSA and OVA were used. To test if the o/w-NP are also suitable for

the formulation with recombinant proteins, α-toxoid from E. coli was tested. Furthermore, α-toxoid derived from Clostridium perfringens was also tested.

The PLGA o/w-NP were loaded with α-toxoid as described in chapter 3.2.1. Before the proteins were incubated with the o/w-NP the nanoparticles were freeze dried as previously described (3.4). The protein solution was then incubated for 3 h with the freeze dried nanoparticles. PLGA nanoparticles were used in a concentration of 12.5 mg/ml in the loading experiment.

The α-toxoid from E. coli was added to yield a final concentration of 0.065 mg/ml and the α-toxoid from Clostridium perfringens was added to yield a concentration of 0.0215 mg/ml in the nanoparticle formulation.

The α-toxoid from E. coli was easier to formulate with nanoparticles, except for the CTAB-NP all formulations formed stable nanoparticle suspension (Table 16). Visual aggregation after blending of nanoparticle formulation and protein was considered as “instable”.

The α-toxoid from Clostridium perfringens was not stable when blending with the ionic o/w-NP. Precipitation was observed during incubation of the α-toxoid from Clostridium perfringens with SDS-NP, sodium cholate-NP, and CTAB-NP. The formulation was physically stable when the nonionic PVA or Tween 20 was used for the preparation of the o/w-NP.

Table 16: *Compatibility of different O/W-Nanoparticle formulations with α-toxoid from E. coli and α-toxoid from Clostridium perfringens. (+) indicates that blend of nanoparticle formulation and protein solution is suitable for further testing. (-) indicates that precipitation occurred during blending process (n= 3-4).*

Nanoparticle formulation	α-toxoid (E.coli)	α-toxoid (Clostridium perfringes)
PVA (1%)	+	+
Tween 20 (1%)	+	+
Sodium cholate (0.05%)	+	-
SDS (0.01%)	+	-
CTAB (0.05%)	-	-

The protein is not extensively purified, which is visible in the SDS-PAGE gels (Fig. 29). The α-toxoid from E. coli has a purity of approximately 50% and the α-toxoid from Clostridium perfringens has a purity of approximately 25%. As the proteins are unpurified a BCA-assay cannot give reliable results concerning the adsorption of the toxoids on the surface, because the total amount of protein is measured when applying a BCA-assay, the method is not specific for α-toxoid. Therefore, SDS-PAGE was used to measure the amount of the different proteins on the surface of the nanoparticles. An indirect method was used, as mentioned previously (3.5.2).

It must be noted that some o/w-NP formulations were unstable when blending with the toxoids. Precipitation was observed for some formulations, this is important when examining the gels, as an indirect method was applied measuring the protein in the supernatant of the o/w-NP after incubation. In case of precipitation, the toxoid formed agglomerates with the nanoparticles, and the supernatant did not contain any toxoid. Consequently, even if no protein was detected in the supernatant, which would normally mean that 100% is adsorbed at the nanoparticle surface, adsorption of the toxoid to the nanoparticle surface did not take place, if precipitation occurred during the incubation. In this context, the supernatant of CTAB-NP, for example, contained no toxoid at all (Fig. 29), and this is attributed to the fact that CTAB-NP agglomerated with the

protein solutions (Table 16). CTAB-NP were therefore considered not to be suitable for either, α-toxoid from E. coli or α-toxoid from Clostridium perfringens.

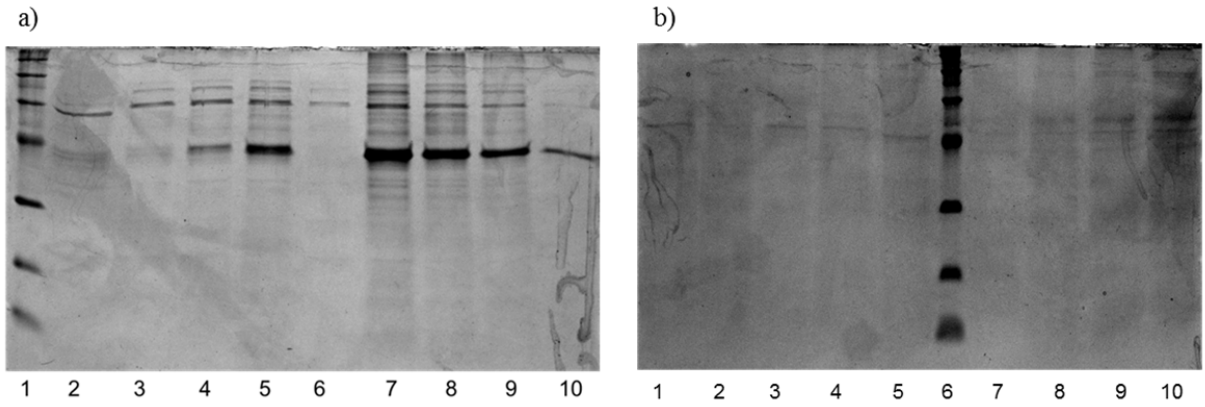

Fig. 29: *SDS-PAGE gels after staining with Coomassie Brilliant Blue, supernatants of o/w-NP formulations after incubation with toxoids and standard of toxoids; a) α-toxoid (E.coli): 1) Marker 2) PVA-NP 3) Tween 20-NP 4) Sodium cholate-NP 5) SDS-NP 6) CTAB-NP 7) α-toxoid (E.coli) 0.065 mg/ml 8) α-toxoid (E.coli) 0.049 mg/ml 9) α-toxoid (E.coli) 0.0325 mg/ml 10) α-toxoid (E.coli) 0.016 mg/ml; b) α-toxoid (Clostridium perfringes): 1) PVA-NP 2) Tween 20-NP 3) Sodium cholate-NP 4) SDS-NP 5) CTAB-NP 6) Marker 7) α-toxoid (Clostridium perfringes) 0.0054 mg/ml 8) α-toxoid (Clostridium perfringes) 0.0108 mg/ml 9) α-toxoid (Clostridium perfringes) 0.0161 mg/ml 10) α-toxoid (Clostridium perfringes) 0.0215 mg/ml*

The o/w-NP using anionic surfactants for the preparation (SDS and sodium cholate) also precipitated when mixing with the α-toxoid from Clostridium perfringens. Hence, these formulations are not appropriate for this protein. However, the formulations with α-toxoid from E. coli were successful regarding their physical stability. Here, the amount of protein in the supernatant could be used to calculate the loading rate of the toxoid to the nanoparticle surface. For the o/w-NP using nonionic surfactants (PVA and Tween 20) formulations with both toxoids were physically stable, consequently supernatant was used to determine the amount of toxoid on the o/w-NP surface.

The SDS-PAGE gels were visualized with an Intas® camera system and a densiometric analysis was performed using the imageJ software. The experiments in which the loading of o/w-NP with α-toxoid from E. coli was tested could be easily evaluated, as the proteins from the vaccine

formulation were clearly separated and had a high enough concentration to be sufficiently visible for a quantitative measurement (Fig. 29a).

The o/w-NP prepared with the nonionic surfactants PVA and Tween 20 showed the highest loading with α-toxoid from E. coli with loading rates of 94% ± 6% and 96% ± 1%, respectively (Table 17). The sodium cholate-NP also showed a high loading rate of 80% ± 1% and the SDS-NP had a loading rate of 41% ± 10%.

Table 17: *Loading rate of o/w-NP with α-toxoid (E.coli)*

Nanoparticle formulation	**α-toxoid (E.coli) loading rate [%]**
PVA (1%)	94 ± 6
Tween 20 (1%)	96 ± 1
Sodium cholate (0.05%)	80 ± 1
SDS (0.01%)	41 ± 10
CTAB (0.05%)	-

The analysis of the o/w-NP with α-toxoid from Clostridium perfringens was challenging, as the bands of the targeted protein were not clearly visible (Fig. 29). Therefore, in addition to testing the supernatant of the o/w-NP after incubation with the vaccine formulation, the o/w-NP themselves were tested as well. Here, the centrifuged o/w-NP were redispersed with 10% SDS and 2.3% DTT. The test does not give a quantitative result for the loading rate of the α-toxoid on the o/w-NP, because some agglomerates remained after redispersing the sample. A qualitative conclusion could be made nevertheless, as it is clear that at least some part of the α-toxoid from Clostridium perfringens was adsorbed at the surface of the o/w-NP (Fig. 61).

The loading of o/w-NP with the two toxoids could be achieved when using the nonionic surfactants PVA and Tween 20 for the preparation of the nanoparticles. Furthermore, the SDS-

NP and sodium cholate-NP could be used for the α-toxoid from E.coli, but not for α-toxoid from Clostridium perfringens. The CTAB-NP are not suitable, as precipitation occurred regardless which of the two toxoids were used. Apparently, the cationic nanoparticles interacted with compounds in the protein solution. The protein solution was manufactured with E.coli or Clostridium perfringens and the purity was under 50%. Recombinant proteins solutions with such a poor purity can contain DNA and proteolytic degradation products, which can lead to aggregates with ionic substances (Seetharam and Sharma, 1991).

The characteristics of the α-toxoid from E. coli are similar to those of BSA and OVA regarding its size. It has a molecular weight of 43kDa, OVA has a molecular weight of 45 kDa and BSA 66 kDa.

The exact mechanism according to which a protein adsorbs to the surface of PLGA nanoparticles is not completely identified (Lynch et al., 2007). Hydrophobic interactions of the protein and the o/w-NP seem to play a role in the adsorption of the protein to the PLGA surface. A prediction of the loading rate for a protein cannot be calculated without experimental testing as the mechanism of the adsorption process is not clear. It can be stated that the surfactants that were used to prepare the o/w-NP had an effect on the amount of protein that was loaded to the surface. Different o/w-NP formulations may lead to different results in regard to the loading rate (Table 17). The properties of the protein are also important for the loading rate, as different proteins result in different loading rates when using the same o/w-NP formulation (Fig. 27).

4.2.1.6 Investigation of possible adsorption mechanisms

To investigate the protein-nanoparticle interaction several experiments were conducted. The loading rate for different proteins at the surface of nanoparticles with different surfactants has been described above. Moreover, the surface area was investigated regarding its influence on the loading of the proteins. Another aspect, which is crucial for a loading of the proteins on the surface of nanoparticles, is the ability of the protein to accumulate on the surface of the nanoparticle. This means that the protein must be surface-active. Therefore, the interfactial

tension of protein solutions was measured to investigate the influence of the surface tension on the loading rate of proteins on the surface of nanoparticles.

The surface tension of the surfactants and the proteins were tested. As expected the surface tension decreases with increasing surfactant and protein concentrations (Table 18 and Table 24). Proteins possess the ability to accumulate at interfaces as they have hydrophilic and lipophilic properties. In comparison, BSA is more surface-active than OVA. The ability of the model proteins to accumulate on interfaces may be one reason, as to why they are adsorbing onto the nanoparticles.

Table 18: *Surface tension of protein solutions (mean* ± SD; n = 3)

Concentration protein [mg/ml]	Surface tension [mN/m]	
	OVA	BSA
0.1	61.8 ± 0.9	58.8 ± 0.2
0.5	57.9 ± 0.3	56.2 ± 0.2
1	56.5 ± 3.9	53.8 ± 3.2

The exact physicochemical interaction between proteins and nanoparticles remains not fully understood (Fleischer and Payne, 2012; Lundqvist et al., 2011; Lundqvist et al., 2008; Lynch et al., 2007). Simple ionic interactions are not the driving force for the nanoparticle-protein complex, as the proteins showed to be adsorbed on anionic surfaces in conditions above their isoelectric point, meaning that the protein itself was also negatively charged. If ionic interactions are responsible for the nanoparticle-protein interaction negatively charged proteins could not adsorb at SDS-NP or sodium cholate-NP. It has been discussed that hydrophobic interactions are responsible for the PLGA-protein complex (Chen et al., 2004; Rahman et al., 2013). A prediction, as to how high an adsorption of a protein is to a given nanoparticle formulation cannot be made, as of now each protein must be tested individually for each nanoparticle formulation.

The fact that proteins adsorb at the surface of nanoparticles must be carefully considered before administration of nanoparticles in-vivo, as proteins in the blood can interact with the nanoparticles.

Also, experiments with nanoparticles in the cell culture must be revisited, when surface modifications are responsible for certain interactions with cells, e.g. uptake in cells. The conditions in-vivo are much more complex and adsorption of proteins onto the surface of nanoparticles can change their properties and thereby change their interactions with cells. Protein free media or even PBS as media should therefore not be used for nanoparticle cell culture experiments as results are most likely not applicable for in-vivo conditions.

4.2.1.7 Stability of nanoparticles

The o/w-NP were tested regarding their stability to determine, if fresh samples must be produced for further experiments or if o/w-NP were sufficiently stable over a prolonged period of time.

The o/w-NP formulations were stored at different temperatures, and either as nanoparticle suspensions or as freeze dried nanoparticles. All samples were stable over 4 weeks regarding their particle size properties when stored at 4 °C as nanoparticle suspensions (Table 19). However, the nanoparticle suspensions were not stable when stored at -20 °C or 20 °C. Surprisingly, the nanoparticle suspensions were not completely re-dispersible by simple shaking after storage at -20 °C, as aggregates were clearly visible. The nanoparticle suspensions were re-dispersible by ultrasonication for 5 minutes. However, this was not necessary for the original nanoparticle suspension before storage.

Ultrasonication can be harmful to proteins, therefore it should be avoided for specific nanoparticle formulations, as mild processing conditions were a major driver for the development of these nanoparticles. That is why the samples are listed as instable, when stored at -20 °C.

Freeze dried nanoparticles were stable over 4 weeks of storage at 4 °C and easily re-dispersible, except for the CTAB-NP. Trehalose was added to the nanoparticle suspension at a concentration of 5% prior freeze drying as a cryoprotectant.

Table 19: *Stability of o/w-nanoparticles over 4 weeks storage; Samples were stored either as nanoparticle suspension at -20 °C, 4 °C or 20 °C or as freeze dried nanoparticles at 4°C. (-) indicates that sample was not redispersible or aggregation occurred*

Nanoparticle formulation	Nanoparticle suspension			Freeze dried nanoparticles
	-20 °C	4 °C	20 °C	4 °C
PVA-NP	-	146.9 nm	-	139.3 nm
Tween 20-NP	-	183.2 nm	-	173.3 nm
Sodium-cholate-NP	-	126.7 nm	-	164.6 nm
SDS-NP	-	211.9 nm	-	187.4 nm
CTAB-NP	-	220.7 nm	-	-

4.2.1.8 Characterization of Lipopolysaccharides loaded nanoparticles

The findings about the nanoparticles with the surface adsorbed protein with different surfactants showed a simple method to prepare protein loaded, polymeric nanoparticles. Derived from this method, LPS-NP were prepared, by using the emulsification-evaporation method. LPS-NP were developed to be used as an adjuvant formulation to be applied in combination with an antigen. Here, LPS was added to the outer water phase during the emulsification-evaporation method, technically acting as the surfactant, leading to polymeric nanoparticles with surface adsorbed LPS. LPS-NP are currently investigated regarding its potential as vaccine adjuvants (Gómez et al., 2008). In this work, a novel preparation of the LPS-NP was employed.

LPS-NP were prepared by a simple emulsification-evaporation method and the active ingredient LPS also operated as the surfactant so that no additional surfactant was necessary. The resulting LPS-NP had a LPS concentration of 1 mg/ml and a PLGA concentration of 2.5 mg/ml. As the quantitative measurement of LPS is normally very complex (Binding et al., 2004) an indirect method was applied to quantify the amount of LPS on the nanoparticles. FITC-labeled LPS was used to prepare LPS-NP, afterwards the nanoparticles were centrifuged and the supernatant was

tested regarding its FITC-LPS content. It was observed that almost 70% of the LPS was bound to the nanoparticles (Table 20). The prepared LPS-NP had a particle size with a mean diameter of around 200 nm. This particle size was desired as LPS-NP in that size range showed an improved immune response in mice in previous studies (Gómez et al., 2008). The L2 formulation was subsequently used as an adjuvant formulation in combination with CpG in the mice studies, as LPS and CpG are PAMPs and therefore TLR-4 receptor agonist that induce dendritic cell maturation and T-lymphocytes activation.

Table 20: *Particle size and loading rate of LPS-NP (mean ± SD; n = 3)*

Sample	LPS formulation	Mean diameter [nm]	Loading rate [%]
L1	2 ml of LPS-solution [1 mg/ml]	227 ± 13	-
L2	4 ml of LPS-solution [1 mg/ml]	175 ± 8	-
L3	3.8 ml of LPS-solution [1 mg/ml] + 0.2 ml FITC-LPS	179 ± 2	68 ± 2

4.2.2 Cell culture experiments

The investigation of toxicity of nanoparticles was conducted using a RAW 264.7 cell line. The uptake as well as the localization of the nanoparticles in the cells following incubation was also investigated.

4.2.2.1 Cytotoxicity of nanoparticles

The cell viability after incubation with the o/w-NP was tested using a MTT-assay as described in chapter 3.6.2.1. It was observed that the anionic SDS-NP and sodium cholate-NP were untoxic as the cell viability was between 80-100% regardless of the applied nanoparticle concentration (Fig. 30). The same untoxic effect on the cell viability was seen when using the nonionic PVA-NP. The cell viability was above 90% for all nanoparticle concentrations that were tested. However, when testing the nonionic Tween 20-NP, a toxic effect was clearly visible. For a Tween 20-NP concentration of 3 mg/ml a cell viability of less than 20% was determined. CTAB-NP were even more toxic compared to the Tween 20-NP as a cell viability of less than 20 % was detected when using a CTAB-NP concentration of only 0.3 mg/ml.

It must be kept in mind that different surfactant concentrations were used for the preparation of each formulation (Table 15). This partly explains why the SDS-NP do not show any toxicity as the used SDS concentration in the nanoparticle preparation was just 0.01%. Tween 20 on the other hand was used at a concentration of 1%.

It can be concluded that for further studies a nanoparticle concentration of 0.1 mg/ml is suitable for experiments as problems regarding the cell viability are minimal.

However, Tween 20-NP and CTAB-NP did show a toxic effect on the cells. This toxicity has to be carefully monitored for the in-vivo studies. On the other hand, a mild toxicity might be beneficial for immunization studies as it could attract macrophages and dendritic cells.

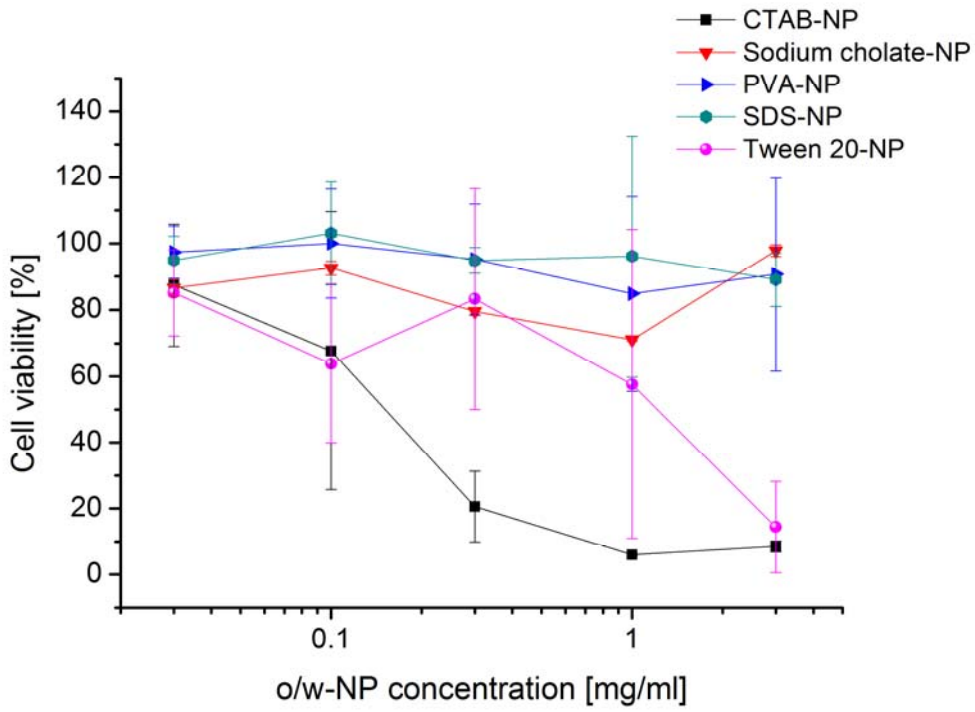

Fig. 30: *Cell viability of o/w-NP formulations using concentrations of 0.03 mg/ml – 3 mg/ml (mean ± SD; n = 3)*

4.2.2.2 Uptake of nanoparticles in macrophages

The uptake of o/w-NP into macrophages was measured as described in chapter 3.6.2.2, after the particles were stained with Nile red. All five available o/w-NP formulations were tested to investigate, if the surfactant has an impact on the cell uptake. Furthermore, it must be considered that the adsorbed OVA on the surface also influence the uptake of the o/w-NP into the cells. The uptake studies were conducted using the RAW 264.7 macrophage cell line.

In preliminary tests it was seen that an incubation period of 2 h is beneficial for investigation as the uptake of the o/w-NP is nearly complete after 2 h (Fig. 62). A slight increase can be observed after 2 h, but the standard deviation increases by 3-5 times at 4-8 h of incubation time, making the results after 2 h much more reliable.

Therefore, each o/w-NP formulation was tested for its uptake into RAW 264.7 cells after 2 h.

The uptake of the nonionic and anionic o/w-NP formulation were similar with an uptake of 37 - 44% (Fig. 31). The Tween 20-NP had the highest uptake of 44% ± 6%. PVA-NP had an uptake of 39% ± 1%, sodium-cholate-NP of 39% ± 2% and SDS-NP of 38% ± 8%. The uptake of the cationic CTAB-NP formulation was significantly lower compared to the other formulations. The uptake of the CTAB-NP was 33% ± 1%.

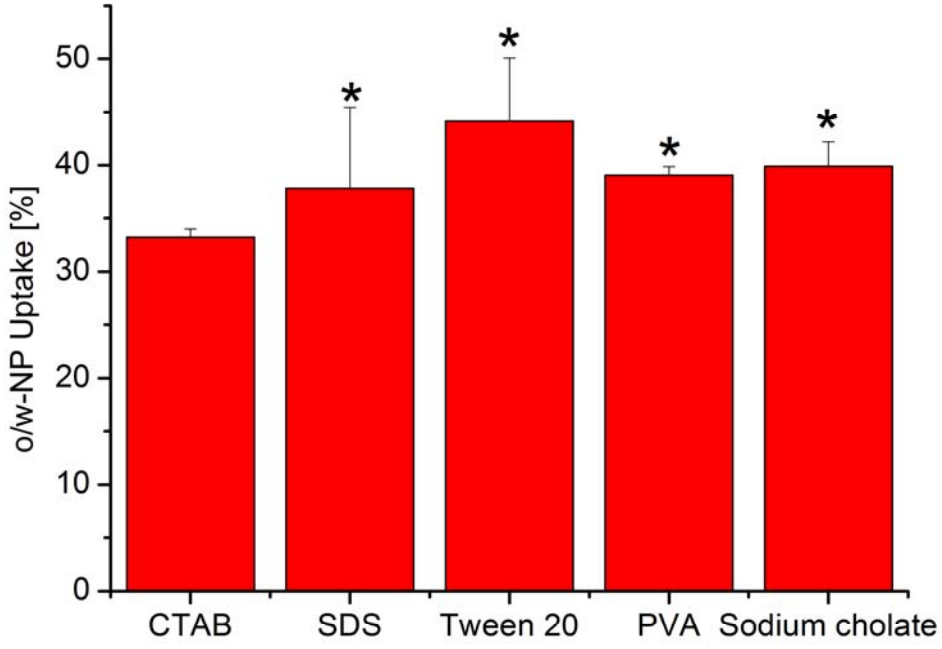

Fig. 31: *Uptake of o/w-NP in RAW 264.7 cells after 2 h (mean ± SD; n = 3; *p < 0.05 compared to CTAB, Kruskal-Wallis one way analysis of variance on ranks followed by Student-Newman-Keuls test)*

4.2.2.3 Localization of nanoparticles in cells (CLSM)

To investigate the localization of the nanoparticles in RAW 264.7 cell, CLSM was applied to nanoparticles that were previously stained with Nile red.

It is clearly visible that for all o/w-NP formulations the particles are located inside the cells as opposed to the cell membrane (Fig. 32). It can be concluded that, the o/w-NP have been taken up into the RAW 264.7 cells. This is important as the results of the uptake studies do not prove that the o/w-NP are really inside the cells. The uptake study only gave a quantitative analysis of the cell associated particles, while the location of the particles remained unknown, because the uptake study only quantified how much of the nanoparticles was adsorbed at the cell membrane or taken up into the cells in total. A differentiation of whether the nanoparticles are located at the cell membrane or inside the cells was not investigated by the uptake study. However, with the CLSM images a qualitative characterization about the localization of the cell associated particles was possible and it could be concluded that the o/w-NP were inside the cells.

The Nile red-NP are accumulating as red dots in the cells. This most likely means that the nanoparticles are not located dispersed in the cytosol, but inside lysosomes and endosomes.

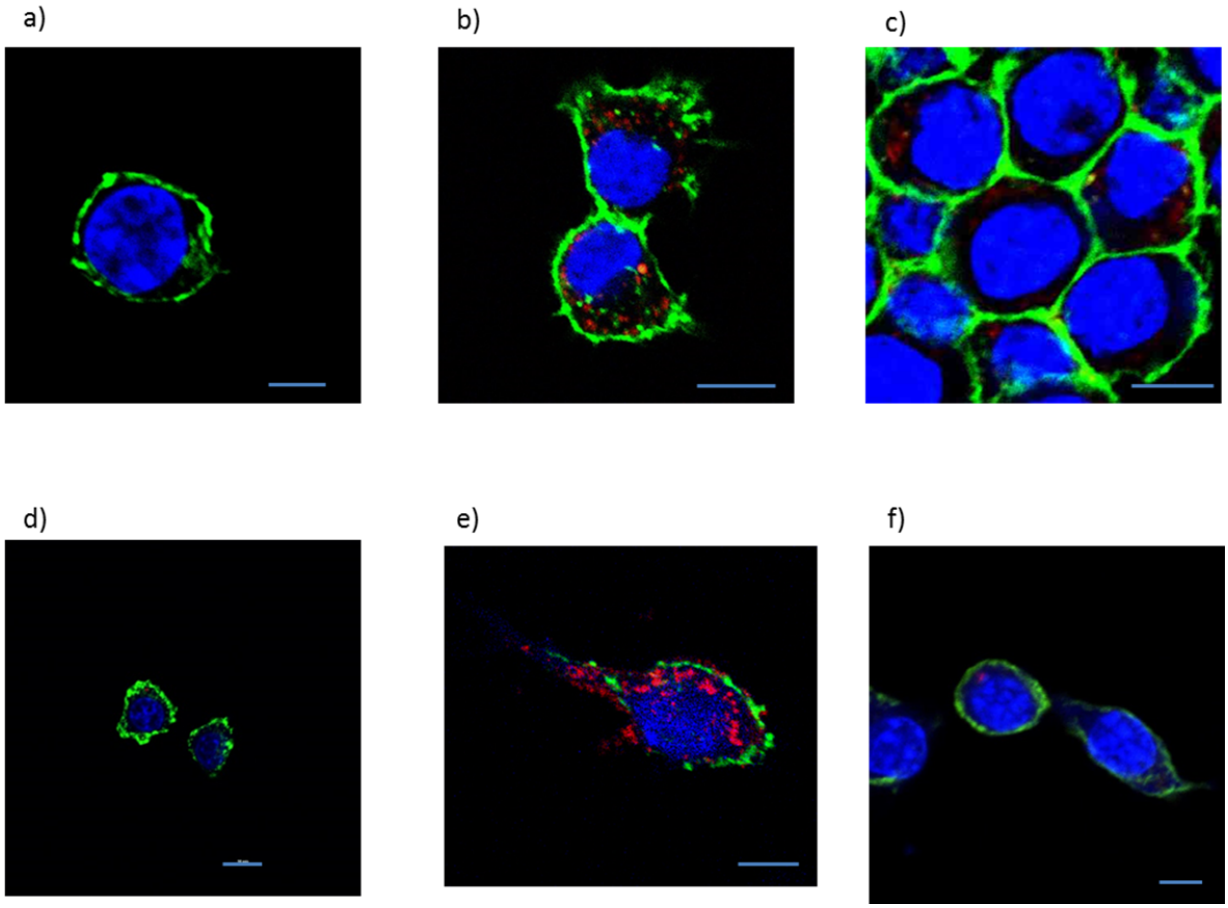

Fig. 32: *CLSM images of RAW 264.7 cells after incubation with different nanoparticle formulations: a) cells without nanoparticles as control b) PVA-NP c) Tween 20-NP d) Sodium cholate-NP e) SDS-NP f) CTAB-NP; Nanoparticles were stained with Nile red (red), cell membrane was stained with concanavalin A (green) and cell nucleus was stained with DAPI (blue). The scale bar represents 10 µm.*

4.2.3 In vivo studies

The ability of proteins to adsorb at the o/w-NP surface was shown in this work. The surface of the nanoparticles was modified, depending on the surfactant that was used. The different formulations were characterized amongst other things regarding their loading rate of the proteins and their ability to be taken up by cells. LPS-NP already showed the potential to increase an immune response (Gómez et al., 2008; Gómez et al., 2009), therefore the LPS-NP prepared in

this work with an emulsification-evaporation method were tested regarding their ability to influence the immune response.

To investigate the adjuvant effect of the o/w-formulations in-vivo studies were conducted. IgG titres were examined to quantify the immune response after immunization. OVA was used as a model antigen, as it already proved to be a suitable antigen in mice for immunization studies (Kasturi et al., 2011) and the IgG concentration was tested using an ELISA-Kit specifically for Anti-OVA IgG. Blood samples were drawn on study day 0, study day 20 and study day 35. The first blood sample was simply to control, if the antibody titer was not elevated before the start of the immunization. On day 20 a low IgG antibody titre was expected, but conclusions about the adaptive immune response cannot be made, as the immune effects are mainly results of the innate immune system. Essential for an evaluation of the adaptive immune response are the IgG-titres at study day 35. After the second vaccination IgG is being released by B-cells, and the concentration reduces very slowly over a prolonged period of time (Dario-Becker, 2013; Schütt and Bröker, 2009).

4.2.3.1 Carbopol and ovalbumin loaded nanoparticles in mice

In the first two in-vivo studies, the nonionic OVA loaded o/w-NP formulations (Tween 20-NP and PVA-NP) were tested regarding their immune response. Carbopol was added as an additional adjuvant as it was unknown, if the o/w-NP itself would elicit an antibody response that is measurable. In both studies 6 groups were tested. The first three groups were OVA loaded Tween-20 NP, OVA loaded PVA-NP and PBS with OVA. The other three groups were exactly the same besides that they also contained Carbopol.

It was expected that there would be no Anti OVA IgG detected on study day zero (SD 0) before the first immunization as the mice did not come in contact with OVA. The food was strictly OVA free.

On SD 20 the IgG titres may already be elevated a little bit as the IgG production starts typically two weeks after the first immunization (Schütt and Bröker, 2009). For non-live, attenuated vaccines, one vaccination is not enough, therefore a second vaccination was performed at SD 20

and blood samples were drawn on SD 35 and SD 42. The IgG titres were clearly elevated on SD 35 and SD 42 (Fig. 33). Moreover, since no IgG was found on SD 0, all mice were evaluable for this study.

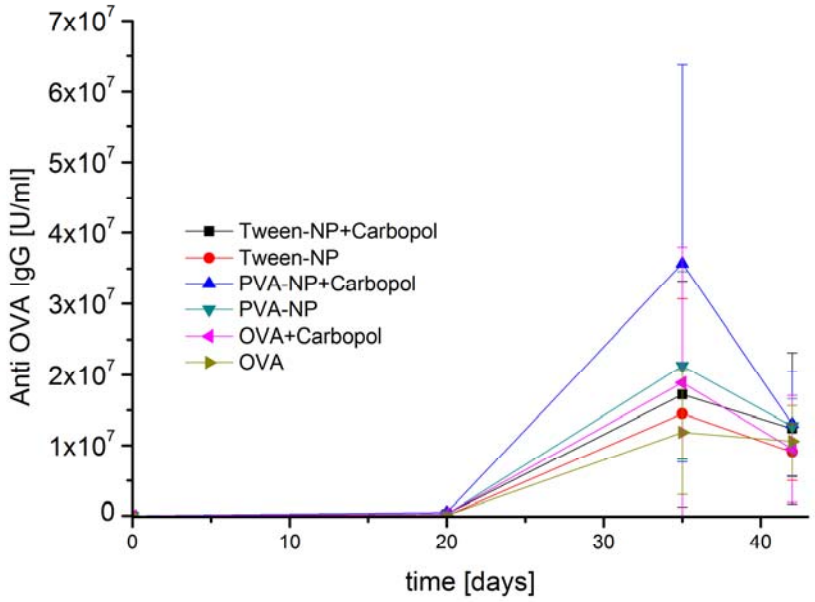

Fig. 33: *Serum IgG-titres of mice after immunization – in vivo study I (mean ± SD, n=4-5), vaccinations on SD 0 and SD 20*

A statistical difference between the groups could not be detected. Differences within the groups were not surprising as the results of in-vivo immunization studies often appear with relatively big standard deviations. However, when examining each group individually, it was surprising that in every group some mice elicit a strong immune response and some no immune response at all (Fig. 34). Even though differences within each groups were expected, it was not expected that some mice showed an immune response following immunization and some did not, when examining the same group. A statistical difference could not be found, because a high variability of the immune response within the groups was detected and a low test population was available.

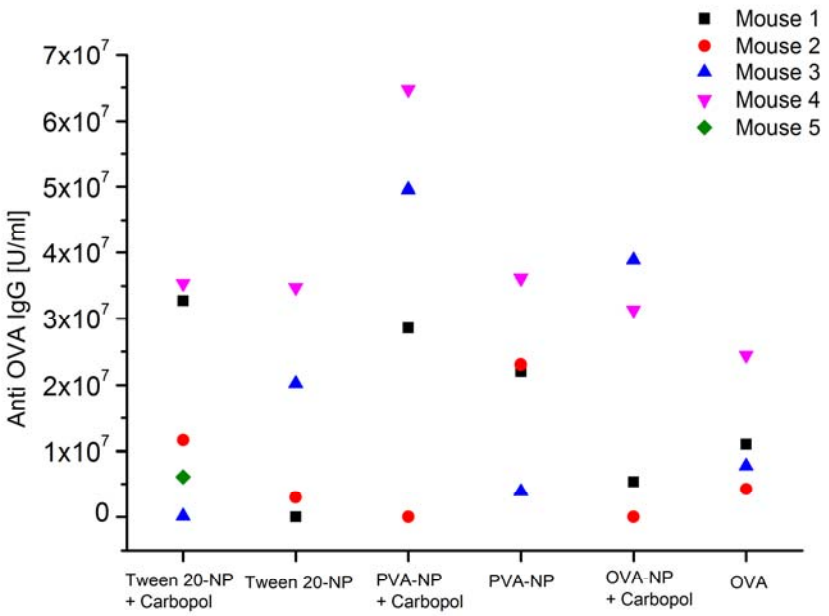

Fig. 34: *Serum IgG-titres of each mouse after study day 35 – in vivo study I (n= 4-5)*

The highest Anti OVA IgG titres were detected for PVA-NP with Carbopol followed by the PVA-NP group. Surprisingly, the control group OVA in PBS with Carbopol elicited a higher immune response than the Tween-20 NP with Carbopol group. However, a statistical difference was not observed as the differences within the groups were considered too high.

Therefore, a second in-vivo study was performed using the same protocol.

Here, the results were in stark contrast to those in the first immunization study. The Tween 20-NP group and the Tween 20-NP with Carbopol group showed the highest IgG titres on SD 35 and SD 42, followed by the PBS with OVA and Carbopol group. Surprisingly, the PVA-NP with Carbopol group did not just elicit a smaller immune response than the PBS with OVA and Carbopol group, but also it did have smaller IgG titres than the PVA-NP group without the additional Carbopol (Fig. 35). However, a statistical difference comparing each group was not found.

As Carbopol is a well-known, widely tested adjuvant it cannot be explained why the group without Carbopol should have elicited a higher immune response, when using OVA loaded PVA-NP.

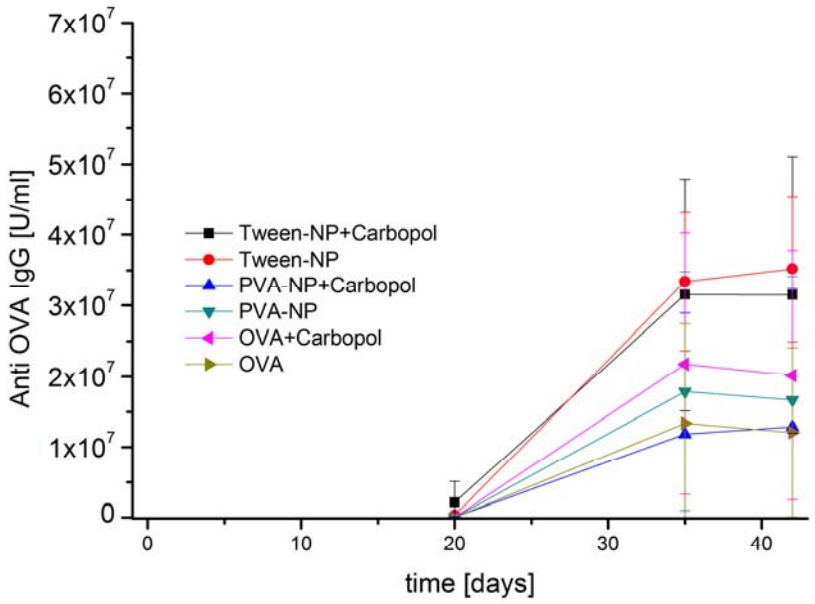

Fig. 35: *Serum IgG-titres of mice after immunization – in vivo study II (mean ± SD, n= 5), vaccinations on SD 0 and SD 20*

When examining each mouse within each group a similar conclusion as to the first immunization study can be made. In every group, except for the Tween 20-NP group, there were mice that showed an immune response and some that did not (Fig. 36). As BALB/c mice are a widely used mice strain for immunization studies these results are very surprising. Differences within each groups are expected, but not a qualitative difference within a group as to if there is an immune response or not.

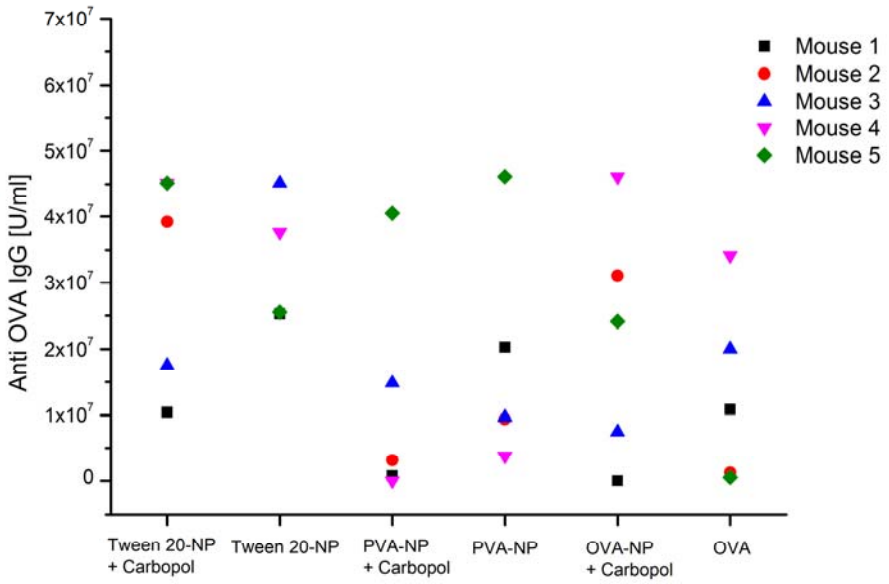

Fig. 36: *Serum IgG-titres of each mouse after study day 35 – in vivo study II (n= 5)*

These results suggest that there may have been a technical error during the immunization. Problems with the mixing of the Carbopol and nanoparticle formulation and erroneous administration of the samples in the neck fold might result in variable IgG titres.

Therefore, further in-vivo studies are necessary to determine, if the o/w-NP do or do not have an adjuvant effect. In-vivo study I and in-vivo study II were inconclusive.

4.2.3.2 In vivo testing of different adjuvants

In the next in-vivo study different adjuvant formulations were tested. CFA/IFA is a well-known adjuvant that elicits very high antibody titres, but is not used in humans or farm animals due to toxicity issues. As the use of this adjuvant is very dangerous, the mice were anaesthetized with isofluran before immunization. CFA/IFA was used as a positive control group. The test groups were LPS-NP with CpG and LPS in solution with CpG. PBS with OVA was used as another

control group to see if the test groups show a beneficial influence regarding the immune response in mice following their administration.

The diagram of the IgG antibody response shows the typical process of an immunization study (Fig. 37). The IgG titres are at 0 U/ml before the first immunization for all formulations, meaning that the mice did not possess any Anti OVA IgG before the study. Before the second immunization at SD 20, the IgG titres are not higher than 5×10^6 for any group. This is also typical for immunization studies, where the immunizations are three weeks apart. Following the first immunization IgG starts to be build up after two weeks, but a fast decrease of IgG occurs afterwards (Schütt and Bröker, 2009). After the second immunization, a high IgG concentration is immediately existent that decreases very slowly over a long period of time, depending on the intensity of the immune response.

As expected, the CFA/IFA formulations showed the highest immune response (Fig. 37). The difference to the other groups was significant. In addition, the LPS-NP group was significantly better than the LPS and PBS group regarding its antibody response.

Here, it was shown that the LPS-NP caused a significantly higher antibody response than the LPS solution, meaning that the TLR-4 agonist LPS is taken up by dendritic cells and macrophages to provoke a strong immune response. LPS is one class of PAMP that leads to the maturation of dendritic cells and subsequently to the activation of T-lymphocytes (Gómez et al., 2009).

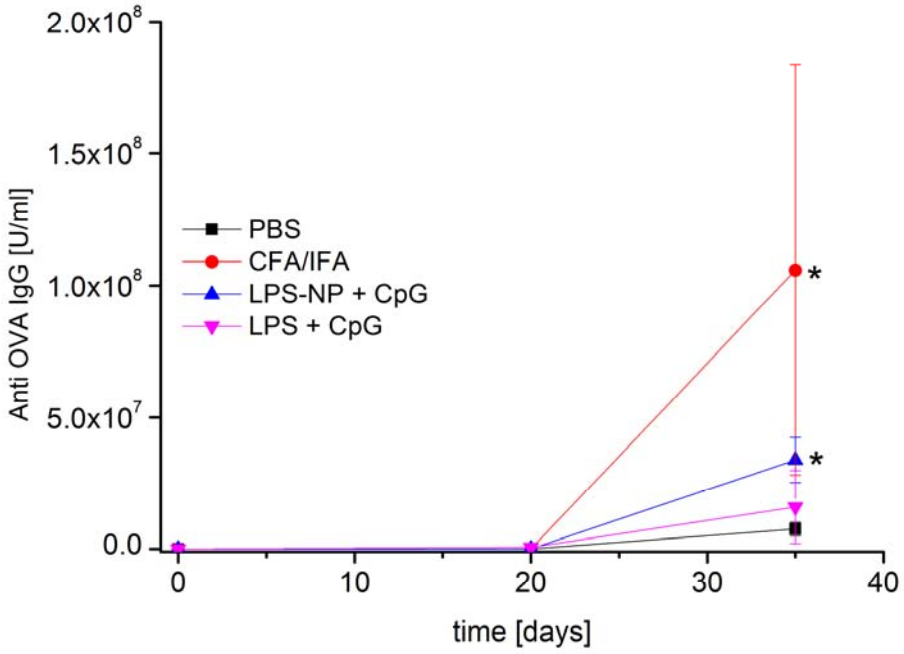

Fig. 37: *Serum IgG-titres of mice after immunization – in vivo study III (mean ± SD, n= 5-6; *p < 0.05 compared to PBS and LPS + CpG, Kruskal-Wallis one way analysis of variance on ranks followed by Student-Newman-Keuls test)*

When comparing the IgG titres of each mouse within each group, it is clearly visible that this immunization study is much more viable than the first two immunization studies (Fig. 34, Fig. 36, Fig. 38). The elicited antibody response is much more homogenous in in vivo study III compared to the first two in-vivo studies.

This strongly suggests that in the first two immunization studies a methodical error occurred during the immunization.

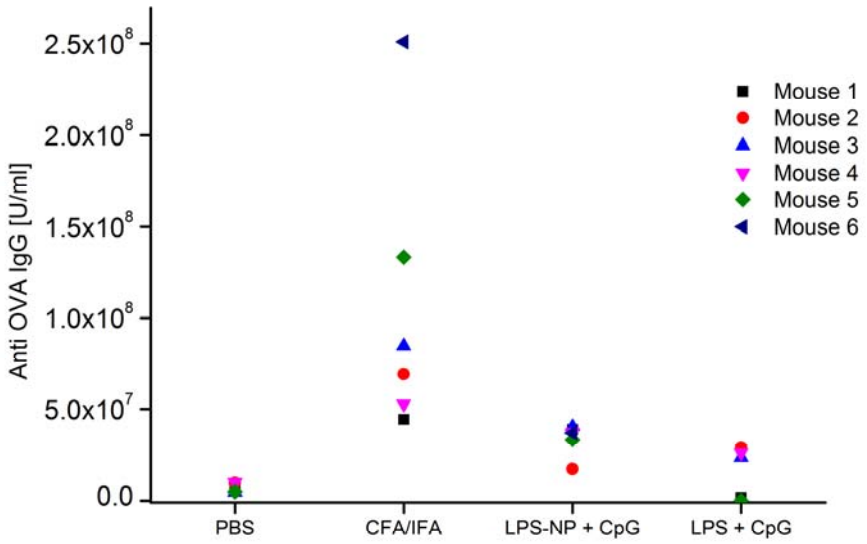

Fig. 38: *Serum IgG-titres of each mouse after study day 35 – in vivo study III (n= 5-6)*

It can be concluded that LPS-NP are favorable compared to LPS in solution. The immune response in the LPS-NP and LPS in solution group is of course also a consequence of the CpG, but since it was present in both groups, the difference between the groups can be attributed to the usage of nanoparticles. The nanoparticles are able to get inside the cells, TLR are located at the cell surface as well as inside cells at endosomes. The application of LPS-NP is advantageous as LPS does not only fulfill its agonistic properties on TLR on the cell surface, but also inside the cells on endosomes following a better uptake into the cells with the nanoparticles.

4.2.3.3 Lipopolysaccharides loaded nanoparticles and ovalbumin loaded nanoparticles in mice

The next in-vivo study was performed to test the different OVA loaded o/w-formulations regarding their ability to enhance the immune response compared to LPS-NP with OVA. As OVA is located onto the surface of the o/w-NP, it is fast released and can be recognized immediately by cells of the immune system, like dendritic cells and macrophages. Due to its adsorption on nanoparticles, OVA might even be better taken up by cells compared to OVA alone.

It must be noted that the loading rate of the different o/w-NP formulations were different. Since no washing step was performed, all formulations had the same OVA amount within one nanoparticle suspension, but the ratio of OVA loaded on the o/w-NP and OVA in solution was different, e.g. for the CTAB-NP no loading was observed.

All o/w-NP formulations that were injected also contained LPS-NP and CpG in the same concentration as in the control group.

As already shown in the previous in-vivo studies, the time-diagram of the antibody response had a typical progress (Fig. 39).

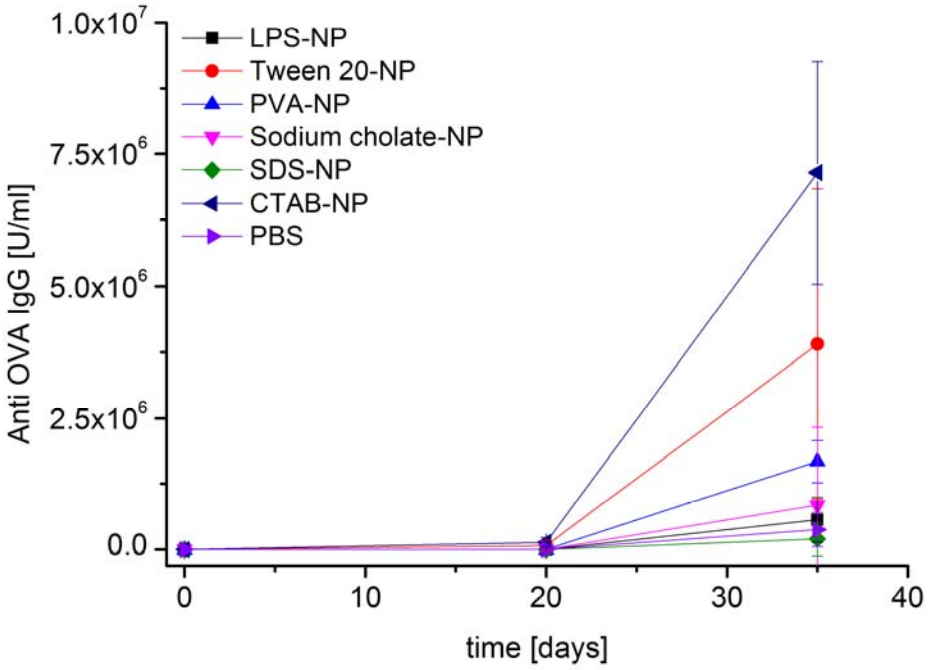

Fig. 39: *Serum IgG-titres of mice after immunization – in vivo study IV (mean ± SD; n= 5-6)*

The CTAB-NP showed the highest immune response following administration in mice (Fig. 40). The antibody response was significantly higher compared to all other groups. The OVA loaded Tween 20-NP and OVA loaded PVA-NP elicited a significantly higher immune response compared to the control group PBS without additional LPS, but the difference compared to the control group with LPS-NP was not significant. The anionic o/w-NP formulations did not provoke a higher immune response than the PBS control group.

For the SDS-NP it can be assumed that the SDS linearizes the protein, therefore reducing its immunogenic properties. It was expected that significantly higher immune response would be produced by the other formulations, because of the good cell uptake of the PVA-NP, Tween 20-NP and sodium cholate-NP into macrophages coupled with high loading rates for these o/w-NP formulations. The loading of the nonionic o/w-NP was relatively high (71% - 83%). In cell culture studies it was already shown that nonionic o/w-NP can be taken up by cells and that they are located inside the cells. However, a significant effect regarding their antibody response in

mice was not observed. It can be hypothesized that the cell uptake and delivery of the protein into the cells of the immune system is not the mode of action here, but that the toxic properties of the nanoparticles play an important role.

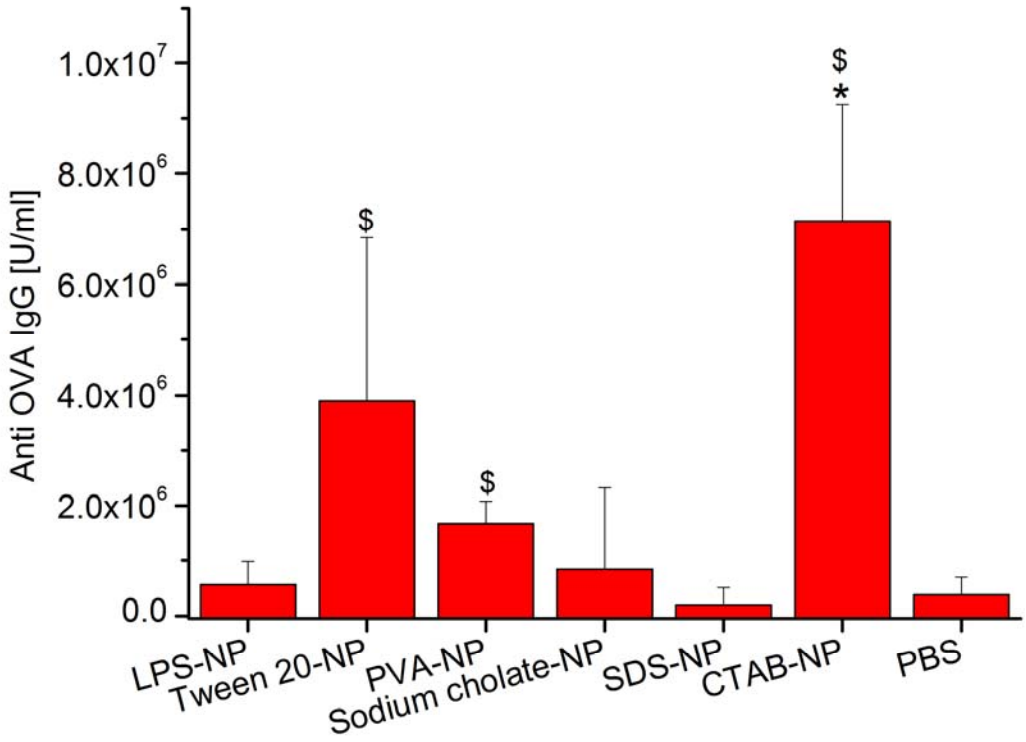

Fig. 40: *Serum IgG-titres of mice after immunization at SD 35 – in vivo study IV (mean ± SD; n= 5 – 6; *p < 0.05 compared to I, $p < 0.05 compared to VII, Kruskal-Wallis one way analysis of variance on ranks followed by Student-Newman-Keuls test)*

The high immune response of the CTAB-NP might be explained by their toxic characteristics. As previously described, the CTAB-NP and Tween-NP showed the highest toxicity in the cell culture model using RAW 264.7 cells. Those two formulations showed the highest antibody response after immunization in mice. The Tween-NP showed a good loading with OVA, but the CTAB-NP were not loaded at all with OVA. Therefore, the effect of an enhanced cell uptake via

nanoparticles of OVA cannot be the reason for the high immune response. More likely is that, because of its toxic potential, cells of the immune system are being released to the injection site, making it more probable for OVA to be processed. This is a mode of action similar to other adjuvants, where the cell uptake is not the primary concern. Many adjuvants induce an inflammation, e.g. CFA/IFA and Alum, thereby activating the innate immune system and subsequently leading to adaptive immunity in combination with an immunogenic. Therefore, the activation of the innate immune system by the nanoparticles might be responsible for the higher immune response compared to the control group.

4.2.3.4 Influence of nanoparticle concentration on immune response in mice

In the previous in-vivo study it was observed that CTAB-NP had a significant influence on the immune response after immunization in mice in combination with LPS-NP and OVA. The nonionic o/w-NP formulations also elicited high immune responses, but a statistical difference was not obtained. The anionic o/w-formulations showed the smallest antibody response; therefore further testing was conducted without these anionic o/w-NP formulations.

Here, the influence of the nanoparticle concentration was supposed to be determined. As in the previous study, all formulations contained LPS-NP and CpG in the same concentration as in the control group. The concentration of the PLGA-NP was varied, but the surfactant content stayed the same for each o/w-NP formulation. A difference in the immune response could therefore be attributed to the nanoparticles and not to the “free” surfactant in solution.

As already shown in the previous in-vivo studies, the time-diagram of the antibody response had a typical progress (Fig. 41).

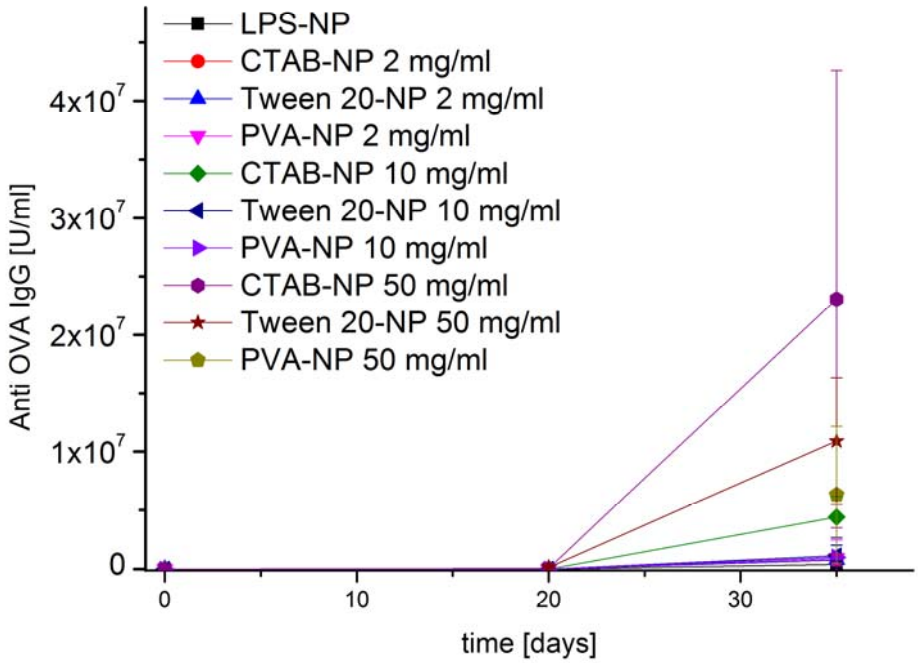

Fig. 41: *Serum IgG-titres of mice after immunization – in vivo study V (mean ± SD, n= 4-5)*

When comparing the IgG titres at SD 35, it can be clearly seen that the dose of the nanoparticles has an effect on the immune response (Fig. 42).

Groups II-IV with a nanoparticle concentration of 2 mg/ml for each o/w-NP formulation have the smallest IgG titres, followed by the formulations with 10 mg/ml, while formulations with 50 mg/ml nanoparticles provoked the highest immune response.

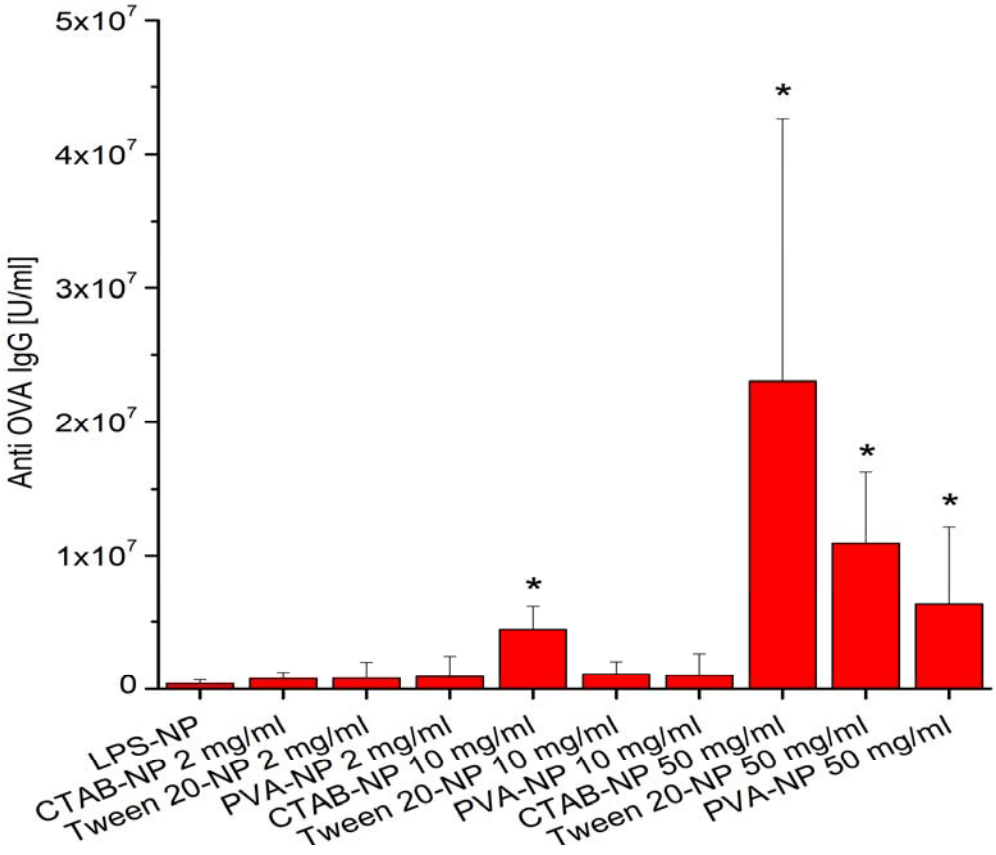

Fig. 42: *Serum IgG-titres of mice after imm*

*unization at study day 35 – in vivo study V (mean ± SD, n= 4-5; *p < 0.05 compared to LPS-NP, Kruskal-Wallis one way analysis of variance on ranks followed by Student-Newman-Keuls test)*

When comparing the CTAB-NP at different concentrations with each other it can be observed that, when using the highest nanoparticle concentration (50 mg/ml), a statistical difference to the other used concentrations (10 mg/ml and 2mg/ml) and to the control group is existing (Fig. 43). As already seen in the previous study, also the CTAB-NP formulation with 10 mg/ml elicits a higher antibody response than the control group. The results of the previous study could be confirmed in that regard.

This clearly means that the concentration of the nanoparticles has an influence on the antibody response in mice. As discussed earlier, an inflammatory effect might be the cause for the immune

response following immunization with CTAB-NP. Therefore, a higher immune response with a higher nanoparticle concentration is comprehensible.

The inflammatory effect of CTAB-NP was visible at a concentration of 50 mg/ml as four out of five mice had a mild inflammation at the injection site. Two weeks after the immunization in the neck fold the immunization was still visible on the neck. This suggests that a strong inflammation occurred during immunization, making the CTAB-NP at such high concentrations inapplicable as adjuvants, as safety and tolerability is of utmost importance for adjuvants. Adjuvants that on the one hand elicit a very strong antibody response and on the other hand are toxic or highly inflammatory are not suitable for parental application. An example for this would be CFA/IFA, high antibody titres can be obtained, when a vaccine is administered with CFA/IFA, but due to toxicity issues CFA/IFA is only used for research and development.

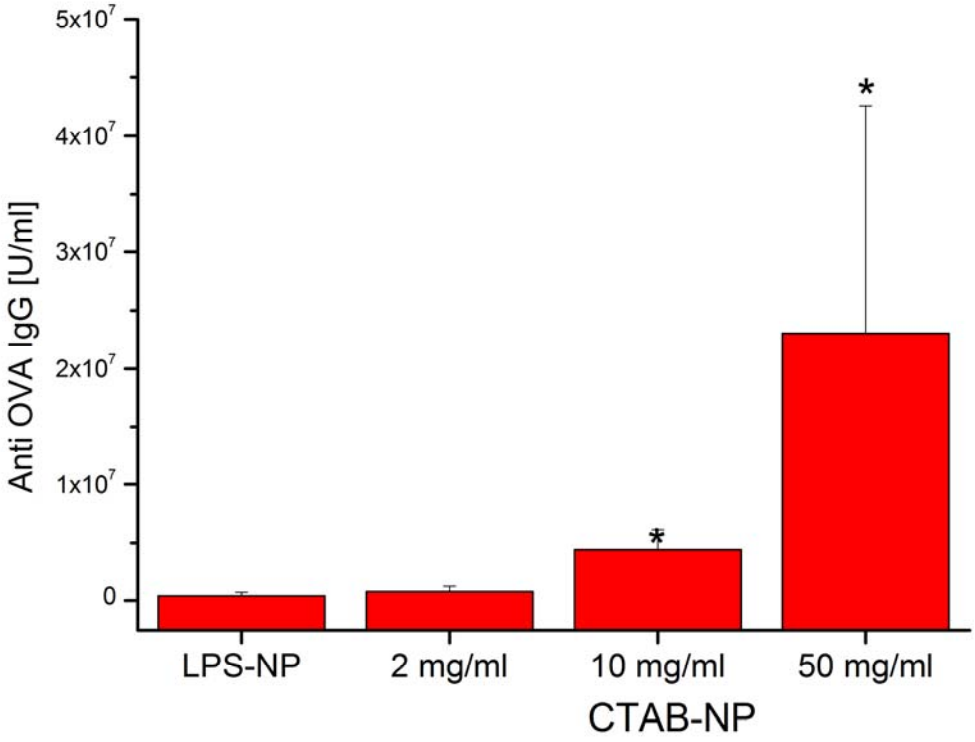

Fig. 43: *Serum IgG-titres of mice after immunization at study day 35 – in vivo study V – CTAB-NP at different concentrations (mean ± SD, n= 4-5; *p < 0.05 compared to LPS-NP, Kruskal-Wallis one way analysis of variance on ranks followed by Student-Newman-Keuls test)*

The PVA-NP showed a similar behavior as the other o/w-NP formulations, as the IgG titres at SD 35 increased with increasing concentrations of the nanoparticles (Fig. 44). The PVA-NP with the highest nanoparticle concentration (50 mg/ml) provoked an antibody response at SD 35 that was significantly higher compared to the control group. The titres caused by PVA-NP at the other concentrations were also higher than the control group, but a statistically significant difference was not observed. The results of the previous study could be confirmed in that regard.

An inflammation at the injection site was not visible for any concentration of PVA-NP that was used for this immunization study, making the PVA-NP better tolerable to the CTAB-NP at the highest concentration, even though it must me noted that the CTAB-NP at 50 mg/ml provoked a much higher immune response than the PVA-NP.

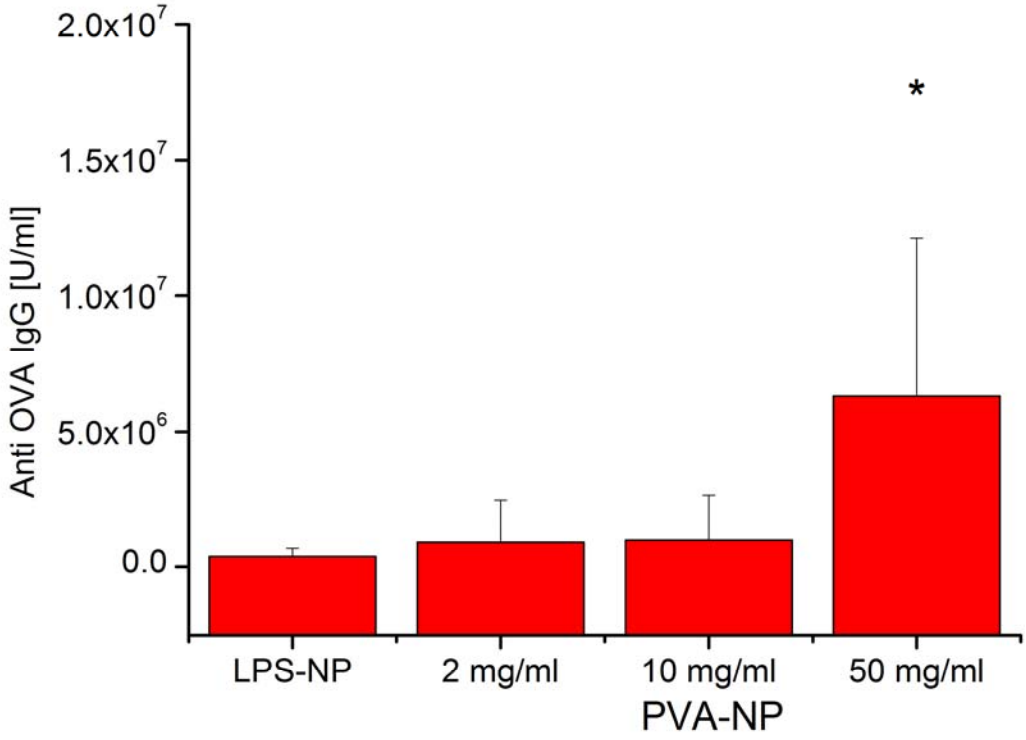

Fig. 44: *Serum IgG-titres of mice after immunization at study day 35 – in vivo study V – PVA-NP at different concentrations (mean ± SD, n = 5; *p < 0.05 compared to LPS-NP, Kruskal-Wallis one way analysis of variance on ranks followed by Student-Newman-Keuls test)*

The Tween 20-NP showed a similar behavior as the other o/w-NP formulations, as the IgG titres at SD 35 increased with increasing concentrations of the nanoparticles (Fig. 45). Tween-NP at a concentration of 50 mg/ml provoked an immune response that was significantly higher than the LPS-NP (control group). At the other concentrations of the Tween 20-NP a significant difference compared to the control group was not observed, even though a slight increase of the immune response was visible when comparing the Tween 20-NP with the control group. The results of the previous study could be confirmed in that regard.

Tween 20-NP like the also non-ionic PVA-NP did not induce any visible inflammation at the injections site, meaning that they are superior to the CTAB-NP regarding their safety and tolerability.

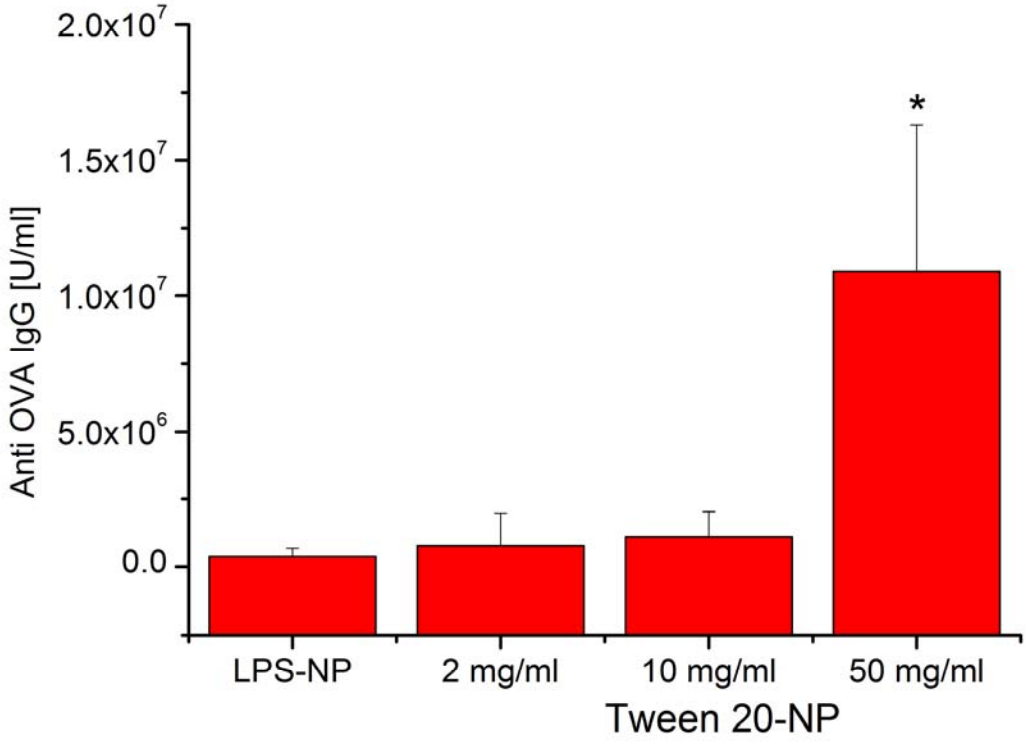

Fig. 45: *Serum IgG-titres of mice after immunization at study day 35 – in vivo study V – Tween 20-NP at different concentrations (mean ± SD, n = 5; *p < 0.05 compared to LPS-NP, Kruskal-Wallis one way analysis of variance on ranks followed by Student-Newman-Keuls test)*

The in-vivo studies revealed insight into the strength of immune responses following the application of different adjuvants.

Surprisingly, the first two in-vivo studies were inconclusive due to huge variations within each group regarding their antibody response after immunization.

The testing of different adjuvant formulations revealed that LPS-NP in combination with CpG are beneficial to LPS in solution in combination with CpG. This is of particular interest as TLR-4 agonists pose as an intriguing way to trigger a strong immune response to obtain adaptive immunity. LPS itself is too toxic to be used in humans, but similar TLR-4 agonists are already

being tested in clinical trials. Preparation of TLR-4 agonists with nanoparticles might be beneficial in terms of the adjuvant effect as the LPS-NP showed an improved immune response compared to the LPS in solution. Furthermore, it was seen that CFA/IFA showed significantly higher antibody responses than the LPS-NP, but the CFA/IFA formulation was just tested to have a positive control. Due to toxicity issues CFA/IFA is obsolete, although very high antibody responses can be produced with CFA/IFA.

The experiments with the five different o/w-NP formulations revealed that the CTAB-NP elicit the highest antibody response. This was particularly surprising as it was previously observed that no OVA was adsorbed at the surface of the CTAB-NP, meaning that the uptake into cells with the nanoparticles was not the mode of action here. Besides, CTAB-NP showed to have the lowest uptake rate into cells in cell culture experiments conducted with RAW 264.7 cells. Rather than a drug targeting with CTAB-NP, an activation of the immune system due to inflammation seems to be responsible for the high immune response. This hypothesis is supported by the fact that the antibody response increases with higher CTAB-NP concentration and inflammation was visible at the injection site for CTAB-NP with the highest nanoparticle concentration.

The antibody response for the nonionic o/w-NP formulations was also slightly increased compared to the control group. The nonionic o/w-NP formulations did not alter the immune response compared to the control at a concentration of the nanoparticles of 10 mg/ml. A significant difference in the antibody response for the nonionic o/w-NP formulations was just observed at the highest nanoparticle concentration, suggesting that a dose-dependent inflammatory effect may also be the mode of action here. Even for low dosage nanoparticle formulations a high loading rate, similar to high dosage nanoparticle formulations, was observed, which leads to the assumption that not the loading rate, but the nanoparticle dosage is deciding for the immune response.

It has been reported that nanoparticles and microparticles with conjugated antigens show a stronger immune response than soluble antigen (Kasturi et al., 2011; Singh et al., 2007). In these studies a size dependent effect was seen, as particles smaller than 10 µm showed a significantly higher immune response (Singh et al., 2007). Nanoparticles in a size range of 50 – 200 nm elicited a stronger immune response than larger and smaller particles (Kuroda et al., 2013). It has

also been previously investigated that dendritic cells are able to internalize PLGA-NP (Hamdy et al., 2011).

However, nanoparticles used in those studies were prepared by a double-emulsion method and it was postulated that the antigen is encapsulated inside the nanoparticle (Blanco and Alonso, 1997; Hamdy et al., 2011; Kasturi et al., 2011; Lamprecht et al., 1999). In this work we showed that the protein is not located inside the nanoparticles, but adsorbed at the particle surface. This does not contest the findings of the other studies, but the mode of action must be revisited, as phagocytosis of the nanoparticles with the encapsulated antigen was considered crucial for the stimulation of the immune system (Kuroda et al., 2013).

LPS loaded nanoparticles combined with antigen showed a proinflammatory effect, which ultimately led to an increase of the immune response in mice studies (Demento et al., 2009). In the study of Demento et al. it was also hypothesized that the antigen encapsulated in a nanoparticulate carrier was better internalized into the dendritic cells.

However, the strongest immune response in this work was observed for CTAB-NP, which did not have OVA adsorbed at the particle surface. OVA was dissolved in the nanoparticle suspension, suggesting that an uptake into the cells with the nanoparticle was not important for the strong antibody response. Moreover, it can be hypothesized that the CTAB-NP activate the immune system due to their toxic surface properties. The toxicity has been previously discussed (see 4.2.2.1).

The potential of nanoparticles as vaccine adjuvants has already been tested in-vivo and proven successful in regard to a significantly higher immune response compared to soluble antigen (Demento et al., 2009; Hamdy et al., 2011; Kasturi et al., 2011). However, a comprehensive understanding about the mode of action of nanoparticles as vaccine adjuvants is still not available.

Further testing would be required to investigate the exact mode of action of the o/w-NP, prepared in this work. The nonionic o/w-NP were only an improvement at a nanoparticle concentration of 50 mg/ml, regarding their adjuvant capabilities. The CTAB-NP were showing an adjuvant effect at lower concentrations, but those nanoparticles are most likely not suitable for vaccinations, due

to their toxic potential. An inflammation was visible at the injection site in the mice studies conducted in this work, when using CTAB-NP.

PLGA nanoparticles already showed to increase the immune response as vaccine adjuvants in mice. However, further studies are necessary, to determine if the nanocarriers are an improvement to alternative adjuvant systems as PLGA-NP are very expensive and the toxic effects following administration might outweigh the benefits.

4.3 Microparticles prepared with double-emulsion-solvent-extraction method

All microparticle samples were prepared using the double-emulsion-solvent-extraction method, because it is a suitable technique to encapsulate hydrophilic drugs like proteins into microparticles, and it can be easily performed in the laboratory without needing costly equipment.

Microparticles have long been investigated for their adjuvant potential (O'Hagan and Singh, 2003), in the present work different microparticle formulations were characterized regarding their physicochemical characteristics.

All particle sizes are being portrayed as d_{50} values. All microparticle formulations were loaded with BSA as a model antigen.

4.3.1 Physicochemical characterization of microparticle properties

4.3.1.1 Influence of polymer and surfactant on particle size and loading rate

PLGA is commonly used as a polymer for micro- and nanoparticulate carriers for parental use, as its biocompatibility and biodegradability has been observed and its use is approved for humans by the FDA (Jain, 2000).

When applying the double-emulsion method as described in chapter 3.3.1 with different PLGAs, but not changing anything other in the setting of the preparation, different results regarding the particle size and the encapsulation efficiency (Table 21) are obtained. In this work, the microparticles were prepared under the same conditions to investigate the influence of the polymer on the process.

The particle size increases when the molecular mass of the used polymer increases. RG 502 H has the smallest molecular mass of the tested polymer and yields the smallest particle size. This effect can be attributed to the higher viscosity of polymers with a higher molecular mass, e.g. the

inherent viscosity of RG 502 H is 0.16 - 0.24 dl/g, of RG 503 H 0.32 – 0.44 dl/g, of RG 504 H 0.45 – 0.60 dl/g and of RG 505 0.61 – 0.74 dl/g. When using the same concentrations the inherent viscosity is proportional to the viscosity. As always the same amount of each polymer was used it can be assumed that the viscosity of the polymer phase in the manufacture of the microparticles increases from RG 502 H to RG 505.

The only sample in which the particle size does not increase when the viscosity increases is RG 505, but here the properties of the polymer are a little different to the other tested PLGAs as the end groups are not carboxylated. Therefore, the conditions are not the same as this structural difference also leads to different behavior of the polymer in solution, e.g. regarding its ability to accumulate on interfaces.

Table 21: *Particle size of microparticles prepared with different PLGA's (mean ± SD, n = 3)*

Polymer	D10 [µm]	D50 [µm]	D90 [µm]	Encapsulation efficiency [%]
RG 502 H	13.7 ± 0.6	34.6 ± 6.1	92.0 ± 10.9	54.4 ± 2.5
RG 503 H	11.3 ± 0.9	59.9 ± 1.0	87.9 ± 0.9	42.7 ± 1.5
RG 504 H	16.7 ± 15.2	65.3 ± 19.7	95.7 ± 18.3	65.9 ± 10.5
RG 505	10.6 ± 2.0	56.3 ± 13.1	86.7 ± 21.8	55.6 ± 3.7

The microparticle formulations were further tested regarding their encapsulation efficiency. The microparticles were loaded with BSA. When comparing the different PLGAs with each other no clear correlation to the viscosity or the particle size was observed (Fig. 46). The encapsulation efficiencies were between 42% - 66%, if no Span 60 was added to the oil phase during the preparation. A statistical difference regarding the encapsulation efficiency was not observed when comparing the samples without Span 60.

Surprisingly, the samples that were prepared with Span 60 showed a very low encapsulation rate, although the other processing conditions remained the same. The same polymers were used to investigate the influence of Span 60.

The encapsulation efficiency was below 7.5 % for all formulations. Theoretically it was assumed that Span 60 would stabilize the interface between the inner water phase and the oil phase, and thereby prevent leaking of the protein. However, it was observed that the opposite effect was happening leading to very low encapsulation efficiencies, when using Span 60 in the oil phase.

Therefore, Span 60 was not used for further studies as poor encapsulation efficiencies are not acceptable, especially when working with proteins, which are in general very expensive.

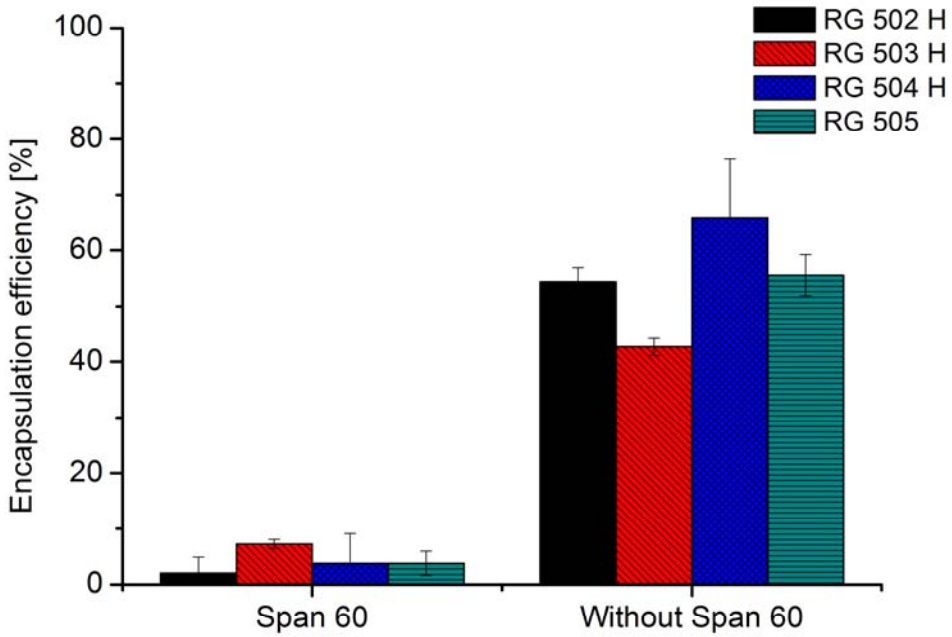

Fig. 46: *Influence of Span 60 in the inner water phase on the encapsulation efficiency of microparticles prepared with different PLGA's (mean ± SD, n = 3)*

4.3.1.2 Influence of emulsification process on particle size and loading rate

The conditions of the preparation method were further altered regarding the emulsification process. The rest of the conditions were kept constant, using RG 502 H as a polymer, and no Span 60.

First, the influence of the emulsification of the double-emulsion was investigated. The conditions for the first emulsifications step were kept constant for these experiments. Using different stirring speeds from 500 rpm – 1000 rpm in the second emulsification step, it was observed that the particle size decreased with increasing stirring speed. The first emulsification step is the deciding factor for the particle size, but apparently, the second emulsification step is also important, as higher stirring speeds resulted in smaller particles (Table 22).

Table 22: *Influence of stirring speed of propeller stirrer during emulsification of double emulsion on particle size and encapsulations efficiency (mean ± SD, n = 3)*

Stirring speed of Propeller stirrer [rpm]	D10 [µm]	D50 [µm]	D90 [µm]	Encapsulation efficiency [%]
500	15.3 ± 0.3	64.5 ± 0.3	115.0 ± 9.2	41.7 ± 0.8
850	13.7 ± 0.6	34.6 ± 6.1	92.0 ± 10.9	54.4 ± 2.5
1000	5.0 ± 1.6	24.6 ± 7.2	52.0 ± 9.5	53.5 ± 1.6

Furthermore, the influence of the first emulsification step in the double-emulsion method was tested regarding its influence on the particle size and the loading rate (Table 23). The conditions of the other parameters were kept the same; the second emulsification step was performed by constant conditions using a propeller stirrer.

Three different devices were tested for the first emulsification process, ultrasound using a Sonicatior, and two Ultra turrax devices (UT 8 and UT 18). Both Ultra turrax devices were adjusted to the same speed. However, the machinery itself was different as the UT 18 has more power, which can be attributed to its superior motor.

As expected, the particle size was influenced by the different dispersing instruments. The microparticle samples that were prepared with ultrasound had the smallest particle size; the samples with UT 18 were smaller compared to the ones prepared with UT 8.

Table 23: *Influence of emulsification method during emulsification of primary emulsion on particle size and encapsulations efficiency (mean ± SD, n = 3)*

Sample	Emulsification method for primary emulsion	D10 [µm]	D50 [µm]	D90 [µm]	Encapsulation efficiency [%]
M1	Ultrasonication	1.9 ± 0.8	14.2 ± 6.3	81.1 ± 59.9	83.9 ± 2.0
M2	UT 8	13.7 ± 0.6	34.6 ± 6.1	92.0 ± 10.9	54.4 ± 2.5
M3	UT 18	3.2 ± 0.3	21.3 ± 3.9	40.39 ± 0.7	83.3 ± 2.5

The particle size of microparticles can be altered using a lot of different parameters, when a double-emulsion method is being applied. Especially the emulsifications steps are critical, if adjustments regarding the particle size are being desired. Furthermore, the particle size of microparticles can be adjusted using different polymers, different polymer concentrations and different stabilizers.

4.3.1.3 Release profile

The microparticle samples were tested regarding their in-vitro release profile.

The samples were incubated in PBS and tested over several weeks. An evaporation of the buffer during the release study was not observed, as the samples were kept in Eppendorf cups.

An initial burst was observed for all preparations. The formulations with the smallest particle size (M1 and M3) showed a higher initial burst. After three days no additional release of BSA was observed for those particles. The microparticle formulation with the biggest particle size (M2)

also showed a high immediate release of over 40 %, the release continued to be over 60% after one week.

The release of all formulations was not complete in the experiment, which may be attributed to the fact that due to hydrophobic interactions the BSA can also be adsorbed at the surface of the PLGA microparticles. It is also possible that a complete release of the active compound was simply not done after three weeks. Consequently, longer release studies need to be performed in the future. Release studies described in the literature had duration of 1 day to several months (Determan et al., 2004; Freiberg and Zhu, 2004; Uchida et al., 1995). Results in the literature were not in agreement with each other. Some studies showed the same release profile as presented in this work (Blanco and Alonso, 1998; Ravi et al., 2008; Uchida et al., 1995; Ye et al., 2010), where a complete release was not observed. However, this is most likely due to the short duration of the study. In other studies it was reported that a complete release of the protein is possible (Giteau et al., 2008; Luan et al., 2006; Porjazoska et al., 2004).

It must be stated that due to the acid environment in microparticles following degradation of the polymer the protein is highly stressed. This acid environment might also lead to the inactivation of the encapsulated protein. Previous studies, in which very long release profiles of several weeks to month were reported, must be viewed carefully, as the simple detection of the released amount of protein does not allow a statement on whether it remained still active.

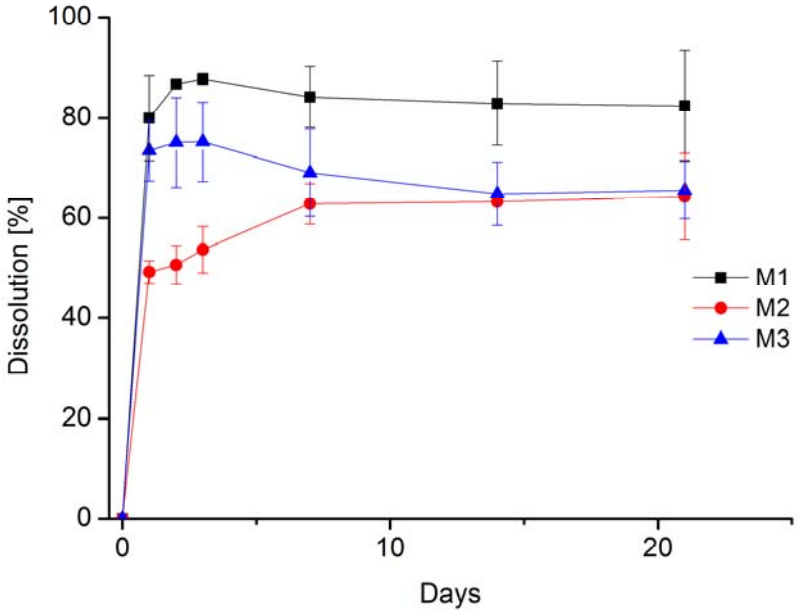

Fig. 47: *Dissolution test of microparticle samples M1-M3 (mean ± SD, n = 2)*

4.3.1.4 Morphology of microparticles

The morphology of the microparticle formulations was investigated using SEM. The formulations with the immediate release within 3 days (M1 and M3) had a different morphology compared to microparticle formulation M2, which had a sustained release over two weeks.

It must be stated that the particles of M1 and M3 formulations were also smaller than of the M2 formulations (Table 23).

The particles of M1 and M3 formulations had an irregular morphology. Some particles were spherical, but some particles had a drop like structure. In addition, the particles with the drop like structure were hollow. It can be stated that the bigger particles within one formulation were of a drop like structure and that the smaller particles were spherical in their morphology.

The M2 formulation was very homogenous, no particles with a drop like structure were found. The particles were round and had a clearly visible sponge like internal morphology. This internal

structure is in agreement with the findings of the dissolution test, where a release of the active compound over two weeks was determined. Protein that was located near the polymeric shell was faster released than protein that was located in the inner core of the microparticle.

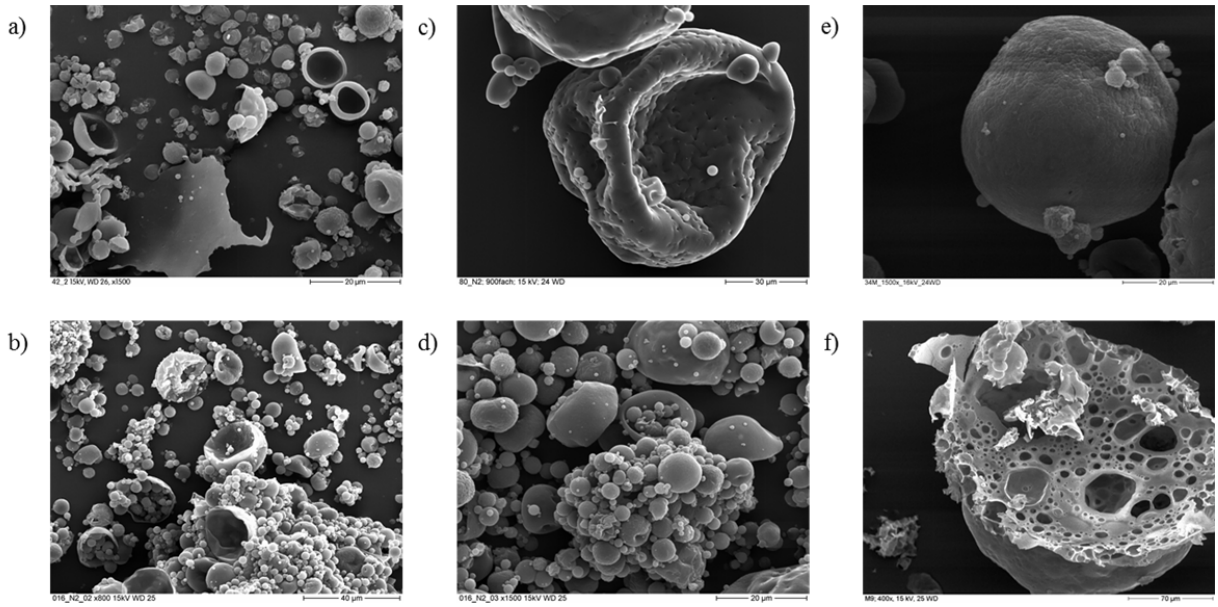

Fig. 48: *SEM images of w/o/w-MP: a) and b) microparticles prepared with ultrasound during first emulsification; c) and d) microparticles prepared with UT 18 during first emulsification; e) and f) microparticles prepared with UT 8 during first emulsification; samples were investigated at 15 kV with magnifications of 400 - 1500 x*

5 Summary and Conclusion

Live, attenuated vaccines consist of virus or bacteria that are not virulent, but have the ability to proliferate. Therefore, a strong immune response can be generated, as the vaccine is distributed throughout the body, due to the proliferation properties of the microorganisms. Mutation of the vaccine can cause the microorganisms to reverse to virulence. Therefore, inactivated, non-live vaccines are more desirable on the grounds of safety issues. However, inactivated vaccines rarely induce a strong enough immune response to achieve adaptive immunity. That is why adjuvants are essential for successful vaccinations (Rosenthal and Zimmerman, 2006).

The objective of this work was to develop protein loaded micro- and nanoparticles as parental carrier systems for the antigen delivery, as particulate, polymeric carrier systems have a huge potential to pose as adjuvants.

Antigens can be encapsulated in microparticles, causing the active compound to be released over several weeks. A pulsatile release would also be possible, mimicking several injections. Moreover, microparticles can even be taken up by cells, if the particle size is below 10 µm (O'Hagan et al., 2006).

Nanoparticles have a similar size as pathogens, making them particularly interesting for antigen delivery. Besides, nanoscale drug delivery systems can enhance the transport of the active compound across absorption barriers, leading to high amounts of antigen within dendritic cells and macrophages (Singh et al., 2007).

In the presented work, microparticles were prepared with a double-emulsion solvent extraction method. The influence of different parameters on the microparticle properties was investigated.

Interestingly, our findings showed that not only the first emulsification process to obtain the primary emulsion is decisive on the resulting particle size, but also the second emulsification process to obtain the double emulsion.

Furthermore, it was discovered that microparticles that contained Span 60 as a surfactant in the oil phase during the preparation, had a significantly lower encapsulation rate than particles

without Span 60. Instead of stabilizing the interfaces Span 60 increased the leakage of the protein from the inner phase to the outer water phase, yielding in low encapsulation rates.

In this work, a physicochemical characterization of nanoparticulate drug carriers was performed to better understand their properties. Protein loaded nanoparticles were prepared using a double-emulsion-method. This technique has been widely described as a simple method to encapsulate a hydrophilic drug inside polymeric nanoparticles (Blanco and Alonso, 1997; Lamprecht et al., 2000b). Moreover, this preparation method is manageable in a laboratory scale, as expensive and big instruments are unnecessary. Many in-vivo studies for various medical applications have been performed with nanoparticles prepared by this method (Jiao et al., 2002; Kasturi et al., 2011).

The biocompatible and biodegradable PLGA, which is an excipient that has already been used in pharmaceutical products, was used as a polymer and BSA was used as a model protein. First, nanoparticles were prepared using different amounts of stabilizer, in this case PVA, in the outer water phase. It was observed that the mean diameter of the prepared particles decreases with increasing PVA concentrations. At a concentration of 0.03% PVA in the outer phase, microparticles were prepared. By increasing the PVA amount to 0.1%, nanoparticles were obtained. Higher PVA concentrations led to a decrease of the particle size of the nanoparticles. Interestingly, the loading rate of the nanoparticles with BSA was almost proportional to the mean diameter of the nanocarriers. The loading rate increased with smaller obtained nanoparticles. This effect is not in accordance to the theory that the active compound is encapsulated inside the nanoparticles. To analyze the loading behavior in detail, the preparation method was modified in the regard that the protein was not present in the inner water phase, but was later added to the outer water phase. For this modified version of the double-emulsion method, the protein was definitely located at the surface of the nanoparticles. Surprisingly, the loading rates for these nanoparticles showed a similar behavior compared to those prepared in the conventional way. Further testing regarding the release profile strengthens the suspicion that the protein is not encapsulated, but located at the surface. A fast release within one hour was observed, and the release profiles of the particles prepared by the conventional method were identical to those prepared by the modified version. A sustained release could only be determined for particles with a mean diameter in the micrometer range. Here, some part of the protein seems to be

encapsulated, as a complete release was not observed after 24 hours. To get a comprehensive understanding of the prepared particles, FE-SEM was used to investigate the morphology of the particles. In previous studies, the imaging techniques were used to determine the shape of nanoparticles and to confirm the particle size (Sahana et al., 2010; Zambaux et al., 1998). However, the internal morphology was never visualized. Therefore, ion-milling coupled FE-SEM was used to reveal the morphology of the nanoparticles. Furthermore, the model protein BSA was substituted with Gold-BSA as Gold-BSA is visible as bright spots in FE-SEM images. The internal morphology was clearly visible using this method and it was observed that most of the gold-labeled protein was located at the surface of the nanoparticles. It was revealed that only particles with a mean diameter above 600 nm contained an inner phase. Thereby, the previously postulated structure of nanoparticles prepared by the double-emulsion method needs to be revisited.

It can be concluded that ion-milling coupled field-emission scanning electron microscopy is a novel approach to characterize nanoparticles and is suitable to visualize the interior morphology of nanoparticles, which has never been described before. The method should be applied to all nanoparticle formulations described in the literature that have an active ingredient encapsulated to determine the interior morphology.

The findings in this work revealed that the double-emulsion method is not a proper preparation technique to produce nanoparticles that have the hydrophilic drug encapsulated inside a polymeric matrix. This should impact further studies regarding protein loaded nanoparticles as novel preparation methods are necessary to ensure that proteins can be encapsulated inside nanoparticles.

Furthermore, it can be discussed, whether the double-emulsion technique qualifies at all as a proper preparation method for nanoparticles loaded with hydrophilic drugs. The method can be altered, by first producing polymeric nanoparticles and in a second step adsorbing the active compound onto the surface of the nanoparticles. Thus, shear stress, pressure and high temperatures can be avoided for the hydrophilic drug.

Taking the previous discoveries into account, a simplified method was used to obtain protein loaded nanoparticles. The particles were prepared using an emulsification-evaporation method

followed by an incubation process, in which the hydrophilic drug, in this case OVA or BSA, was adsorbed at the nanoparticle surface. The obtained PLGA-NP were prepared with different surfactants, yielding in nanoparticles with modified surface properties. The nonionic surfactants Tween 20 and PVA, the anionic surfactants SDS and sodium cholate and the cationic surfactant CTAB were utilized. The particles were characterized regarding their particle size, loading rate with OVA and BSA, as well as their release profile. A fast release within one hour was observed for all formulations. In most cases BSA was adsorbed at a higher rate than OVA on the nanoparticles, an exact mode of action on how the adsorption takes place is still unknown. The different formulations were tested regarding their toxicity and their cell adhesion properties in cell culture experiments. It was observed that the Tween 20-NP and the CTAB-NP showed a toxic potential at concentrations of 1 mg/ml, the other formulations were not toxic for the tested concentrations. The cell uptake of the CTAB-NP was significantly lower compared to the other formulations. This might be due to the fact that the other formulations were loaded with OVA, a loading of the CTAB-NP with OVA was not obtained as the loading rate was 0%.

The five different nanoparticle formulations were also tested for their potential to adsorb Clostridium perfringes α-toxoids. Two different α-toxoids were tested. One was formalin inactivated α-toxoid from Clostridium perfringens and the other was expressed in genetically modified E.coli. Using SDS-PAGE it could be observed that both proteins were not pure, leading to aggregation with the cationic CTAB-NP. The anionic SDS-NP and sodium-cholate-NP were incompatible with the α-toxoid from Clostridium perfringens. PVA-NP and Tween 20-NP showed a satisfying behavior in regard to the compatibility with the proteins. Furthermore, it was discovered that most of the α-toxoid was adsorbed at the surface of the nonionic nanoparticles.

The exact mechanism in which the protein adsorbs to nanoparticles is the target of many studies, but it has not been fully explained (Fleischer and Payne, 2012; Lynch et al., 2007). It is believed that the proteins arrange themselves as a “protein corona” around the nanoparticles (Lundqvist et al., 2011). Hydrophobic interactions seem to be the deciding force during the adsorption of proteins on nanoparticles (Rahman et al., 2013).

In immunization studies with BALB/c mice the immune response following application of the different OVA loaded nanoparticle formulations was determined. CTAB-NP showed a significantly higher antibody response compared to the other formulations. This was very

surprising as OVA was not located at the surface of the CTAB-NP, but was just dissolved in the nanoparticle suspension. An increased transport into the cells with the CTAB-NP was therefore not likely. The second highest antibody response was elicited by Tween 20-NP, which suggests that the toxicity of these two formulations might be the reason for the high antibody response. When investigating the influence of different concentrations of the nanoparticle formulations, it was revealed that at the highest CTAB-NP concentration a severe inflammation at the injection site was visible. This suggests that a pronounced inflammation occurred, leading to an accumulation of cells of the immune system like dendritic cells and macrophages, which are crucial for adaptive immunity.

Another adjuvant formulation that was developed were LPS-NP. LPS are TLR-4 agonists and therefore an interesting substance as they activate and facilitate the maturation of dendritic cells (Foged et al., 2002; Hamdy et al., 2011). An emulsification-evaporation method was used for the preparation of LPS-NP. It was determined that almost 70% of the LPS was bound on the nanoparticles. Using an in-vivo study the adjuvant potential of LPS-NP was investigated. It can be concluded that LPS-NP, when combined with CpG, was significantly beneficial regarding its antibody response compared to LPS and CpG in solution. These findings might be interesting for the development of novel adjuvants, as new TLR-ligands can be used in combination with nanoparticles to improve their adjuvant properties.

The preparation of the protein loaded o/w-NP had several advantages compared to the double-emulsion method as the protein is not exposed to shear stress and temperature, when adsorbing them onto the nanoparticle surface after the preparation step. It can be concluded, that simple adsorption of the protein onto the nanoparticle surface after preparation of the nanoparticles by an emulsification-evaporation method is a suitable technique to obtain protein loaded nanoparticles. Here, it has the advantage, compared to the double-emulsion method, that the “blank” nanoparticles can be freeze dried or stored at 4°C and that the incubation with the protein and following adsorption of the protein onto the nanoparticle surface can be carried out just before administration of the nanocarriers. This is a major advantage, as protein stability only has to be ensured for several hours as opposed to several weeks, when the protein is already part of the final formulation.

Based on the results in this work we can also conclude that the surface properties of nanoparticles play a critical role regarding the ability to enhance an immune response. Surfactants have to be selected carefully as the nanoparticle-protein interactions and the toxicity of the prepared nanoparticles are dependent on the chosen surfactants. It can also be concluded that the protein loaded nanoparticles most likely do not increase the immune response by enhancing the antigen delivery into the cells, but that inflammation induced by the antigen loaded nanoparticles causes a significantly increased immune response compared to the soluble antigen.

6 List of Abbreviations

°C	degree Celsius
API	active pharmaceutical ingredient
BCA	bicinchoninic acid
BSA	bovine serum albumin
CFA	Complete Freund's Adjuvant
CLSM	confocal laser scanning microscopy
CTAB	cetyltrimethylammonium bromide
Da/kDa	Dalton/ kilodalton
DMEM	Dulbecco's Modified Eagle Medium
DMSO	dimethyl sulfoxide
DTT	dithiothreitol
e.g.	Latin: exempli gratia (for the sake of an example)
EE	encapsulation efficiency
ELISA	enzyme-linked immunosorbent assay
et al	Latin: et alii (and others)
FDA	Food and Drug Administration
FE-SEM	field emission-scanning electron microscope
Fig.	figure
FITC	fluorescein isothiocyanate
g	acceleration of gravity
G	Gauge
h	hour
IFA	Incomplete Freund's Adjuvant
IgG	immunoglobulin G
kV	kilovolt
LPS	lipopolysaccharides
min	minutes
MTT	methylthiazolyldiphenyltetrazolium bromide
n	number, e.g. of samples
NP	nanoparticles
o/w	oil-in-water
OVA	ovalbumin
PAGE	polyacrylamide gel electrophoresis
PAMP	pathogen associated molecular pattern
PCS	photon correlation spectroscopy
PDI	polydispersity index
PLGA	polylactid-co-glycolid
PVA	polyvinyl alcohol

rcf	relative centrifugal force
rpm	revolutions per minute
s	seconds
s.c.	subcutaneous
SD	standard deviation
SDS	sodium dodecyl sulfate
SEM	scanning electron microscope
STIKO	german: Ständige Impfkommission des Robert Koch-Instituts
TLR	Toll-like receptor
w/o	water-in-oil
w/o/w	water-in-oil-in-water

7 Appendix

7.1 Substances

Table 24: *List of substances used in this work*

Substance	Manufacturer
Bovine Serum Albumin	Boehringer Ingelheim
CpG	Invivogen
CTAB	Roth
Disodium phosphate	Sigma Aldrich
DTT	Roth
Ethyl acetate	ZVE
FBS	Sigma Aldrich
Freund's Adjuvant, complete	Sigma Aldrich
Freund's Adjuvant, incomplete	Sigma Aldrich
LPS	Sigma Aldrich
Methylene chloride	ZVE
MTT	Sigma Aldrich
Nile red	Sigma Aldrich
Ovalbumin	Sigma Aldrich
Penicillin-Streptomycin	Sigma Aldrich
PLGA	Evonik
Potassium chloride	Sigma Aldrich
Potassium dihydrogen phosphate	Sigma Aldrich
PVA	Kuraray
SDS	Sigma Aldrich
Sodium chloride	Sigma Aldrich
Sodium cholate	Sigma Aldrich
Tween 20	Roth
Tween 80	Roth
α-toxoid	Boehringer Ingelheim

7.2 Supplementary Tables and Figures

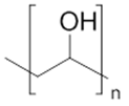

Fig. 49: *Chemical structure of polyvinyl alcohol*

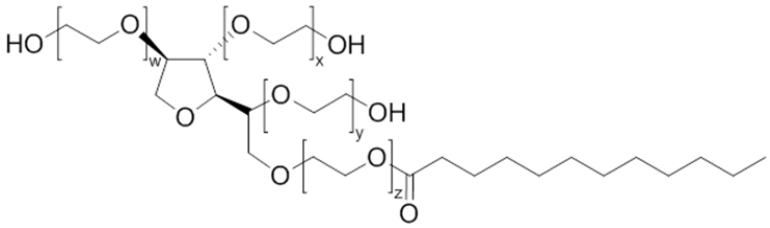

Fig. 50: *Chemical structure of Polysorbate 20*

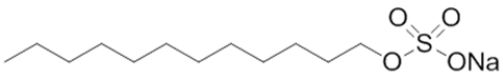

Fig. 51: *Chemical structure of SDS*

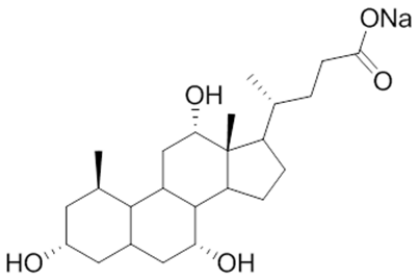

Fig. 52: *Chemical structure of sodium cholate*

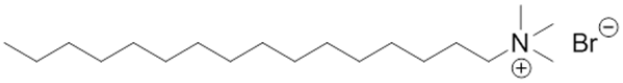

Fig. 53: *Chemical structure of CTAB*

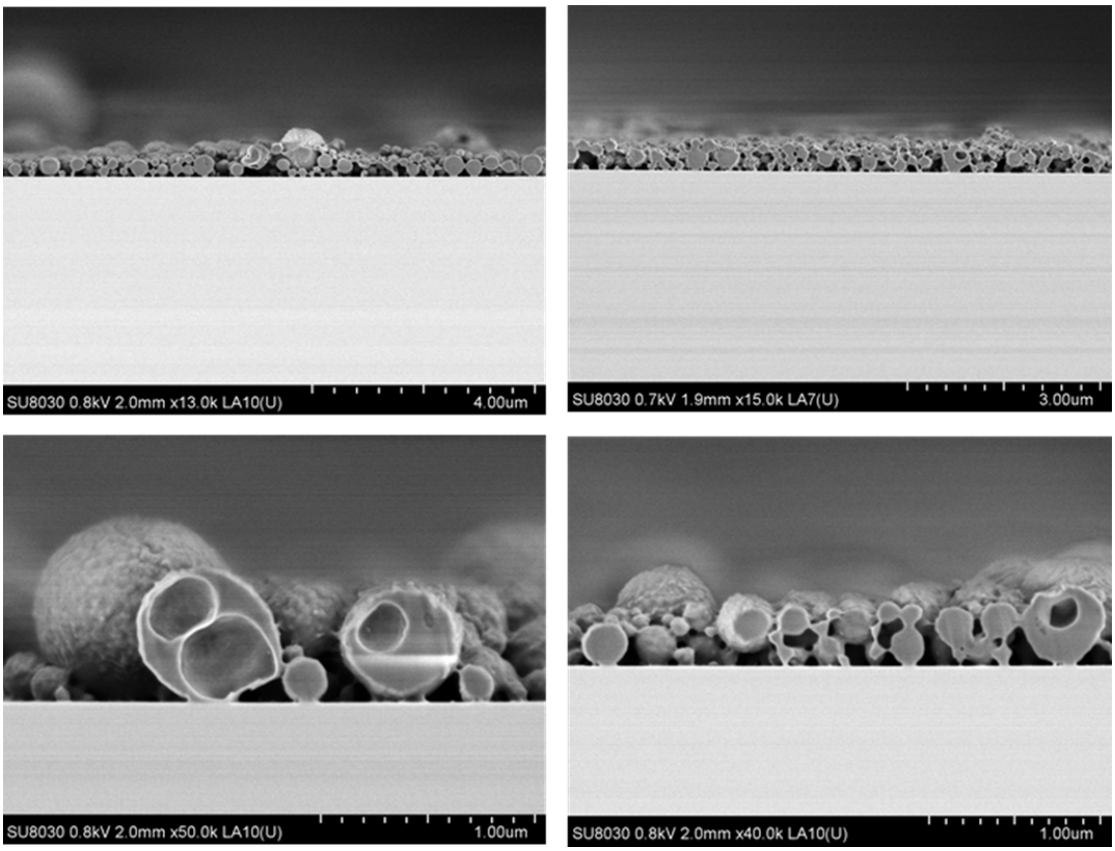

Fig. 54: *FE-SEM images of polyaminomethylmethacrylate-NP prepared by a double-emulsion method at 0.7 – 0.8 kV with magnifications of 13000 – 50000 x after ion milling with an argon beam*

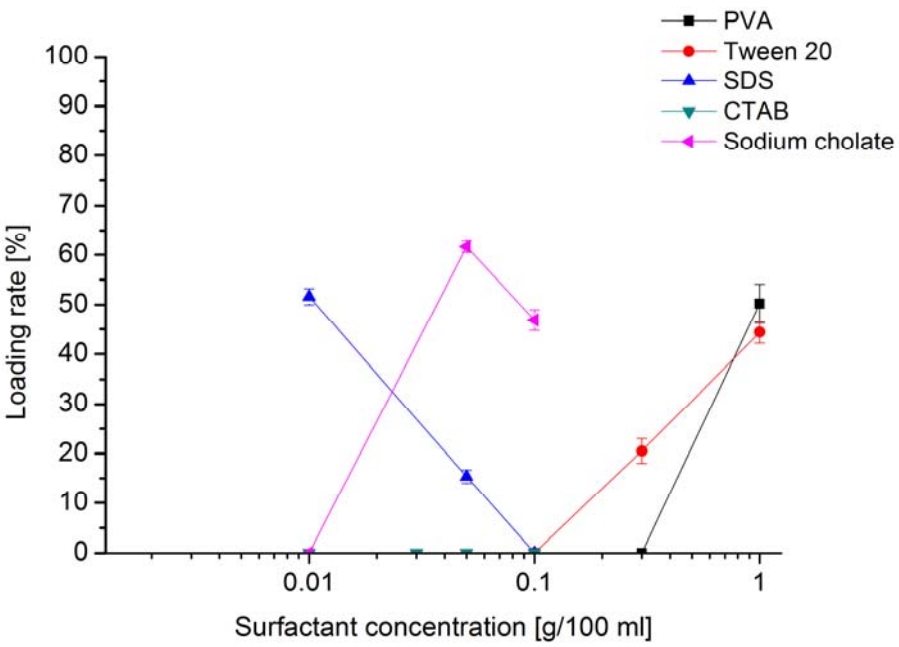

Fig. 55: *Loading rate of O/W-Nanoparticles (10 mg/ml) with 0.5 mg/ml Ovalbumin (mean ± SD, n=3)*

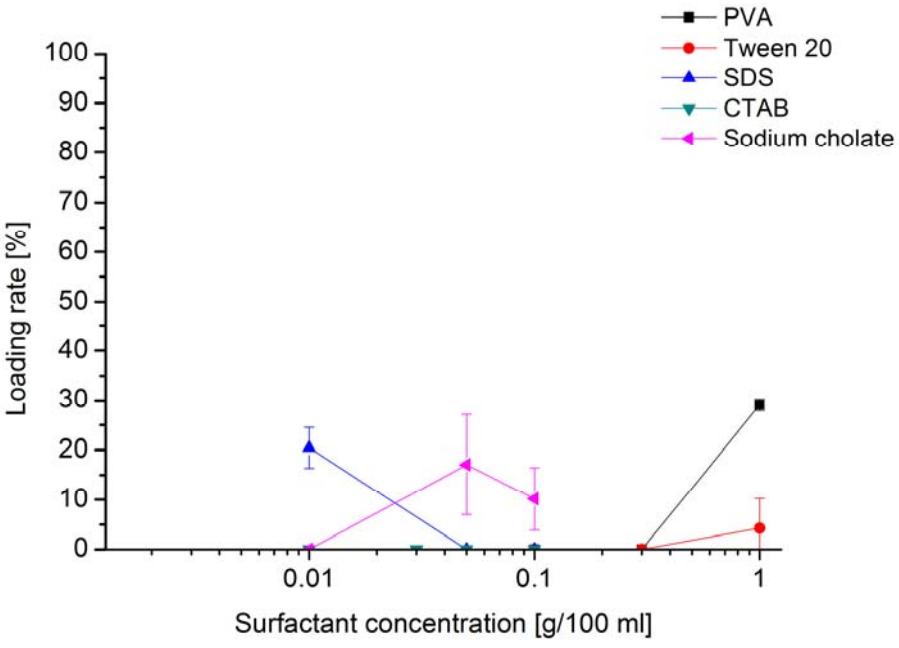

Fig. 56: *Loading rate of O/W-Nanoparticles (10 mg/ml) with 1 mg/ml Ovalbumin (mean ± SD, n=3)*

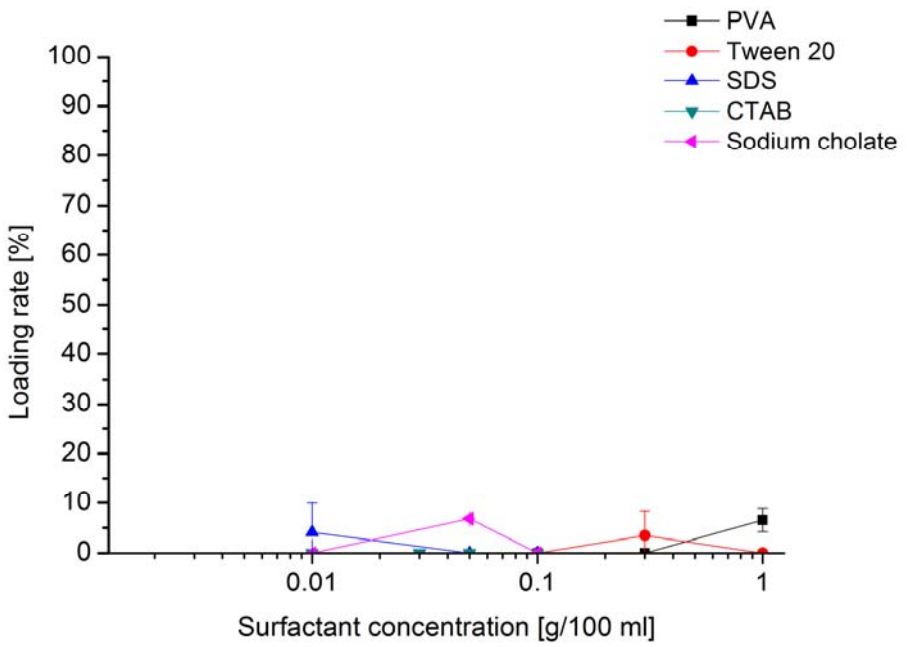

Fig. 57: *Loading rate of O/W-Nanoparticles (10 mg/ml) with 2 mg/ml Ovalbumin (mean ± SD, n=3)*

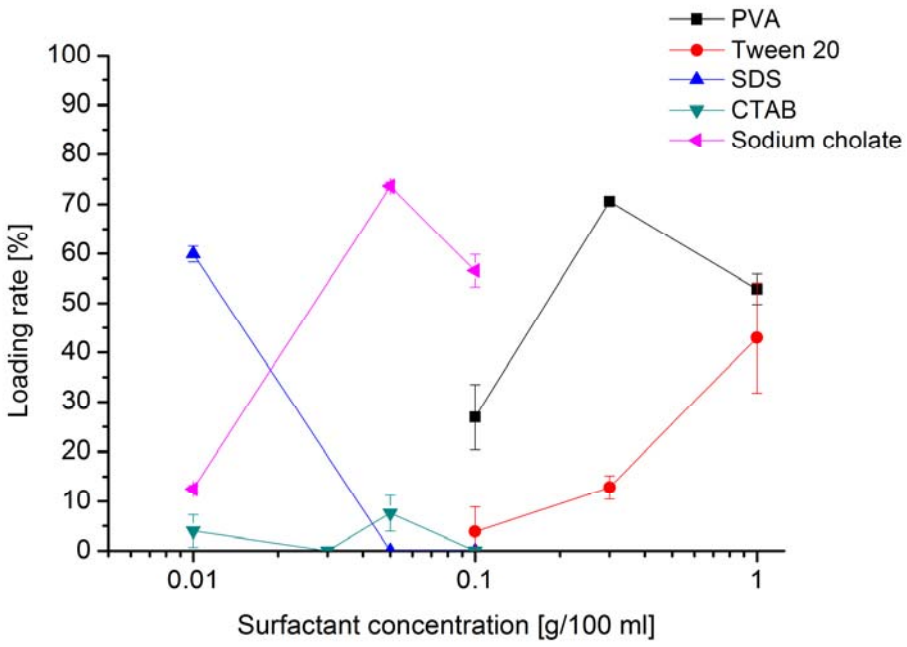

Fig. 58: *Loading rate of O/W-Nanoparticles (10 mg/ml) with 0.5 mg/ml BSA (mean ± SD, n=3)*

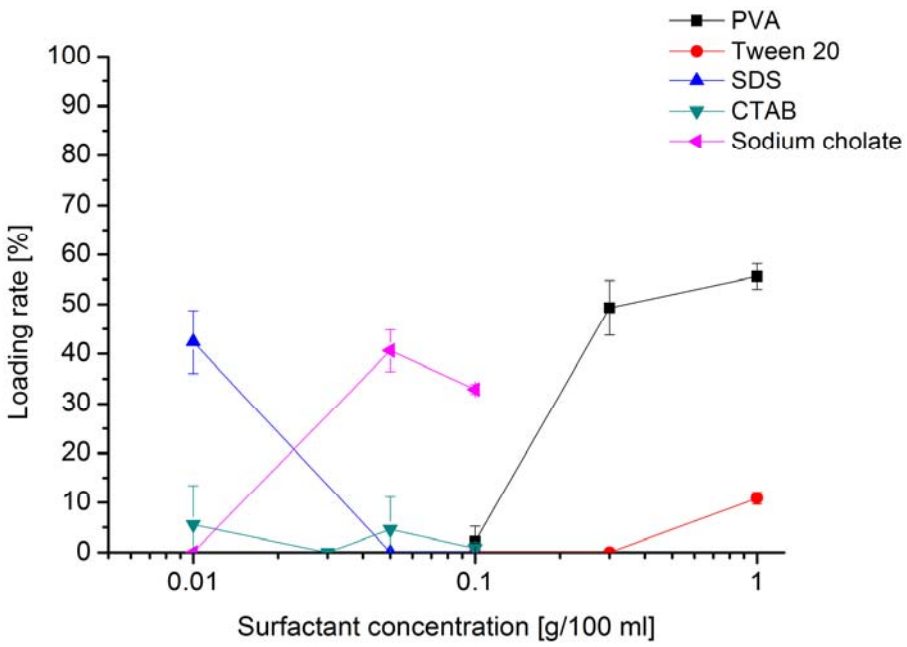

Fig. 59: *Loading rate of O/W-Nanoparticles (10 mg/ml) with 1 mg/ml BSA (mean ± SD, n=3)*

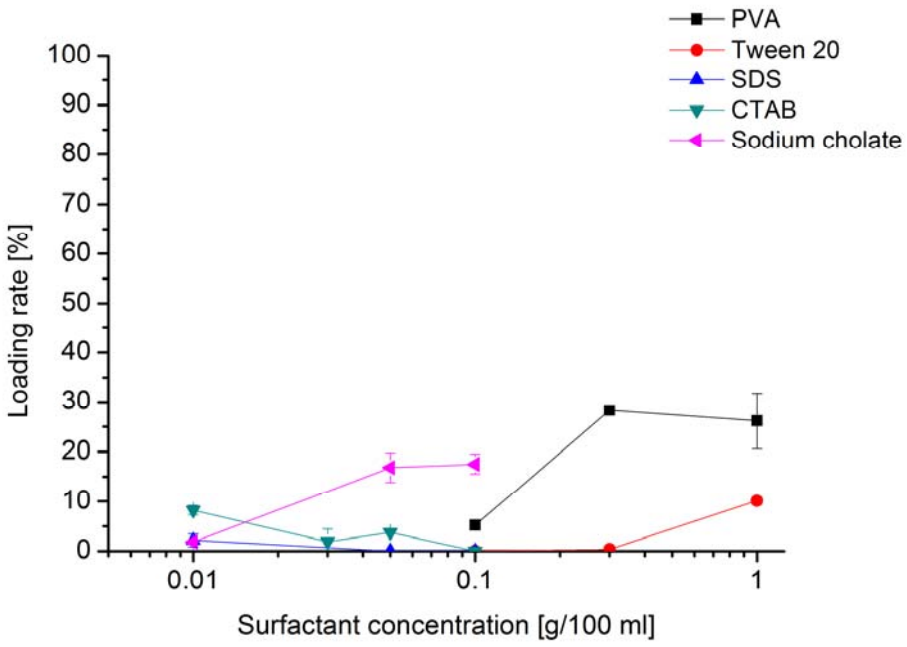

Fig. 60: *Loading rate of O/W-Nanoparticles (10 mg/ml) with 2 mg/ml BSA (mean ± SD, n=3)*

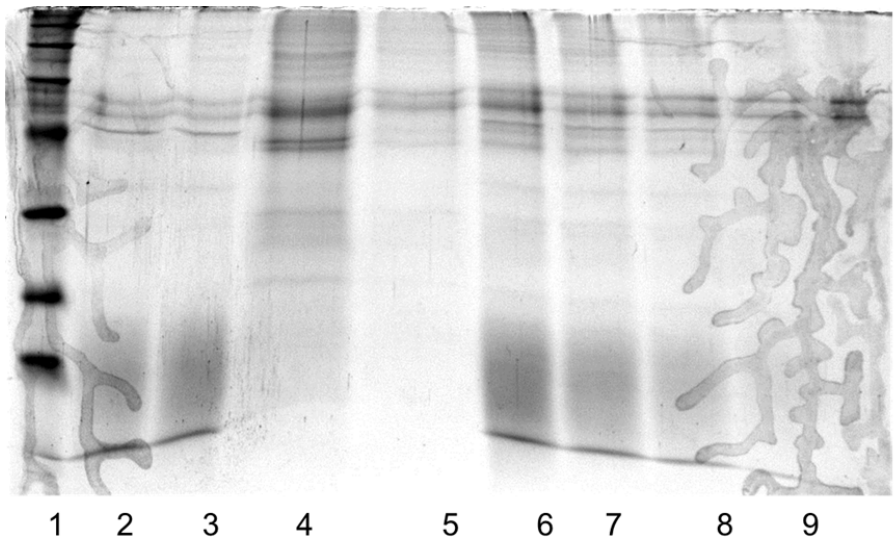

Fig. 61: *SDS-PAGE gels after staining with Coomassie Brilliant Blue, supernatants of o/w-NP formulations after incubation with toxoids, redispersed o/w-NP with SDS and DTT, and standard of α-toxoid (Clostridium perfringes): 1) Marker 2) PVA-NP supernatant 3) PVA-NP supernatant 4) PVA-NP redispersed (4x) 5) PVA-NP redispersed (1x) 6) α-toxoid (Clostridium perfringes) 0.0215 mg/ml 7) α-toxoid (Clostridium perfringes) 0.0161 mg/ml 8) α-toxoid (Clostridium perfringes) 0.0108 mg/ml 9) α-toxoid (Clostridium perfringes) 0.0054 mg/ml*

Table 25: *Surface tension of surfactant solutions (mean* ± SD; n = 3)

Surfactant concentration [g/100 ml]	Surface tension [mN/m]				
	PVA-NP	Tween 20-NP	SDS-NP	Sodium cholate-NP	CTAB-NP
1	44.2 ± 0.4	23.4 ± 0.2			
0.3	44.6 ± 0.4	36.3 ± 0.4			
0.1	48.9 ± 0.1	38.1 ± 0.9	61.6 ± 4.4		
0.05			68.4 ± 0.2	56.3 ± 0.2	34.0 ± 2.6
0.035				59.5 ± 0.1	35.0 ± 0.1
0.01			69.7 ± 0.1	61.0 ± 0.4	35.6 ± 0.1

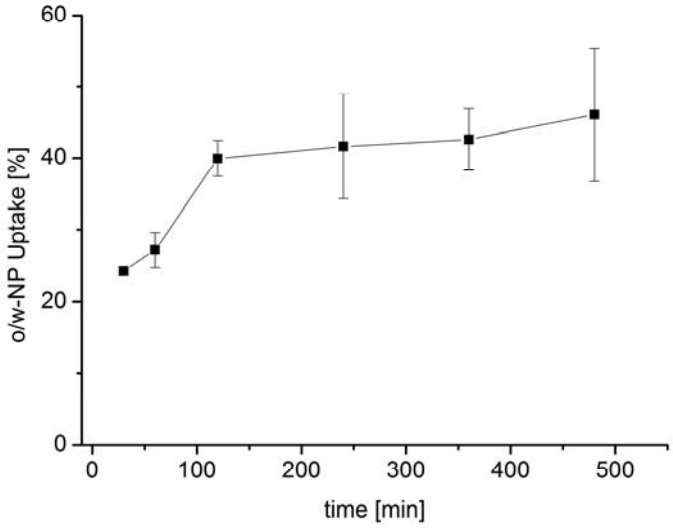

Fig. 62: *Uptake of o/w-NP in RAW 264.7 cells after staining with Nile red at different incubation periods (mean ± SD; n = 3)*

8 References

Akagi, T., Baba, M., Akashi, M., 2012. Biodegradable Nanoparticles as Vaccine Adjuvants and Delivery Systems: Regulation of Immune Responses by Nanoparticle-Based Vaccine, in: Kunugi, S., Yamaoka, T. (Eds.), Polymers in Nanomedicine. Springer Berlin Heidelberg, pp. 31-64.

Ali, M.E., Lamprecht, A., 2013. Polyethylene glycol as an alternative polymer solvent for nanoparticle preparation. International Journal of Pharmaceutics 456, 135-142.

Allhenn, D., Lamprecht, A., 2011. Microsphere preparation using the untoxic solvent glycofurol. Pharm Res 28, 563-571.

Allhenn, D., Neumann, D., Béduneau, A., Pellequer, Y., Lamprecht, A., 2013. A "drug cocktail" delivered by microspheres for the local treatment of rat glioblastoma. Journal of Microencapsulation 30, 667-673.

Anderson, J.M., Shive, M.S., 1997. Biodegradation and biocompatibility of PLA and PLGA microspheres. Advanced Drug Delivery Reviews 28, 5-24.

Arshady, R., 1991. Preparation of biodegradable microspheres and microcapsules: 2. Polyactides and related polyesters. Journal of Controlled Release 17, 1-21.

ATCC, 2014. https://www.lgcstandards-atcc.org/products/all/TIB-71.aspx?geo_country=de&slp=1#generalinformation. Access 06.01.2014.

Aucouturier, J., Dupuis, L., Ganne, V., 2001. Adjuvants designed for veterinary and human vaccines. Vaccine 19, 2666-2672.

Bala, I., Hariharan, S., Kumar, M.N., 2004. PLGA nanoparticles in drug delivery: the state of the art. Crit Rev Ther Drug Carrier Syst 21, 387-422.

Berridge, M.V., Herst, P.M., Tan, A.S., 2005. Tetrazolium dyes as tools in cell biology: New insights into their cellular reduction, in: El-Gewely, M.R. (Ed.), Biotechnology Annual Review. Elsevier, pp. 127-152.

Berridge, M.V., Tan, A.S., 1993. Characterization of the Cellular Reduction of 3-(4,5-dimethylthiazol-2-yl)-2,5-diphenyltetrazolium bromide (MTT): Subcellular Localization, Substrate Dependence, and Involvement of Mitochondrial Electron Transport in MTT Reduction. Archives of Biochemistry and Biophysics 303, 474-482.

Bilati, U., Allemann, E., Doelker, E., 2005. Poly(D,L-lactide-co-glycolide) protein-loaded nanoparticles prepared by the double emulsion method--processing and formulation issues for enhanced entrapment efficiency. J Microencapsul 22, 205-214.

Binding, N., Jaschinski, S., Werlich, S., Bletz, S., Witting, U., 2004. Quantification of bacterial lipopolysaccharides (endotoxin) by GC-MS determination of 3-hydroxy fatty acids. Journal of Environmental Monitoring 6, 65-70.

Blake, C.C.F., Koenig, D.F., Mair, G.A., North, A.C.T., Phillips, D.C., Sarma, V.R., 1965. Structure of Hen Egg-White Lysozyme: A Three-dimensional Fourier Synthesis at 2 A Resolution. Nature 206, 757-761.

Blanco, D., Alonso, M.a.J., 1998. Protein encapsulation and release from poly(lactide-co-glycolide) microspheres: effect of the protein and polymer properties and of the co-encapsulation of surfactants. European Journal of Pharmaceutics and Biopharmaceutics 45, 285-294.

Blanco, M.D., Alonso, M.J., 1997. Development and characterization of protein-loaded poly(lactide-co-glycolide) nanospheres. European Journal of Pharmaceutics and Biopharmaceutics 43, 287-294.

Bobo, W.V., Shelton, R.C., 2010. Risperidone long-acting injectable (Risperdal Consta®) for maintenance treatment in patients with bipolar disorder. Expert Review of Neurotherapeutics 10, 1637-1658.

Buske, J., König, C., Bassarab, S., Lamprecht, A., Mühlau, S., Wagner, K.G., 2012. Influence of PEG in PEG–PLGA microspheres on particle properties and protein release. European Journal of Pharmaceutics and Biopharmaceutics 81, 57-63.

Canfield, R.E., 1963. The Amino Acid Sequence of Egg White Lysozyme. Journal of Biological Chemistry 238, 2698-2707.

Caputo, A., Sparnacci, K., Ensoli, B., Tondelli, L., 2008. Functional Polymeric Nano/Microparticles for Surface Adsorption and Delivery of Protein and DNA Vaccines. Current Drug Delivery 5, 230-242.

Chen, J.L., Yeh, M.K., Chiang, C.H., 2004. The mechanism of surface-indented protein-loaded PLGA microparticle formation: the effects of salt (NaCl) on the solidification process. J Microencapsul 21, 877-888.

Cheng, Z., Al Zaki, A., Hui, J.Z., Muzykantov, V.R., Tsourkas, A., 2012. Multifunctional Nanoparticles: Cost Versus Benefit of Adding Targeting and Imaging Capabilities. Science 338, 903-910.

Cho, M., Sah, H., 2005. Formulation and process parameters affecting protein encapsulation into PLGA microspheres during ethyl acetate-based microencapsulation process. J Microencapsul 22, 1-12.

Cohen-Sela, E., Chorny, M., Koroukhov, N., Danenberg, H.D., Golomb, G., 2009. A new double emulsion solvent diffusion technique for encapsulating hydrophilic molecules in PLGA nanoparticles. J Control Release 133, 90-95.

Coombes, A.G.A., Yeh, M.-K., Lavelle, E.C., Davis, S.S., 1998. The control of protein release from poly(dl-lactide co-glycolide) microparticles by variation of the external aqueous phase surfactant in the water-in oil-in water method. Journal of Controlled Release 52, 311-320.

Cox, J.C., Coulter, A.R., 1997. Adjuvants—a classification and review of their modes of action. Vaccine 15, 248-256.

Crotts, G., Park, T.G., 1997. Stability and release of bovine serum albumin encapsulated within poly(d,l-lactide-co-glycolide) microparticles. Journal of Controlled Release 44, 123-134.

Crotts, G., Park, T.G., 1998. Protein delivery from poly(lactic-co-glycolic acid) biodegradable microspheres: release kinetics and stability issues. J Microencapsul 15, 699-713.

Cruz, L.J., Tacken, P.J., Fokkink, R., Joosten, B., Stuart, M.C., Albericio, F., Torensma, R., Figdor, C.G., 2010. Targeted PLGA nano-but not microparticles specifically deliver antigen to human dendritic cells via DC-SIGN in vitro. Journal of Controlled Release 144, 118-126.

Cu, Y., Saltzman, W.M., 2008. Controlled Surface Modification with Poly(ethylene)glycol Enhances Diffusion of PLGA Nanoparticles in Human Cervical Mucus. Molecular Pharmaceutics 6, 173-181.

Dario-Becker, J., 2013. Adaptive Immune Response. Derived Copy of Biology: Mixed Majors, Part II http://cnx.org/content/m44821/latest/?collection=col11592/latest.

Demento, S.L., Eisenbarth, S.C., Foellmer, H.G., Platt, C., Caplan, M.J., Mark Saltzman, W., Mellman, I., Ledizet, M., Fikrig, E., Flavell, R.A., Fahmy, T.M., 2009. Inflammasome-activating nanoparticles as modular systems for optimizing vaccine efficacy. Vaccine 27, 3013-3021.

des Rieux, A., Fievez, V., Garinot, M., Schneider, Y.-J., Préat, V., 2006. Nanoparticles as potential oral delivery systems of proteins and vaccines: a mechanistic approach. Journal of Controlled Release 116, 1-27.

Desgouilles, S., Vauthier, C., Bazile, D., Vacus, J., Grossiord, J.-L., Veillard, M., Couvreur, P., 2003. The Design of Nanoparticles Obtained by Solvent Evaporation: A Comprehensive Study. Langmuir 19, 9504-9510.

Determan, A.S., Trewyn, B.G., Lin, V.S.Y., Nilsen-Hamilton, M., Narasimhan, B., 2004. Encapsulation, stabilization, and release of BSA-FITC from polyanhydride microspheres. Journal of Controlled Release 100, 97-109.

Dey, A.K., Burke, B., Sun, Y., Hartog, K., Heeney, J.L., Montefiori, D., Srivastava, I.K., Barnett, S.W., 2012. Use of a polyanionic carbomer, Carbopol971P, in combination with MF59, improves antibody responses to HIV-1 envelope glycoprotein. Vaccine 30, 2749-2759.

Doll, T.A.P.F., Raman, S., Dey, R., Burkhard, P., 2013. Nanoscale assemblies and their biomedical applications. Journal of The Royal Society Interface 10.

Dunnebier, E.A., Segenhout, J.M., Kalicharan, D., Jongebloed, W.L., Wit, H.P., Albers, F.W.J., 1995. Low-voltage field-emission scanning electron microscopy of non-coated guinea-pig hair cell stereocilia. Hearing Research 90, 139-148.

Eggerstedt, S.N., Dietzel, M., Sommerfeld, M., Süverkrüp, R., Lamprecht, A., 2012. Protein spheres prepared by drop jet freeze drying. International Journal of Pharmaceutics 438, 160-166.

Faisant, N., Akiki, J., Siepmann, F., Benoit, J.P., Siepmann, J., 2006. Effects of the type of release medium on drug release from PLGA-based microparticles: experiment and theory. Int J Pharm 314, 189-197.

Fleischer, C.C., Payne, C.K., 2012. Nanoparticle Surface Charge Mediates the Cellular Receptors Used by Protein–Nanoparticle Complexes. The Journal of Physical Chemistry B 116, 8901-8907.

Foged, C., Brodin, B., Frokjaer, S., Sundblad, A., 2005. Particle size and surface charge affect particle uptake by human dendritic cells in an in vitro model. International Journal of Pharmaceutics 298, 315-322.

Foged, C., Sundblad, A., Hovgaard, L., 2002. Targeting vaccines to dendritic cells. Pharm Res 19, 229-238.

Freiberg, S., Zhu, X.X., 2004. Polymer microspheres for controlled drug release. International Journal of Pharmaceutics 282, 1-18.

Fu, J., Fiegel, J., Krauland, E., Hanes, J., 2002. New polymeric carriers for controlled drug delivery following inhalation or injection. Biomaterials 23, 4425-4433.

Fuguet, E., Ràfols, C., Rosés, M., Bosch, E., 2005. Critical micelle concentration of surfactants in aqueous buffered and unbuffered systems. Analytica Chimica Acta 548, 95-100.

Garmise, R.J., Staats, H.F., Hickey, A.J., 2007. Novel dry powder preparations of whole inactivated influenza virus for nasal vaccination. AAPS PharmSciTech 8, 2-10.

Gaumet, M., Gurny, R., Delie, F., 2009. Localization and quantification of biodegradable particles in an intestinal cell model: the influence of particle size. Eur J Pharm Sci 36, 465-473.

Ge, S., Kojio, K., Takahara, A., Kajiyama, T., 1998. Bovine serum albumin adsorption onto immobilized organotrichlorosilane surface: influence of the phase separation on protein adsorption patterns. Journal of Biomaterials Science, Polymer Edition 9, 131-150.

Giovino, C., Ayensu, I., Tetteh, J., Boateng, J.S., 2012. Development and characterisation of chitosan films impregnated with insulin loaded PEG-b-PLA nanoparticles (NPs): A potential approach for buccal delivery of macromolecules. International Journal of Pharmaceutics 428, 143-151.

Giteau, A., Venier-Julienne, M.C., Aubert-Pouëssel, A., Benoit, J.P., 2008. How to achieve sustained and complete protein release from PLGA-based microparticles? International Journal of Pharmaceutics 350, 14-26.

Gómez, S., Gamazo, C., San Roman, B., Ferrer, M., Sanz, M.L., Espuelas, S., Irache, J.M., 2008. Allergen immunotherapy with nanoparticles containing lipopolysaccharide from Brucella ovis. European Journal of Pharmaceutics and Biopharmaceutics 70, 711-717.

Gómez, S., Gamazo, C., San Roman, B., Grau, A., Espuelas, S., Ferrer, M., Sanz, M.L., Irache, J.M., 2009. A novel nanoparticulate adjuvant for immunotherapy with Lolium perenne. Journal of Immunological Methods 348, 1-8.

Greenspan, P., Mayer, E.P., Fowler, S.D., 1985. Nile red: a selective fluorescent stain for intracellular lipid droplets. The Journal of Cell Biology 100, 965-973.

Gurny, R., Peppas, N.A., Harrington, D.D., Banker, G.S., 1981. Development of Biodegradable and Injectable Latices for Controlled Release of Potent Drugs. Drug Development and Industrial Pharmacy 7, 1-25.

Gutierro, I., Hernandez, R.M., Igartua, M., Gascon, A.R., Pedraz, J.L., 2002a. Influence of dose and immunization route on the serum Ig G antibody response to BSA loaded PLGA microspheres. Vaccine 20, 2181-2190.

Gutierro, I., Hernandez, R.M., Igartua, M., Gascon, A.R., Pedraz, J.L., 2002b. Size dependent immune response after subcutaneous, oral and intranasal administration of BSA loaded nanospheres. Vaccine 21, 67-77.

GV-SOLAS, 2009. Abbruchkriterien bei Tierversuchen. http://www.gv-solas.de/assets/files/PDFs/pdf_PUBLIKATION/tie_abbruch_herrmann.pdf Access: 08.01.2014.

Hamdy, S., Haddadi, A., Hung, R.W., Lavasanifar, A., 2011. Targeting dendritic cells with nano-particulate PLGA cancer vaccine formulations. Adv Drug Deliv Rev 63, 943-955.

He, Q., Liu, J., Sun, X., Zhang, Z.R., 2004. Preparation and characteristics of DNA-nanoparticles targeting to hepatocarcinoma cells. World J Gastroenterol 10, 660-663.

Heegaard, P., Dedieu, L., Johnson, N., Le Potier, M.-F., Mockey, M., Mutinelli, F., Vahlenkamp, T., Vascellari, M., Sørensen, N., 2011. Adjuvants and delivery systems in veterinary vaccinology: current state and future developments. Archives of Virology 156, 183-202.

Hillaireau, H., Couvreur, P., 2009. Nanocarriers' entry into the cell: relevance to drug delivery. Cell Mol Life Sci 66, 2873-2896.

Hirayama, K., Akashi, S., Furuya, M., Fukuhara, K.-i., 1990. Rapid confirmation and revision of the primary structure of bovine serum albumin by ESIMS and frit-FAB LC/MS. Biochemical and Biophysical Research Communications 173, 639-646.

Hiszczyńska-Sawicka, E., Li, H., Xu, J.B., Olędzka, G., Kur, J., Bickerstaffe, R., Stankiewicz, M., 2010. Comparison of immune response in sheep immunized with DNA vaccine encoding Toxoplasma gondii GRA7 antigen in different adjuvant formulations. Experimental Parasitology 124, 365-372.

Hoffart, V., Lamprecht, A., Maincent, P., Lecompte, T., Vigneron, C., Ubrich, N., 2006. Oral bioavailability of a low molecular weight heparin using a polymeric delivery system. Journal of Controlled Release 113, 38-42.

Huntington, J.A., Stein, P.E., 2001. Structure and properties of ovalbumin. J Chromatogr B Biomed Sci Appl 756, 189-198.

Jain, R.A., 2000. The manufacturing techniques of various drug loaded biodegradable poly(lactide-co-glycolide) (PLGA) devices. Biomaterials 21, 2475-2490.

Jalil, R., Nixon, J.R., 1990. Biodegradable poly(lactic acid) and poly(lactide-co-glycolide) microcapsules: problems associated with preparative techniques and release properties. Journal of Microencapsulation 7, 297-325.

Ji, W., Yang, F., Seyednejad, H., Chen, Z., Hennink, W.E., Anderson, J.M., van den Beucken, J.J.J.P., Jansen, J.A., 2012. Biocompatibility and degradation characteristics of PLGA-based electrospun nanofibrous scaffolds with nanoapatite incorporation. Biomaterials 33, 6604-6614.

Jiang, W., Gupta, R.K., Deshpande, M.C., Schwendeman, S.P., 2005. Biodegradable poly(lactic-co-glycolic acid) microparticles for injectable delivery of vaccine antigens. Advanced Drug Delivery Reviews 57, 391-410.

Jiao, Y., Ubrich, N., Marchand-Arvier, M., Vigneron, C., Hoffman, M., Lecompte, T., Maincent, P., 2002. In Vitro and In Vivo Evaluation of Oral Heparin–Loaded Polymeric Nanoparticles in Rabbits. Circulation 105, 230-235.

Jongebloed, W., Stokroos, D., Kalicharan, D., Van der Want, J., 1999. Is cryopreservation superior over tannic acid/arginine/osmium tetroxide non-coating preparation in field emission scanning electron microscopy. Scanning Microsc 13, 93-109.

Kasturi, S.P., Skountzou, I., Albrecht, R.A., Koutsonanos, D., Hua, T., Nakaya, H.I., Ravindran, R., Stewart, S., Alam, M., Kwissa, M., Villinger, F., Murthy, N., Steel, J., Jacob, J., Hogan, R.J., Garcia-Sastre, A., Compans, R., Pulendran, B., 2011. Programming the magnitude and persistence of antibody responses with innate immunity. Nature 470, 543-547.

Khoee, S., Sattari, A., Atyabi, F., 2012. Physico-chemical properties investigation of cisplatin loaded polybutyladipate (PBA) nanoparticles prepared by w/o/w. Materials Science and Engineering: C 32, 1078-1086.

Khoee, S., Yaghoobian, M., 2009. An investigation into the role of surfactants in controlling particle size of polymeric nanocapsules containing penicillin-G in double emulsion. European Journal of Medicinal Chemistry 44, 2392-2399.

Kim, K.-J., Dickson, M.R., Chen, V., Fane, A.G., 1992. Applications of field emission scanning electron microscopy to polymer membrane research. Micron and Microscopica Acta 23, 259-271.

Korsholm, K.S., 2010. One does not fit all: new adjuvants are needed and vaccine formulation is critical. Expert Review of Vaccines 10, 45-48.

Kuroda, E., Coban, C., Ishii, K.J., 2013. Particulate Adjuvant and Innate Immunity: Past Achievements, Present Findings, and Future Prospects. International Reviews of Immunology 32, 209-220.

Laemmli, U.K., 1970. Cleavage of structural proteins during the assembly of the head of bacteriophage T4. Nature 227, 680-685.

Lamprecht, A., 2010. IBD: Selective nanoparticle adhesion can enhance colitis therapy. Nat Rev Gastroenterol Hepatol 7, 311-312.

Lamprecht, A., Schafer, U., Lehr, C.M., 2000a. Structural analysis of microparticles by confocal laser scanning microscopy. AAPS PharmSciTech 1, E17.

Lamprecht, A., Ubrich, N., Hombreiro Perez, M., Lehr, C., Hoffman, M., Maincent, P., 1999. Biodegradable monodispersed nanoparticles prepared by pressure homogenization-emulsification. Int J Pharm 184, 97-105.

Lamprecht, A., Ubrich, N., Hombreiro Perez, M., Lehr, C., Hoffman, M., Maincent, P., 2000b. Influences of process parameters on nanoparticle preparation performed by a double emulsion pressure homogenization technique. Int J Pharm 196, 177-182.

Lamprecht, A., Yamamoto, H., Takeuchi, H., Kawashima, Y., 2004. pH-sensitive microsphere delivery increases oral bioavailability of calcitonin. J Control Release 98, 1-9.

Langer, R., Folkman, J., 1976. Polymers for the sustained release of proteins and other macromolecules. Nature 263, 793-800.

Leslie, D., Fairweather, N., Pickard, D., Dougan, G., Kehoe, M., 1989. Phospholipase C and haemolytic activities of Clostridium perfringens alpha-toxin cloned in Escherichia coli: sequence and homology with a Bacillus cereus phospholipase C. Mol Microbiol 3, 383-392.

Li, X., Sloat, B.R., Yanasarn, N., Cui, Z., 2011. Relationship between the size of nanoparticles and their adjuvant activity: Data from a study with an improved experimental design. European Journal of Pharmaceutics and Biopharmaceutics 78, 107-116.

Lin, S.-Y., Chen, L.-J., Xyu, J.-W., Wang, W.-J., 1995. An Examination on the Accuracy of Interfacial Tension Measurement from Pendant Drop Profiles. Langmuir 11, 4159-4166.

Lowry, O.H., Rosebrough, N.J., Farr, A.L., Randall, R.J., 1951. Protein measurement with the folin phenol reagent. Journal of Biological Chemistry 193, 265-275.

Lu, J.M., Wang, X., Marin-Muller, C., Wang, H., Lin, P.H., Yao, Q., Chen, C., 2009. Current advances in research and clinical applications of PLGA-based nanotechnology. Expert Rev Mol Diagn 9, 325-341.

Luan, X., Skupin, M., Siepmann, J., Bodmeier, R., 2006. Key parameters affecting the initial release (burst) and encapsulation efficiency of peptide-containing poly(lactide-co-glycolide) microparticles. Int J Pharm 324, 168-175.

Lundqvist, M., Stigler, J., Cedervall, T., Berggård, T., Flanagan, M.B., Lynch, I., Elia, G., Dawson, K., 2011. The Evolution of the Protein Corona around Nanoparticles: A Test Study. ACS Nano 5, 7503-7509.

Lundqvist, M., Stigler, J., Elia, G., Lynch, I., Cedervall, T., Dawson, K.A., 2008. Nanoparticle size and surface properties determine the protein corona with possible implications for biological impacts. Proceedings of the National Academy of Sciences 105, 14265-14270.

Lynch, I., Cedervall, T., Lundqvist, M., Cabaleiro-Lago, C., Linse, S., Dawson, K.A., 2007. The nanoparticle–protein complex as a biological entity; a complex fluids and surface science challenge for the 21st century. Advances in Colloid and Interface Science 134–135, 167-174.

Mäder, K., Bittner, B., Li, Y., Wohlauf, W., Kissel, T., 1998. Monitoring Microviscosity and Microacidity of the Albumin Microenvironment Inside Degrading Microparticles from Poly(lactide-co-glycolide) (PLG) or ABA-triblock Polymers Containing Hydrophobic Poly(lactide-co-glycolide) A Blocks and Hydrophilic Poly(ethyleneoxide) B Blocks. Pharm Res 15, 787-793.

Mäder, K., Weidenauer, U., 2010. Innovative Arzneiformen. Wissenschaftliche Verlagsgesellschaft Stuttgart.

Marvel, C.S., Denoon, C.E., 1938. The Structure of Vinyl Polymers. II.1 Polyvinyl Alcohol. Journal of the American Chemical Society 60, 1045-1051.

McCave, I., Bryant, R., Cook, H., Coughanowr, C., 1986. Evaluation of a laser-diffraction-size analyzer for use with natural sediments. Journal of Sedimentary Research 56, 561-564.

McKenzie, H.A., White, F.H., 1991. Lysozyme and alpha-lactalbumin: structure, function, and interrelationships. Advances in protein chemistry 41, 173-315.

Meeusen, E.N., Walker, J., Peters, A., Pastoret, P.-P., Jungersen, G., 2007. Current status of veterinary vaccines. Clinical microbiology reviews 20, 489-510.

Meng, F.T., Ma, G.H., Qiu, W., Su, Z.G., 2003. W/O/W double emulsion technique using ethyl acetate as organic solvent: effects of its diffusion rate on the characteristics of microparticles. Journal of Controlled Release 91, 407-416.

Mitsui-Chemicals, 2010. http://eu.mitsuichem.com/service/pdf/plga.pdf. Access 20.06.2014.

Mohanan, D., Slutter, B., Henriksen-Lacey, M., Jiskoot, W., Bouwstra, J.A., Perrie, Y., Kundig, T.M., Gander, B., Johansen, P., 2010. Administration routes affect the quality of immune responses: A cross-sectional evaluation of particulate antigen-delivery systems. J Control Release 147, 342-349.

Mosmann, T., 1983. Rapid colorimetric assay for cellular growth and survival: application to proliferation and cytotoxicity assays. J Immunol Methods 65, 55-63.

Mundargi, R.C., Babu, V.R., Rangaswamy, V., Patel, P., Aminabhavi, T.M., 2008. Nano/micro technologies for delivering macromolecular therapeutics using poly(D,L-lactide-co-glycolide) and its derivatives. J Control Release 125, 193-209.

Nair, L.S., Laurencin, C.T., 2007. Biodegradable polymers as biomaterials. Progress in Polymer Science 32, 762-798.

Nicolete, R., dos Santos, D.F., Faccioli, L.H., 2011. The uptake of PLGA micro or nanoparticles by macrophages provokes distinct in vitro inflammatory response. Int Immunopharmacol 11, 1557-1563.

NIH, 2012. Types of Vaccines. http://www.niaid.nih.gov/topics/vaccines/understanding/pages/typesvaccines.aspx Access: 13.02.2014.

Nikon, 2014. A1 Konfokales Laser-Mikroskopsystem. http://www.nikoninstruments.com/en_DE/Products/Microscope-Systems/Confocal-Microscopes/A1R-A1-Confocal2 Access: 03.01.2014.

Nisbet, A.D., Saundry, R.H., Moir, A.J.G., Fothergill, L.A., Fothergill, J.E., 1981. The Complete Amino-Acid Sequence of Hen Ovalbumin. European Journal of Biochemistry 115, 335-345.

O'Hagan, D.T., Singh, M., 2003. Microparticles as vaccine adjuvants and delivery systems. Expert Review of Vaccines 2, 269-283.

O'Hagan, D.T., Singh, M., Ulmer, J.B., 2006. Microparticle-based technologies for vaccines. Methods 40, 10-19.

Okada, H., Heya, T., Ogawa, Y., Shimamoto, T., 1988. One-month release injectable microcapsules of a luteinizing hormone-releasing hormone agonist (leuprolide acetate) for treating experimental endometriosis in rats. Journal of Pharmacology and Experimental Therapeutics 244, 744-750.

Oyewumi, M.O., Kumar, A., Cui, Z., 2010. Nano-microparticles as immune adjuvants: correlating particle sizes and the resultant immune responses. Expert Review of Vaccines 9, 1095-1107.

Paillard-Giteau, A., Tran, V.T., Thomas, O., Garric, X., Coudane, J., Marchal, S., Chourpa, I., Benoît, J.P., Montero-Menei, C.N., Venier-Julienne, M.C., 2010. Effect of various additives and polymers on lysozyme release from PLGA microspheres prepared by an s/o/w emulsion technique. European Journal of Pharmaceutics and Biopharmaceutics 75, 128-136.

Patel, R.P., 2008. Nanoparticles and its applications in field of pharmacy. Latest Reviews 6.

Peek, L.J., Middaugh, C.R., Berkland, C., 2008. Nanotechnology in vaccine delivery. Adv Drug Deliv Rev 60, 915-928.

Pinto Reis, C., Neufeld, R.J., Ribeiro, A.J., Veiga, F., 2006. Nanoencapsulation I. Methods for preparation of drug-loaded polymeric nanoparticles. Nanomedicine: Nanotechnology, Biology and Medicine 2, 8-21.

Porjazoska, A., Goracinova, K., Mladenovska, K., Glavas, M., Simonovska, M., Janjević, E.I., Cvetkovska, M., 2004. Poly(lactide-co-glycolide) microparticles as systems for controlled release of proteins -- preparation and characterization. Acta pharmaceutica (Zagreb, Croatia) 54, 215-229.

Putney, S.D., Burke, P.A., 1998. Improving protein therapeutics with sustained-release formulations. Nat Biotech 16, 153-157.

Rachel, P.J.L., Michael, S.S., Paul, T., Frank, W., David, J.S., Simon, D.W.F., Celia, C.L., David, C.M., Antu, K.D., Indresh, K.S., Quentin, S., Susan, W.B., Jonathan, L.H., 2012. Mixed adjuvant formulations reveal a new combination that elicit antibody response comparable to Freund's adjuvants. PLoS One 7, e35083-e35083.

Rahman, M., Laurent, S., Tawil, N., Yahia, L.H., Mahmoudi, M., 2013. Protein-Nanoparticle Interactions. Springer.

Raschke, W.C., Baird, S., Ralph, P., Nakoinz, I., 1978. Functional macrophage cell lines transformed by abelson leukemia virus. Cell 15, 261-267.

Ravi, S., Peh, K.K., Darwis, Y., Murthy, B.K., Singh, T.R., Mallikarjun, C., 2008. Development and characterization of polymeric microspheres for controlled release protein loaded drug delivery system. Indian J Pharm Sci 70, 303-309.

Rein, H., 2010. ANALYTIK. Rasterelektronenmikroskopie - Theorie und praktische Anwendungen in der Pharmazie. Deutsche Apotheker-Zeitung 150, 50.

Rice-Ficht, A.C., Arenas-Gamboa, A.M., Kahl-McDonagh, M.M., Ficht, T.A., 2010. Polymeric particles in vaccine delivery. Current Opinion in Microbiology 13, 106-112.

Rosenthal, K.S., Zimmerman, D.H., 2006. Vaccines: all things considered. Clinical and vaccine immunology 13, 821-829.

Sah, H., 1999. Stabilization of proteins against methylene chloride/water interface-induced denaturation and aggregation. J Control Release 58, 143-151.

Sahana, B., Santra, K., Basu, S., Mukherjee, B., 2010. Development of biodegradable polymer based tamoxifen citrate loaded nanoparticles and effect of some manufacturing process parameters on them: a physicochemical and in-vitro evaluation. Int J Nanomedicine 5, 621-630.

Schagger, H., von Jagow, G., 1987. Tricine-sodium dodecyl sulfate-polyacrylamide gel electrophoresis for the separation of proteins in the range from 1 to 100 kDa. Anal Biochem 166, 368-379.

Schmitz, S., 2011. Der Experimentator: Zellkultur. Spektrum Akademischer Verlag.

Schnare, M., Barton, G.M., Holt, A.C., Takeda, K., Akira, S., Medzhitov, R., 2001. Toll-like receptors control activation of adaptive immune responses. Nat Immunol 2, 947-950.

Schütt, C., Bröker, B., 2009. Grundwissen Immunologie. Springer.

Schwendeman, S.P., 2002. Recent advances in the stabilization of proteins encapsulated in injectable PLGA delivery systems. Critical reviews in therapeutic drug carrier systems 19, 73-98.

Seetharam, R., Sharma, S.K., 1991. Purification and Analysis of Recombinant Proteins. Taylor & Francis.

Siegrist, C.-A., 2008. Vaccine immunology. http://www.who.int/immunization/documents/Elsevier_Vaccine_immunology.pdf. Vaccines. Saunders.

Siepmann, J., Faisant, N., Akiki, J., Richard, J., Benoit, J.P., 2004. Effect of the size of biodegradable microparticles on drug release: experiment and theory. J Control Release 96, 123-134.

Sigma-Aldrich, 2013a. http://www.sigmaaldrich.com/catalog/product/sigma/c9282?lang=de&region=DE. Access 13.12.2013.

Sigma-Aldrich, 2013b. http://www.sigmaaldrich.com/content/dam/sigma-aldrich/docs/Sigma/Product_Information_Sheet/f5881pis.pdf. Access 12.12.2013.

Singh, M., Chakrapani, A., O'Hagan, D., 2007. Nanoparticles and microparticles as vaccine-delivery systems. Expert Rev Vaccines 6, 797-808.

Singh, M., Kazzaz, J., Ugozzoli, M., Chesko, J., O'Hagan, D.T., 2004. Charged polylactide co-glycolide microparticles as antigen delivery systems. Expert Opinion on Biological Therapy 4, 483-491.

Singh, M., O'Hagan, D.T., 2003. Recent advances in veterinary vaccine adjuvants. Int J Parasitol 33, 469-478.

Smith, E.R.B., 1935. The effect of variations in ionic strength on the apparent isoelectric point of egg albumin. Journal of Biological Chemistry 108, 187-194.

Smith, P.K., Krohn, R.I., Hermanson, G.T., Mallia, A.K., Gartner, F.H., Provenzano, M.D., Fujimoto, E.K., Goeke, N.M., Olson, B.J., Klenk, D.C., 1985. Measurement of protein using bicinchoninic acid. Anal Biochem 150, 76-85.

Soppimath, K.S., Aminabhavi, T.M., Kulkarni, A.R., Rudzinski, W.E., 2001. Biodegradable polymeric nanoparticles as drug delivery devices. Journal of Controlled Release 70, 1-20.

STIKO, 2013. Empfehlungen der Ständigen Impfkommission (STIKO) am Robert Koch-Institut/Stand: http://www.rki.de/DE/Content/Infekt/EpidBull/Archiv/2013/Ausgaben/34_13.pdf?__blob=publicationFile. Access 13.02.2014.

Takada, S., Uda, Y., Toguchi, H., Ogawa, Y., 1995. Application of a Spray Drying Technique in the Production of TRH-Containing Injectable Sustained-Release Microparticles of Biodegradable Polymers. PDA Journal of Pharmaceutical Science and Technology 49, 180-184.

Tetsutani, K., Ishii, K.J., 2012. Adjuvants in influenza vaccines. Vaccine 30, 7658-7661.

Titball, R.W., 2005. Gas gangrene: an open and closed case. Microbiology 151, 2821-2828.

Titball, R.W., 2009. Clostridium perfringens vaccines. Vaccine 27 Suppl 4, D44-47.

Titball, R.W., Naylor, C.E., Basak, A.K., 1999. The Clostridium perfringens alpha-toxin. Anaerobe 5, 51-64.

Treuel, L., Jiang, X., Nienhaus, G.U., 2013. New views on cellular uptake and trafficking of manufactured nanoparticles. Journal of The Royal Society Interface 10.

TVT, 2010. Tierschutzaspekte bei der Immunisierung von Versuchstieren. http://www.tierschutz-tvt.de/merkblaetter.html Access: 29.01.2014.

Uchida, T., Goto, S., Foster, T.P., 1995. Particle size studies for subcutaneous delivery of poly(lactide-co-glycolide) microspheres containing ovalbumin as vaccine formulation. J Pharm Pharmacol 47, 556-560.

Unanue, E.R., 1984. Antigen-presenting function of the macrophage. Annual review of immunology 2, 395-428.

van de Weert, M., Hennink, W.E., Jiskoot, W., 2000. Protein instability in poly(lactic-co-glycolic acid) microparticles. Pharm Res 17, 1159-1167.

Vauthier, C., Bouchemal, K., 2009. Methods for the Preparation and Manufacture of Polymeric Nanoparticles. Pharm Res 26, 1025-1058.

Veitch, N.C., 2004. Horseradish peroxidase: a modern view of a classic enzyme. Phytochemistry 65, 249-259.

Viehof, A., Javot, L., Béduneau, A., Pellequer, Y., Lamprecht, A., 2013. Oral insulin delivery in rats by nanoparticles prepared with non-toxic solvents. International Journal of Pharmaceutics 443, 169-174.

Viehof, A., Lamprecht, A., 2013. Oral Delivery of Low Molecular Weight Heparin by Polyaminomethacrylate Coacervates. Pharm Res 30, 1990-1998.

Wachsmann, P., Lamprecht, A., 2012. Polymeric nanoparticles for the selective therapy of inflammatory bowel disease. Methods Enzymol 508, 377-397.

Wachsmann, P., Moulari, B., Béduneau, A., Pellequer, Y., Lamprecht, A., 2013. Surfactant-dependence of nanoparticle treatment in murine experimental colitis. Journal of Controlled Release 172, 62-68.

Waeckerle-Men, Y., Groettrup, M., 2005. PLGA microspheres for improved antigen delivery to dendritic cells as cellular vaccines. Adv Drug Deliv Rev 57, 475-482.

Wagenaar, B.W., Müller, B.W., 1994. Piroxicam release from spray-dried biodegradable microspheres. Biomaterials 15, 49-54.

Wagner, V., Dullaart, A., Bock, A.-K., Zweck, A., 2006. The emerging nanomedicine landscape. Nat Biotech 24, 1211-1217.

Walczyk, D., Bombelli, F.B., Monopoli, M.P., Lynch, I., Dawson, K.A., 2010. What the Cell "Sees" in Bionanoscience. Journal of the American Chemical Society 132, 5761-5768.

Wendorf, J., Chesko, J., Kazzaz, J., Ugozzoli, M., Vajdy, M., O'Hagan, D., Singh, M., 2008. A comparison of anionic nanoparticles and microparticles as vaccine delivery systems. Hum Vaccin 4, 44-49.

Wetter, L.R., Deutsch, H.F., 1951. Immunological studies on egg white proteins: IV. Immunochemical and physical studies of lysozyme. Journal of Biological Chemistry 192, 237-242.

Williams, R.O., Mahaguna, V., 1998. Preformulation Studies on Freund's Incomplete Adjuvant Emulsion. Drug Development and Industrial Pharmacy 24, 157-162.

Wu, X., Narsimhan, G., 2008. Effect of surface concentration on secondary and tertiary conformational changes of lysozyme adsorbed on silica nanoparticles. Biochimica et Biophysica Acta (BBA) - Proteins and Proteomics 1784, 1694-1701.

Ye, M., Kim, S., Park, K., 2010. Issues in long-term protein delivery using biodegradable microparticles. Journal of Controlled Release 146, 241-260.

Yeo, Y., Park, K., 2004. Control of encapsulation efficiency and initial burst in polymeric microparticle systems. Archives of Pharmacal Research 27, 1-12.

Yoo, J.Y., Kim, J.M., Seo, K.S., Jeong, Y.K., Lee, H.B., Khang, G., 2005. Characterization of degradation behavior for PLGA in various pH condition by simple liquid chromatography method. Bio-Medical Materials and Engineering 15, 279-288.

Yuan, W., Wu, F., Guo, M., Jin, T., 2009. Development of protein delivery microsphere system by a novel S/O/O/W multi-emulsion. European Journal of Pharmaceutical Sciences 36, 212-218.

Zambaux, M.F., Bonneaux, F., Gref, R., Maincent, P., Dellacherie, E., Alonso, M.J., Labrude, P., Vigneron, C., 1998. Influence of experimental parameters on the characteristics of poly(lactic acid) nanoparticles prepared by a double emulsion method. J Control Release 50, 31-40.

Zdziennicka, A., Szymczyk, K., Krawczyk, J., Jańczuk, B., 2012. Critical micelle concentration of some surfactants and thermodynamic parameters of their micellization. Fluid Phase Equilibria 322–323, 126-134.

Zhu, W., Sabatino, P., Govoreanu, R., Verbruggen, K., Martins, J.C., Van der Meeren, P., 2011. Preferential adsorption of polysorbate 20 molecular species in aqueous paliperidone palmitate suspensions. Colloids and Surfaces A: Physicochemical and Engineering Aspects 384, 691-697.